AD NUMBER
AD871194
LIMITATION CHANGES
TO: **Approved for public release; distribution is unlimited.**
FROM: **Distribution authorized to U.S. Gov't. agencies and their contractors; Administrative/Operational Use; MAY 1970. Other requests shall be referred to Armed Services Explosive Safety Board, Forrestal Building, Washington, DC.**
AUTHORITY
ASESB, DOD ltr dtd 24 Jun 1971

EVALUATION OF EXPLOSIVE STORAGE SAFETY CRITERIA

Final Report

By

George H. Custard
James D. Donahue
John R. Thayer

Falcon Research and Development Company
Denver, Colorado

May 1970

PREPARED FOR

ARMED SERVICES EXPLOSIVE SAFETY BOARD
FORRESTAL BUILDING
WASHINGTON, D. C.

Contract No. DAHC04-69-C-0095

FALCON
RESEARCH AND
DEVELOPMENT

Technodyne DIVISION

DENVER COLORADO

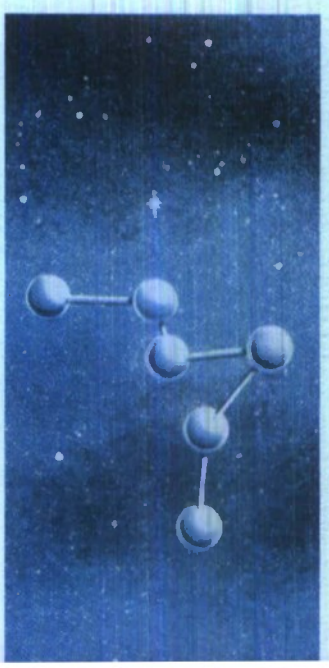

EVALUATION OF EXPLOSIVES STORAGE SAFETY CRITERIA

By

George H. Custard
James D. Donahue
John R. Thayer

Falcon Research and Development Company
Denver, Colorado

Final Report

Prepared for the

Armed Services Explosive Safety Board
Washington, D. C. 20314

May 1970

FOREWORD

The work summarized in this report was conducted under Contract DAHC04-69-C-0095 during the period 1 July 1969 to 28 February 1970. The project was under the direction of the Chairman of the Armed Services Explosive Safety Board, Col. B. B. Abrams. Technical guidance was provided by Mr. Russel G. Perkins, Contract Monitor, and Mr. Robert C. Herman, Alternate Technical Monitor.

The study was conducted by the Falcon Research and Development Company under the guidance of Mr. Arthur M. Krill, President. Mr. George H. Custard served as Project Supervisor and was ably assisted by Mr. James D. Donahue, Mr. Daniel K. Parks, and Mr. John Thayer. Other persons assisting in the project at the Falcon Research and Development Company include Mr. Charles E. Eppinger, Mr. Donald Saum, Mr. Howard Iwata, Mr. Wallace Clark, and Mrs. Jerry Foster. Assistance to the technical effort was also provided by staff members of the Ken R. White Company, an affiliate of Falcon Research and Development.

SUMMARY

This project has sought to develop greater understanding of the interaction of explosive blast forces with the structural targets which require protection from the accidental detonation of stored explosives. The relationships which have been developed will be helpful in understanding the risks which are implied in the established explosive quantity-distance criteria and will provide a basis for estimating the potential damage to structures exposed in a blast field which is sufficient to cause incipient structural failure.

This work differs from many prior blast response studies in that neither the massive structural failure sought by the weapon designer nor the complete structural survival sought by the protective structures programs have been directly applicable. This precise balance between the blast forces and the structural properties has required a more exacting treatment of interactions than is found in much of the earlier work.

This study has been implemented through the definition of ten specific structures which have been "exposed" to the blast forces from five charge sizes through analytical modeling techniques. All charges considered have been spherical, surface burst, bare TNT. The charges considered were limited to the following five sizes: 1,000 pounds, 10,000 pounds, 100,000 pounds, 1,000,000 pounds, and 9,000,000 pounds.

The study has been limited to target response to air blast forces with no consideration to ground shock, fragmentation hazards (except glass), fire hazards or other potential threats. This limitation is imposed only by the defined scope of work and should not be misinterpreted as a lack of concern or awareness relative to the other hazards.

The ten specific target structures selected for consideration were:

1. Modern split-level house constructed of a combination of masonry and frame.

2. A modern church with laminated beams and an A-frame roof.

3. A modern elementary school.

4. A multi-story office building.

5. A passenger bus moving around a curve on a highway.

6. A camper-pickup on a straight highway.

7. A stationary mobile home.

8. Personnel in the open.

9. The front wall of a standard igloo.

10. A commercial jet aircraft.

These targets have been described in precise structural detail so that dynamic responses involving actual component weight, elasticity, strength, and dimensions could be investigated.

Specific levels of damage have been defined as "acceptable" for each type of target. These damage levels have been selected in consultation with the Armed Services Explosive Safety Board to minimize the risk of serious injury to occupants of the structures without requiring separation distances between the stored explosive and the target structure that are excessive. It is recognized by this study that separation distance is often an expensive requirement. Thus, some minor or incipient structural damage to target structures has been considered as acceptable so long as the risk of serious injury to personnel was sufficiently low.

A separate model of blast response has been developed for each structural component of each target which can reasonably be expected to suffer damage within the range of charge sizes and distances considered. Thus, for example, the house is analyzed in terms of the behavior of its frame roof, frame walls, and masonry walls. The first failure of any of the three components (to the established maximum acceptable level) defines a minimum distance requirement for the entire target.

The dynamic interaction models consider both the elastic and plastic deformation involved in target response and rely heavily on the concept of requiring a critical impulse to be

imparted to the target member in no more than one fourth of its fundamental resonant frequency. Where the blast forces act against both front and back surfaces of a target or component, both forces have been considered. The models rely upon the work of the Ballistic Research Laboratories for descriptions of the blast wave phenomena in terms of peak incident pressure, incident impulse, and positive duration. These values, together with appropriate reflection factors and target dimensions have been used to define the reflected pressure and impulse to which a particular target element must respond as a function of time.

The computer program which has been developed to handle the various models performs the iterative steps for each charge-target interaction and will provide data relative to the critical periods of each component, associated critical impulse, required separation distance to meet the maximum acceptable damage criterion, and the blast exposure of the other target components. The program will accept a series of structural properties as inputs to the program so that the effects of variations in tensile strength, elasticity, mass, etc., can be shown for each target element.

While the models and computer program elements are extensively concerned with target structural properties, it will be valuable to remember that the protection of people rather than the protection of structure underlies virtually all of the work. This element of the models is easily lost sight of, since it is implemented through the selection of damage criteria rather than through the later developments of the various failure modes. Note that no building is ever allowed to collapse upon its occupants nor is any vehicle allowed to overturn or be forced beyond the control of the driver.

Experimental verification of target behavior, under the blast loading conditions of greatest interest, has been sought from all known prior tests. Some significant data has been found and the analytical results are generally supported by the data available. In general, however, the documented experimental data available for these types of targets exposed to blast conditions which produce only low levels of structural component damage must be described as meager. This scarcity of experimental evidence has required that results be developed through a reliance on analytical techniques which are believed

to be accurate and appropriate. Confidence in these techniques would be further enhanced by a carefully planned series of tests to experimentally verify target behavior at the threshold of structural failure for each type of target component considered.

The results of the program have been presented in a series of plots showing the computed distance for the defined damage level in each target exposed to each of the five charge sizes. These data may be compared with present standards which are shown on each plot for the convenience of the reader. Plots of the incident pressure and impulse values associated with these distances have also been prepared for each target type. These plots are clearly of the hyperbolic form which was predicted by earlier workers in the field.

CONTENTS

LIST OF ILLUSTRATIONS

LIST OF TABLES

EVALUATION OF EXPLOSIVES STORAGE SAFETY CRITERIA

I. INTRODUCTION

Present quantity-distance explosives storage criteria [28] used for the specification of minimum separation distances between various types and quantities of stored explosives and surrounding facilities, have evolved principally from comprehensive studies of actual blast damage results. Several of the recommended storage separation distances for given types and quantities of explosives specified in these tables were derived from thorough evaluations of the blast damage caused by accidental detonation of these quantities to different types of nearby structures. These damaged structures were classified into general categories (such as inhabitated buildings), and the minimum distance specification for that classification of structure then based on the damage done to the lightest constructed facility. Other separation distances for quantities of explosives for which no accident or experimental data exist were derived through the use of scaling laws.

The current standards have wide use and have proved a significant factor in public safety over the years. However, it seems desirable to revise and expand the tables of recommended separation distances whenever sufficient information with which to consider new types of explosives, larger stored quantities of explosive materials, and/or a wider spectrum of civilian targets becomes available. Quantity-distance explosive storage specifications have undergone several such revisions and expansions since their inception. Recognition of the need to distinguish between the storage requirements for military explosives (bombs, rockets, etc.) and those pertaining to commercial non-fragmenting explosives represents a past event prompting review.

A review of current storage distance specifications again seems warranted in view of the large number of weapons effects studies, experimental and analytical studies of blast wave characteristics, and target response studies conducted in the past few years. In addition, the current standards have been criticized from the viewpoint that they are expressed only in

terms of general categories of civilian targets*; i.e., barricaded or unbarricaded inhabited buildings, passenger railroads, public highways, etc. Obviously, with the specification of a separation distance applied to a general category of targets (such as unbarricaded inhabited buildings, for example), no acknowledgement is made of any significant differences in the response to a given blast force by the different types of potential targets within that category--frame house, brick houses, church building, school buildings, etc. Consequently, specifications of minimum separation distances can vary greatly in the degree of protection afforded the different types of structures classified in one category. When significant differences in the blast responses of specific targets within one general category do exist, an extension of the quantity-distance tables to include specific targets of interest is warranted.

In view of these considerations, this study was conducted for the Armed Services Explosive Safety Board with the intended objectives of critically evaluating existing storage-distance criteria, for blast damage, in light of updated analytical and experimental evidence and of recommending the basis for storage distance requirements applicable to a number of specific civilian target not previously considered. For each target and quantity of explosive considered, analytical methodology has been formulated with which to specify a minimum separation distance which minimizes the probable risk that the blast damage resulting from an accidental detonation will exceed a predetermined acceptable level. These procedures were derived, where possible, through application of results from more recent analytical and experimental blast damage programs in which the structures or structural elements subjected to blast could be related through similar structural properties and construction techniques to the civilian targets of interest. A computer program was developed to facilitate this study and was used to obtain the results of the analysis presented herein.

---

*The term "target" is used throughout this report to refer to personnel and to public structures which normally require protection from accidental detonation of stored explosives. Such targets include civilian personnel, various types of private dwellings and buildings, mobile houses, commercial aircraft, automotive vehicles, other storage magazines, etc.

It is programmed in FORTRAN and can be adapted to several types of computers. A description of the program, flow charts, and operating instructions are presented in Reference 32.

II. SELECTION OF TARGETS AND ESTABLISHMENT OF ACCEPTABLE DAMAGE CRITERIA

The prediction of the blast response of existing structures is an exceedingly complex problem involving many unresolved aspects of both the air blast loading on, and the failure mechanism of, structures. Therefore, a combined knowledge of air blast phenomena and the construction practices used with many types of structures is important to the ultimate success of any blast damage study.

In reviewing the current quantity-distance explosives storage specifications, a realistic spectrum of civilian targets requiring protection against blast damage hazards was first established so that representative or generic types of structures could be selected, and a detailed study of their construction techniques made. Therefore, as an initial step, ten specific types of civilian targets considered to be representative of the spectrum of targets requiring protection were selected by cognizant personnel of the Armed Services Explosive Safety Board. These are listed below and each is discussed in detail in Section IV.

1. Split-level, frame-brick house
2. A-frame construction church building
3. One-story masonry school building
4. Multistory, concrete block panel office building
5. Mobile home
6. Passenger bus
7. Camper-pickup unit
8. Commercial jet aircraft
9. Man
10. Standard explosives storage igloo

Before recommended quantity-distance criteria for stored explosives could be established or critically reviewed, the levels of damage against which the selected targets are to be protected had to be ascertained. This, of course, is a complex task because of the difficulty in meaningfully describing the exact extent of structural degradation caused by observable damage in an experimental test. For example, the description for a large crack in a section of concrete wall as "severe structural damage", may or may not accurately describe the loss in load-carrying capacity of the particular type of wall.

The approach to this problem was to determine blast overpressures which cause different, uniquely describable, degrees of acceptable damage to a structure.

In establishing "acceptable damage" criteria for each of the above targets, a number of unacceptable degrees of damage were first considered for each structure. The explosive storage separation distance for a given explosive quantity was then established with relationship to a "worst case" or first damage level. For the stationary targets (home, church, school, office building, and the mobile home), two levels of unacceptable damage or risk levels were considered. The first was damage which constituted a critical hazard to occupants from high velocity glass fragments from broken windows. The second was blast damage sufficient to cause an immediate hazard to occupants of the building as a result of collapse of the roof or walls of the structure. In the analysis of these structures, levels of pressure-impulse--for each selected explosive quantity--which cause each of these types of damage were established. The greatest separation distance at which unacceptable damage occurs denotes the critical damage, and, thus, is designated as the "worst case".

Acceptable damage to each structure is identified as all structural damage of a degree up to but not including the specified critical damage. For example, if a house roof is expected to fail before the brick or frame walls--and also before flying glass becomes a significant hazard--then the acceptable level would include all damage up to, but not including, roof collapse. In this case, a distance corresponding to the blast forces required to crack the roof rafters, but not sufficient to structurally collapse the roof, would be identified as the recommended separation distance.

With respect to the passenger vehicles, targets 6 and 7, the levels of risk considered were those which cause: (1) loss of control on high speed, heavily travelled highways so as to endanger other vehicles; (2) crushing of the wall sections of the vehicles so as to endanger occupants; or (3) overturning, whichever represents the worst case.

For the commercial jet aircraft, damage sufficient to cause loss of control when landing or taking off was considered.

The level of risk considered for personnel targets was that of being violently thrown to the ground, down stairs, or against nearby structures. Collapse of the door of the explosives storage igloo was specified as the level of risk for that target.

The computer program has been used to generate separation distances for the above ten targets and the specified damage levels. Five explosive charge sizes (1,000, 10,000, 100,000, 1 and 9 million pounds of TNT) have been considered.

Specific degrees of acceptable damage to each target have been defined with respect to the hazards discussed above. The quantity-distance criterion for each target has been based on the first to occur of the different types of acceptable damage. These are:

1. House - (1) cracking, but not complete severance, of one or more roof rafters; (2) cracking of one or more frame wall support members; (3) a 5-inch deflection of the center section of the brick wall; or (4) a glass fragment serious injury probability up to 30 percent.

2. Church - (1) cracking of one or more of the laminated beams, (2) cracking of one or more decking members, or (3) a glass fragment serious injury probability up to 30 percent.

3. School - (1) cracking of one or more roof beams, (2) a 5-inch deflection of the center section of the stone wall, or (3) a glass fragment serious injury probability up to 30 percent.

4. Office Building - (1) a 5-inch deflection in either type of wall, or (2) a glass fragment injury probability up to 30 percent.

5. Passenger Bus, Camper-Pickup Unit, and Mobile Home - (1) all damage associated with the pressure-impulse corresponding to 80 percent of the impulse required for overturning.

6. Explosives Storage Igloo - (1) all damage associated with the pressure-impulse required to deform the doors so that they open.

7. Personnel - (1) overpressures up to but not including those causing eardrum rupture, or (2) pressure-impulse forces causing translation of the man at a maximum velocity of 3.5 fps.

8. Commercial Aircraft - (1) threshold deformation of the substructive frame member supporting the weakest skin panel.

III. BLAST EFFECTS MODELS AND RELATED STUDIES

A. GENERAL CONSIDERATIONS

A model or method to accurately relate the damage characteristics of a shock wave to the structural characteristics of a specific target is required in order to determine the blast damage potential of an explosive detonation. Theoretically, the response of a structure to the dynamic blast loading can be estimated with a knowledge of (a) the complete dynamic response of the structure; (b) the aerodynamic properties of the specific structure; and (c) the pressure, time, and position characteristics of the blast wave relative to the structure. These essential factors have been treated, more or less independently, in a large number of military target vulnerability and weapons effectiveness studies, target descriptions, and experimental and analytical studies of blast wave characteristics. Sufficient experimental data have been obtained from field testing so that the pressure, time, and position characteristics of a shock wave resulting from explosive detonation can be approximated with reasonable accuracy. Formulae and extensive tabulations giving values of these parameters for various weights and types of explosives are available [57, 71].

Accurate estimates of the complete dynamic response of a structure to blast are greatly complicated by its complex structural nature and by the number of various phenomena of a blast wave which render damage to the structure. A completely acceptable theory or method of approximation for this response by all types of targets has not been developed. Many experimental studies have been conducted in which the structural responses to blast of simple structural shapes, such as cylinders [86, 87], beams [66], plates [59, 72], and shells [15] have been measured. Methods for predicting the blast levels sufficient to cause permanent deformation in the structure are formulated from the empirical data. Many investigators have attempted to obtain approximations of the structural response of targets by viewing the targets as a composite system of simple structural shapes and utilizing empirical methods to predict the structural response of each individual component. However, this procedure has usually resulted in obtaining only gross approximations. Based on these considerations, the dynamic response of a complex target is considered the most

difficult-to-quantify factor in the study of this type of damage mechanism.

B. ANALYTICAL AND EXPERIMENTAL MODELS OF STRUCTURAL BLAST DAMAGE

As an initial step in attempting to quantify the dynamic response to blast loading of the targets of interest, a detailed study of their structural properties and construction techniques was made. This study was intended to indicate how the external surfaces of each target might react under blast loading. While from a structural analysis viewpoint, different types of single story houses, for example, all might conceivably be classified as being of "rigid roof" construction (the columns are of sufficient strength and rigidity to resist relative motion between columns), it is inconceivable that their different types of exterior walls would react identically to identical blast loadings. Therefore, it was necessary and desirable to classify the potential mode of behavior to blast loading of different types of exterior surfaces of each class of target through a detailed structural study at the outset of this program.

Results from several experimental blast studies which have been conducted on targets or structural elements, related through similar structural properties to the specified civilian targets, have been used. In several cases, the descriptions of structures and structural elements treated in these experimental studies have been well documented and it can be definitely ascertained that they are similar to the structural peoperties of the selected civilian targets considered in this study. Thus, their resistance to blast loading has been equated.

In this phase of the study, numerous documented experimental and analytical investigations were reviewed; several are listed in the Reference section. The more useful results are reviewed in the following paragraphs.

1. Wall Sections of Houses and Other Buildings

The essential difference between the response to blast loading of the walls of different types of single story frame, brick, stucco, etc., houses, can be attributed to the varying strength

properties of the different types of walls. The resistance of wall sections can be idealized as elastic, elasto-plastic, plastic, strain hardening, and decaying or unstable. The blast response of a wall is dependent upon the type of wall construction and more specifically on its support conditions and mode of response. For each type of wall construction, simple support, fixed support, and fixed-hinged support construction must be considered.

The exterior walls of buildings are also generally categorized as panel, curtain, and load-bearing. Panel walls can be defined as nonload-bearing walls that are supported by the structural framework of the building at each floor level. In general, such walls are designed for wind pressure only; in actual buildings, panel walls can act as diaphragms or shear walls in resisting deformations of the structure, especially for large blast forces. Curtain walls are self-supporting exterior walls that are independent of the frame, although they are usually laterally anchored to the frame at each floor level. Except for their own dead weight, curtain walls are also nonload-bearing. On the other hand, the exterior walls make up the main structural member of a load-bearing wall building. As such, load-bearing walls support primary building loads in addition to their own dead weight.

a. Simply Supported Walls

The resistance of a simply supported masonry unit wall, for example, subjected to a uniformly distributed dynamic load is a function of the bending resistance of the wall and its vertical load (see Figure 1). Masonry walls which are loaded from the side will fail in a three-step process composed of an elastic phase, tensile failure of mortar or mortar bonds, and a deformation phase in which internal crushing takes place, and components of the wall are translated or deflected beyond a point where they can support their usual load.

The resistance-deflection relationships which make it possible to evaluate the work required to fail the wall have been presented in an OCD report, "Existing Structures Evaluation - Part I, Walls" [106]. The maximum elastic resistance, Q_1, for a 1-inch wide section or beam of this type of wall (8 inches thick), is developed when the moment at the center section is a maximum, or

$$M = \frac{Q_1 L}{8} , \tag{1}$$

where L is the height of the wall section (inches) as indicated in Figure 1.

If it is assumed that a linear relationship exists between stress and strain across a section of the wall, the extreme fiber stress, σ, is given by

$$\sigma = \frac{M \cdot C}{I} \pm \frac{P_V}{A} \tag{2}$$

where:

P_V = the vertical wall load acting on the end section A (inches^2),

C = the maximum distance from the neutral axis of the wall to the extreme fiber, and

I = the moment of inertia of the wall section.

P_V includes the blast forces acting on structures supported by the wall or bearing on the wall.

Substituting equation (1) into equation (2), rearranging terms, and assuming that the tensile stress governs the initial wall failure, the maximum elastic resistance, Q_1, for the 1-inch wide wall column is

$$Q_1 = \frac{4T_W}{3L} (f \cdot T_W + P_V) \tag{3}$$

where:

T_W = thickness of the wall (inches) and

f = tensile bond strength (lbs/in^2).

The maximum deflection (inches) for the elastic phase is

$$y_1 = \frac{5Q_1 L^3}{384EI} , \tag{4}$$

where E is Young's modulus.

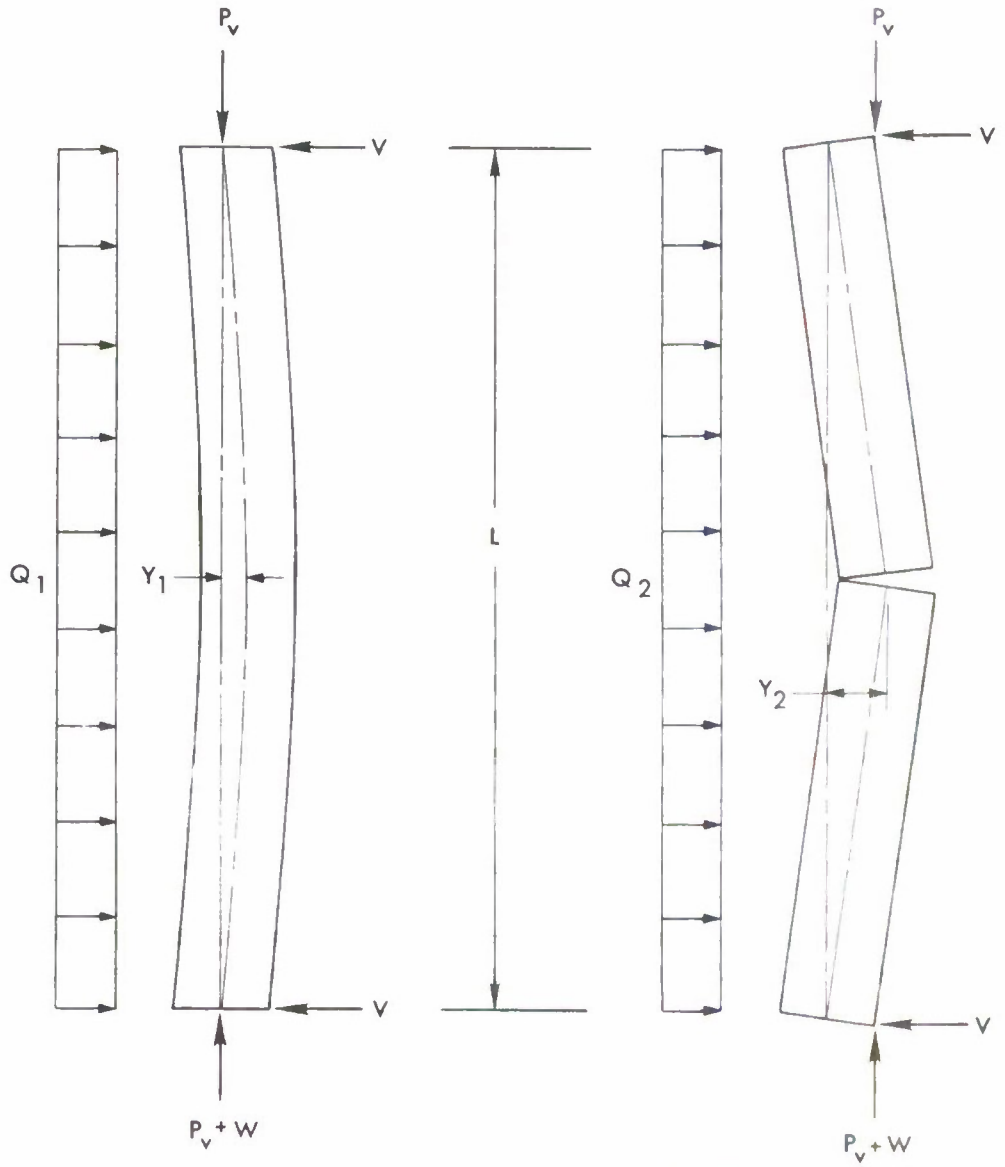

Figure 1. Assumed Model for Behavior of Masonry Unit Wall

The above equations are not exact, since the effect of the eccentricity of the axial load, which results from the deflection of the wall under the lateral load, is neglected. However, for unreinforced walls of the type considered, the elastic deflections are very small, and therefore, the increase in moment and deflection caused by the eccentricity are also small.

Subsequent to the initial bending failure of the wall during the elastic phase, a crack is developed in the vicinity of the point of maximum moment, and the bending resistance of the wall reduces to zero. However, the wall does not necessarily collapse, since the axial force in the plane of the wall provides a restoring force, which results in a decaying type of resistance function. It is apparent that for a static or long duration dynamic lateral load, a structural member with a decaying resistance function would collapse if the load equaled the maximum resistance. However, for situations where the clearing time of the reflected overpressure is relatively short, the influence of a decaying resistance function can be important for the prediction of the collapse pressure, even for long duration blast loads.

The tensile failure occurs very nearly instantaneously at the limit of elastic deformation. Beyond the point of the tensile failure deformation proceeds in accordance with the relationship between the blast loading and a linear resistance decay from a maximum resistance level, Q_2. To develop an equation for the resistance during the secondary phase, it was assumed that the wall will crack along a horizontal section and that the two resulting wall segments will rotate about the supports as rigid bodies, as shown on Figure 1(b). The resistance in the secondary or decaying phase is related to the vertical axial load, the wall dead load, the wall dimensions, and the deflection. By taking moments about one of the supports, it can be shown that the maximum resistance during the decaying phase is equal to

$$Q_2 = \frac{4}{L} (T_w - y_1) (2 P_v + w), \qquad (5)$$

where w is the weight of the wall column. As shown in Figure 2, this maximum resistance may be greater than, equal to, or less than the maximum elastic resistance.

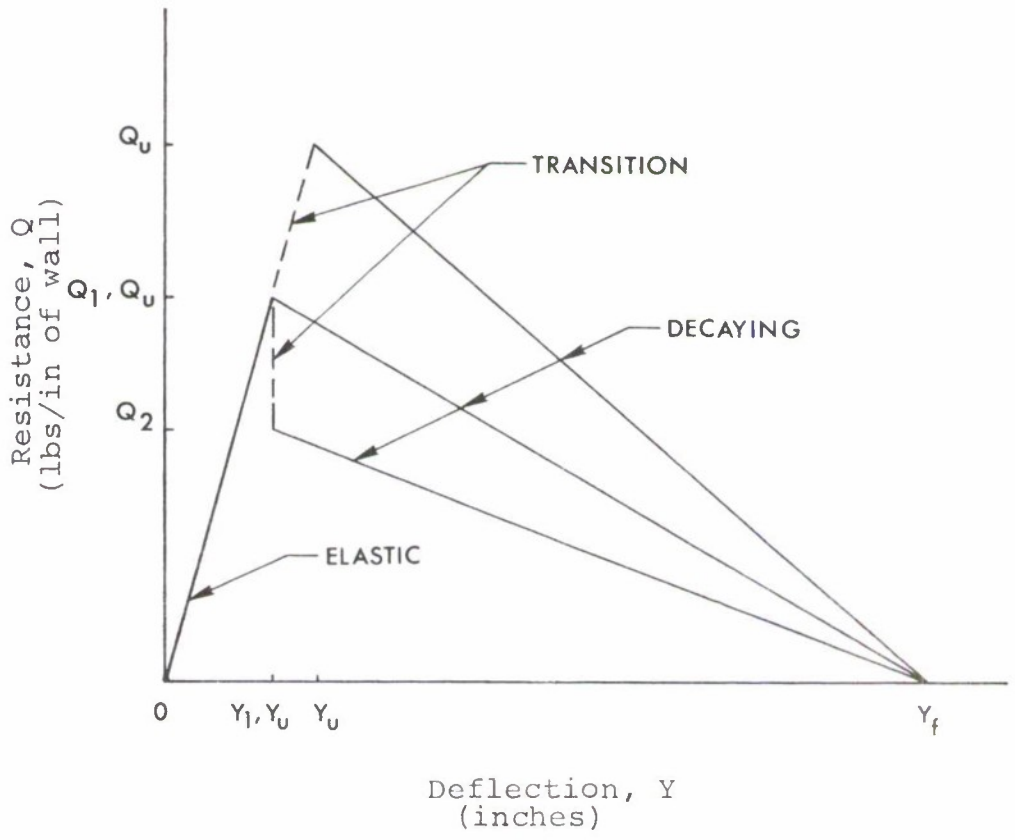

Figure 2. Resistance Function for a Simply Supported Masonry Unit Wall Without Arching

The assumption for the location of the vertical dead weight and blast loading, P_v, during the secondary phase affects both the maximum resistance and the deflection at which collapse is predicted. The actual location of the resultant of the vertical forces during the response of the wall depends on a number of factors, such as the point of application of the floor loads and the deflection of the wall, and is therefore indeterminate. It can be logically assumed that before cracking of the wall the vertical dead load will act at the centroid of the wall section. After cracking, the vertical dead load will act in the plane of the inner wall surface.

The resistance in the decaying phase will decrease linearly from Q_2 at y_1 to zero at $y = T_w$. The integration of the resistance functions shown in Figure 2 defines the blast energy required to fail the wall by the mechanism shown in Figure 1 with an instantaneous uniform load.

The uniform blast impulse first accelerates every element of the wall section imparting kinetic energy to it. If the initial velocity of the components of the wall is sufficient at the end of the instantaneous loading period, failure of the wall will follow, and the kinetic energy required to fail the wall will have been provided by the blast wave. The kinetic energy which must be available in the blast wave which strikes a wall half section can be equated to one-half of the work defined by the integration of the full wall resistance function, and is expressed as

$$1/2W = KE = 1/2m\ v^2 \tag{6}$$

where:

m = mass of the half wall, and

v = initial velocity of the wall elements.

As the restraints come into play, the motion of the wall sections becomes rotational about the restraining points and approximately half the initially imparted energy converted to wall deflection work. The total impulse required to provide this amount of kinetic energy is:

$$\begin{aligned} H &= F_o \cdot \Delta t \\ &= (F_o - F_r)\ \Delta t + F_r\ \Delta t \end{aligned} \tag{7}$$

where:

H = total blast impulse applied to the half wall

F_o = blast force acting at the center of the half wall

Δt = the time interval that the force acts

F_r = resisting force at the point of rotation for the half wall.

Expressed in terms of mass and velocity, equation (7) may be written as

$$H = mV_{cg} + \frac{I_{cg} \cdot V_{cg}}{h^2} \tag{8}$$

where h is one-quarter of the wall height. The unit impulse (psi-ms) required to fail the 1-inch wall column or beam is

$$i_c = \frac{H \cdot 1000}{(\text{area of the half wall beam } (in^2))} \tag{9}$$

b. Fixed-End Walls

The resistance function for a simply supported, one-way reinforced wall is bilinear, with an elastic and a decaying resistance phase. The resistance function for a uniformly loaded fixed-end wall is similar, except that the maximum elastic resistance is developed when the moment at support is a maximum, or

$$M_{max} = \frac{Q_1 L}{12} \tag{10}$$

The maximum elastic resistance is given by

$$Q_1 = \frac{2T_w}{L} (f\ T_w + P_v), \tag{11}$$

where the terms are defined as in (3). The maximum deflection for the elastic phase of a fixed-end wall is

$$y_1 = \frac{Q_1 L^3}{384EI} \quad . \tag{12}$$

After cracking occurs at the fixed support, the bending resistance at the support is reduced to zero, and the wall responds as a simply supported wall. The resistance and deflection during this phase can be determined by equations (3) and (4), respectively. However, since the maximum resistance for a simply supported element is only two-thirds that for a fixed-end element, the influence of this phase on the predicted wall collapse is not important. Therefore, the resistance for the secondary phase for a fixed-end wall is assumed to be identical to the decaying resistance determined by (5) for a simply supported wall.

c. Propped-Cantilever Wall

The shape of the resistance function for a wall fixed at one end and simply supported at the other end is identical to that for a fixed-end wall. The maximum elastic resistance for the propped cantilever is developed when the moment at the fixed support is maximum and is equal to equation (1) for a simply supported wall. The maximum elastic resistance is therefore given by equation (3).

The maximum deflection for the elastic phase occurs at a distance of 0.4215 L from the simply supported end and is equal to

$$y_1 = \frac{Q_1 L^3}{185EI} \quad . \tag{13}$$

For the reasons discussed in the previous subsection for fixed-end walls, the resistance for the secondary phase for a propped-cantilever wall is assumed to be identical to the decaying resistance function given by equation (5) for a simply supported wall.

2. Experimental Work With Wall Sections

A number of experimental tests utilizing full-size test panels or wall sections have been documented. Reference 109 reports shock tube tests with wall sections of the same type and methods of construction as are prevelant in the civilian structures of interest. Twenty-one tests with brick and sheetrock wall panels were conducted in this referenced study. In the tests with 8-inch-thick brick walls (simply supported with no openings), peak reflected pressures ranged from 3.5 to 10.3 psi. In all cases, the wall failed (cracked) and subsequently collapsed. In the lower range of reflected overpressures, 3.5 to 4.0 psi, the walls tended to crack along a generally horizontal line within 1 foot of the center of the wall, and to collapse in several large pieces near their original position. Most of the resultant debris scattered within 10 feet of the wall. The loading pulse was essentially a three-stage, flat-topped pulse in which much of the decay took place in the last one-half of the duration. The duration of the pulse was approximately 90 to 100 msec. The corresponding theoretically computed reflected impulse was approximately 139 psi-msec.

No firm data were obtained with which to establish the threshold failure level, but it was inferred from the existing data and preliminary theoretical work that the collapse threshold is about 1.0 psi reflected overpressure for the 8-inch-thick, simply supported wall (assuming a tensile bond failure stress of 50 lbs/in^2). On this assumption, the computed reflected impulse required to produce threshold collapse is approximately 55 psi-msec. Using the wall collapse model presented in equations (1) through (9), a comparison of actual results and theoretical predictions can be made. Allowing P_v to reflect only the dead weight of the structures supported by the wall (blast loading on these structures assumed negligible) and assuming a tensile bond failure stress of 50 lbs/in^2, the calculated impulse by equations (1) through (9) to cause threshold collapse of the 8-inch, simply supported, brick wall is 60 psi-msec. The general agreement in these predicted and observed results is thought to justify use of the theoretical model presented. It therefore has been used extensively in the analysis section.

C. GLASS FRAGMENT PROPERTIES AND LETHALITY

Reference [73] presents the blast loadings associated with the 50-percent probability of failure for many weights, thicknesses, and maximum sizes of window glass that are available commercially. Data on weight, velocity, and spatial density of glass fragments resulting from window failure were reported for Operation Teapot tests. The incipient failure blast pressures for front-face loading as a function of pane area and thickness are summarized in Figure 3. Characteristics of window and plate glass are presented in Tables I and II.

When a structure is examined to determine its response to a range of air blast overpressures, the lowest overpressure causing building damage is usually found to be that associated with window glass failure. Glass failure is not structurally detrimental; however, if the glass fragments accelerated by air blast attain sufficient velocity, the injury to humans is of major concern. Thus, the need exists for a study of window behavior.

The mass and velocity of actual fragments produced by the breaking of windows due to blast phenomena have been extensively studied by the staff of the Lovelace Foundation. Figure 4 presents data relative to the wounding potential of glass fragments. Probabilities of serious wounds, expressed as functions of fragment mass and velocity, are given in this figure. Fragments which are below the P = 0.0 line must be considered to be of no serious threat to personnel except for chance hits in the eye or other points of extreme vulnerability.

Most of the related work has shown that fragment size varies inversely with the peak pressure of the blast wave striking the window. Figure 5 presents the relationship for the most common varieties of glass. While these mean values are well documented, the range of fragment sizes encountered in experimental tests, particularly for low incident pressures, is extreme. For example, data from the recent China Lake tests involving 10,000 pounds of TNT at a distance of 865 feet, produced fragments from less than 0.02 gram size to more than 60 grams. The front windows only are represented in this range. Incident pressure was about 1 psi and the glass was double strength.

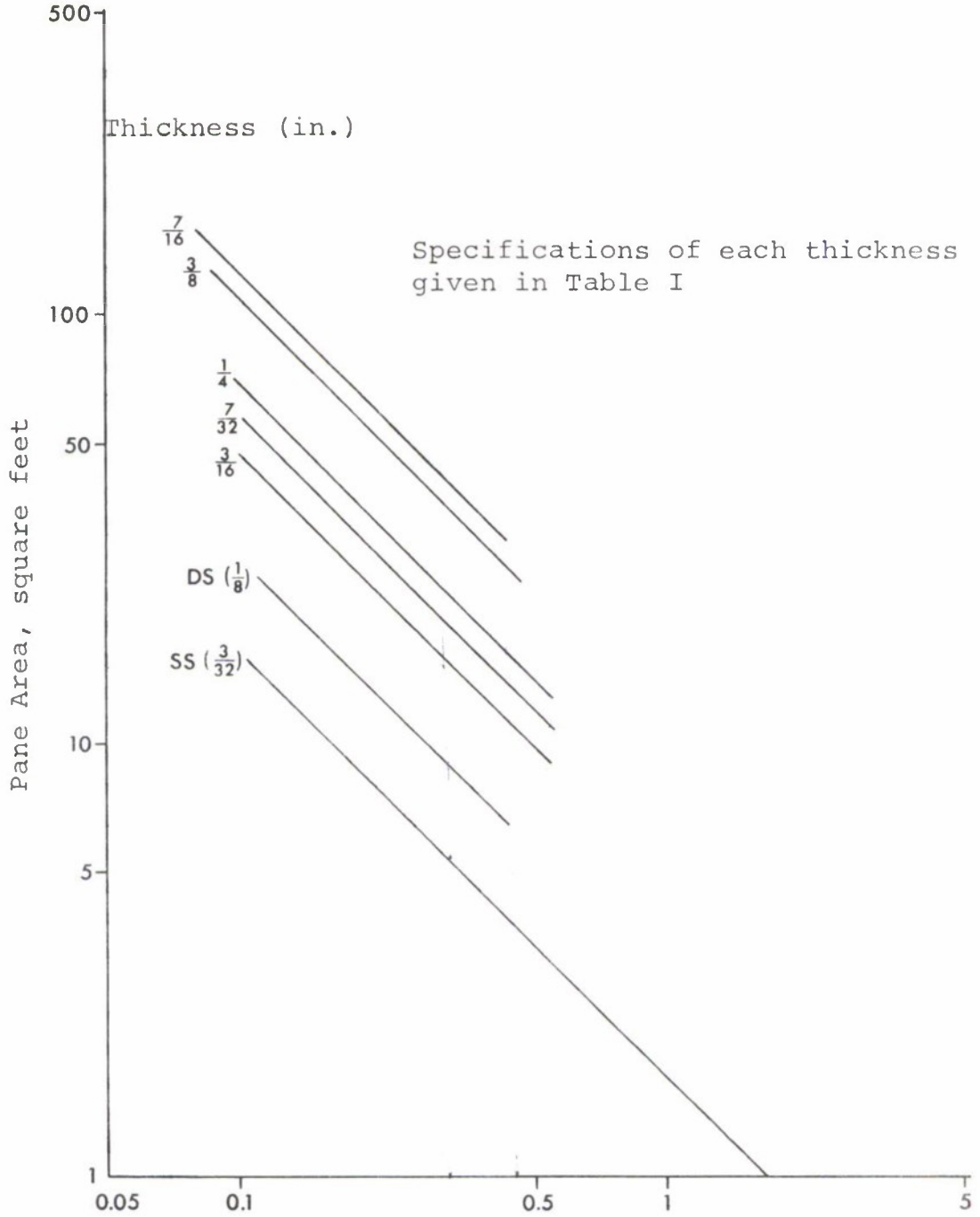

Figure 3. Sheet Glass Incipient Failure Pressures for Front-Face Loading as a Function of Pane Area and Thickness

TABLE I. Sheet Glass Specifications

Type	Thickness (in) Nominal	Thickness (in) Range	Approximate Weight per Square Foot Ounces	Approximate Weight per Square Foot Pounds	Maximum Size (in)
Single strength	3/32	(.085-.097)	19	1.20	40x50
Double strength	1/8	(.117-.131)	26	1.60	60x80
3/16" heavy sheet	3/16	(.182-.200)	40	2.51	120x84
7/32" heavy sheet	7/32	(.212-.230)	45	2.82	120x84
1/4" heavy sheet	1/4	(.240-.260)	52	3.23	120x84
3/8" heavy sheet	3/8	(.356-.384)	77	4.78	60x84
7/16" heavy	7/16	(.400-.430)	86	5.36	60x84

Source: Reference 73.

TABLE II. Plate Glass Specifications

Type	Thickness (in) Nominal	Thickness (in) Tolerance	Approximate Weight per Square Foot (pounds)	Maximum Size (in)
Float	1/4	±1/32	3.24	122x200
Regular plate	1/8	±1/32	1.64	76x128
Regular plate	1/4	±1/32	3.28	127x226
Regular plate	5/16	±1/32	4.10	127x226
Regular plate	3/8	±1/32	4.92	125x281
Regular plate	1/2	±1/32	6.56	125x281
Regular plate	3/4	+1/32 -3/64	9.85	120x280
Regular plate	1	+3/64 -1/16	13.13	74x148

Source: Reference 73.

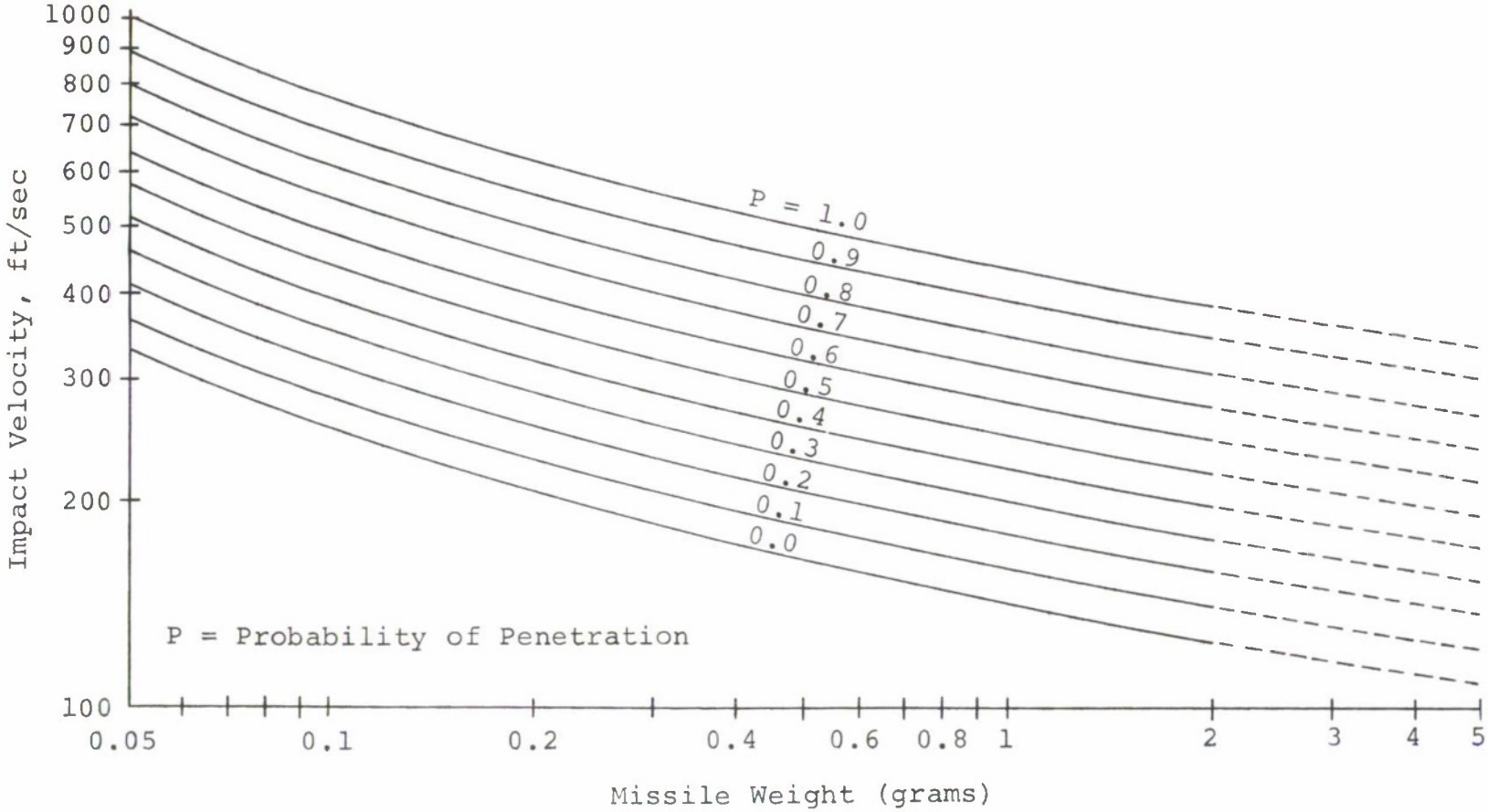

Figure 4. Probability of Penetration of Glass Fragments to Produce Serious Wounds

Source: Bowen, I. G., et al., "Biological Effects of Blast From Bombs", AECU-3350. Prepared by Lovelace Foundation, June 1956.

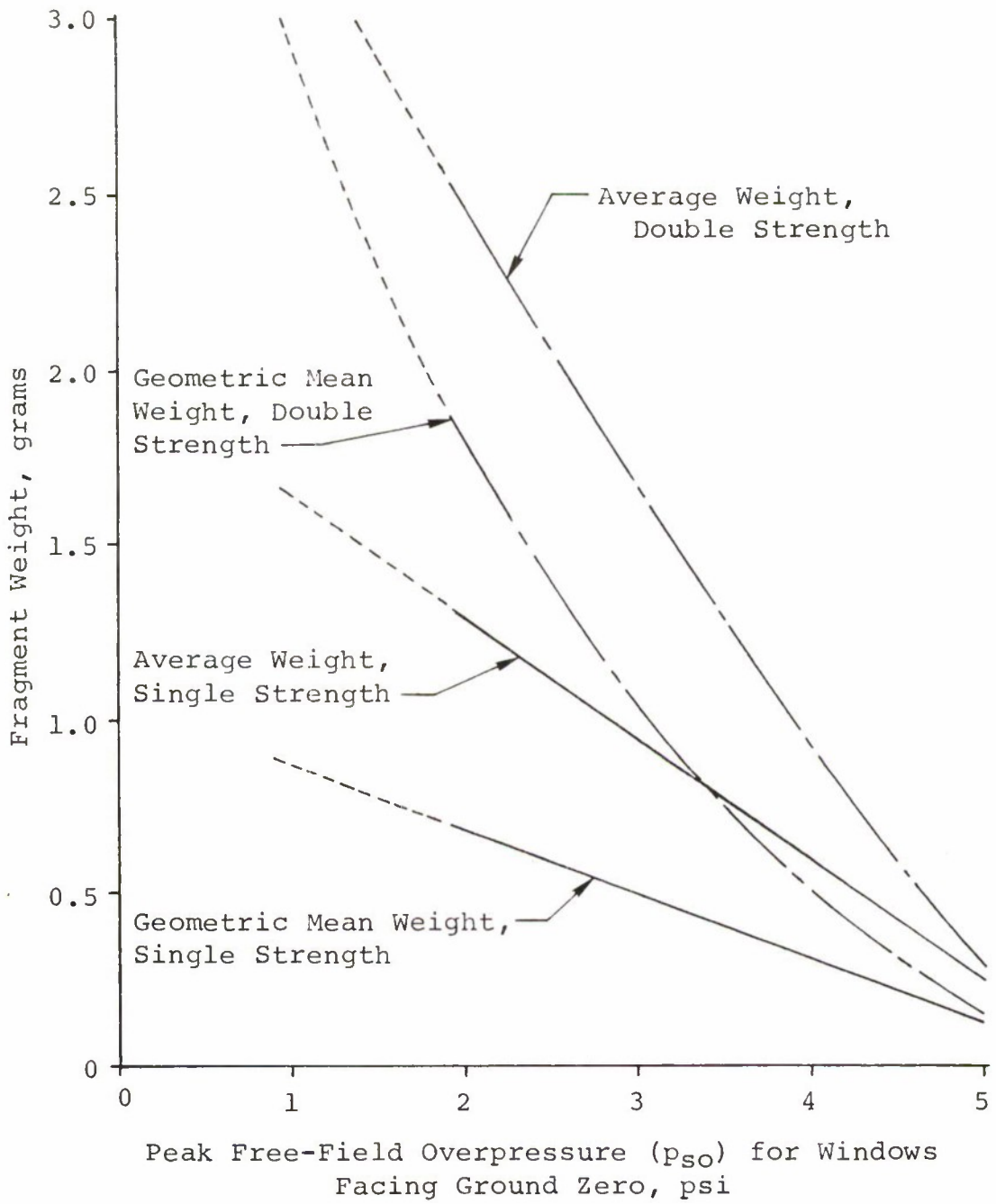

Figure 5. Mean Fragment Weight for Window Glass Broken by Blast

A similar test at Prairie Flat involving 1,000,000 pounds of TNT at a distance of 4,000 feet produced fragments with about the same size spread, even though the glass was only single strength and the mean fragment size was clearly less. Peak pressure for this test was very close to the 1 psi value of the China Lake test even though impulse was greater by at least a factor of three. The scatter of glass fragment mass and velocity values for all windows in both the Prairie Flat and China Lake tests is shown in Figure 6.

Fragment velocity is inversely proportional to fragment size and is directly affected by the duration of the pressure pulse. It has been shown that a window fragment is accelerated by the reflected pressure, since the total pane surface is always large in relation to the dimensions of an individual fragment. Figure 7 indicates the pressure-velocity relationship for the geometric mean fragments. The spread of data is great as indicated by the standard error values plotted on the figure.

In the Prairie Flat test, 822 fragments from front windows were examined. Of these no fragments greater than ten grams mass had velocities greater than 100 feet per second. Only 12 fragments greater than 1 gram exceeded 100 feet per second and the highest velocity indicated for any of these was only 150 feet per second. An additional ten fragments with masses between 0.1 and 1 gram exceeded 150 feet per second, but none of these exceeded 200 feet per second. Thus, there was very little probability of causing serious injury from the glass fragments produced in these tests.

It must be concluded that this type of glass fragment represents a minimum hazard at incident overpressure levels below 1 psi; becomes a marginal hazard at levels of 1.5 to 2 psi; and becomes a more serious hazard only at higher levels.

D. ANALYTICAL MODELS FOR PREDICTING BLAST DAMAGE EFFECTS

In this and other related studies, Falcon personnel have conducted extensive surveys of many analytical and empirical evaluations of conventional explosives blast effects. It has been concluded from these investigations that the most feasible approaches to the prediction of the blast loading response of a structure must be based on theory utilizing both the peak

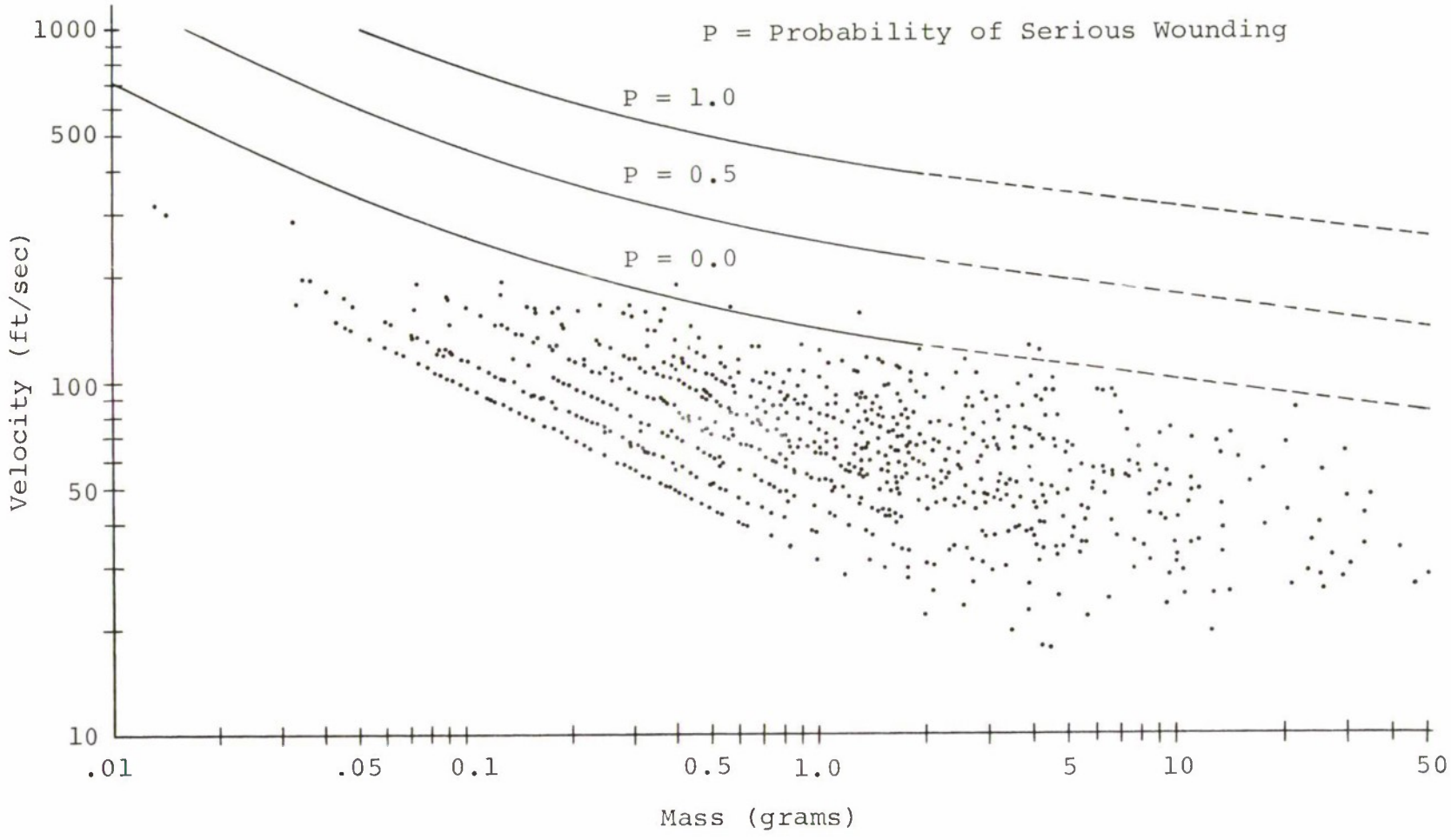

Figure 6. Wounding Potential of Glass Fragments From the China Lake and Prairie Flat Tests, all Windows

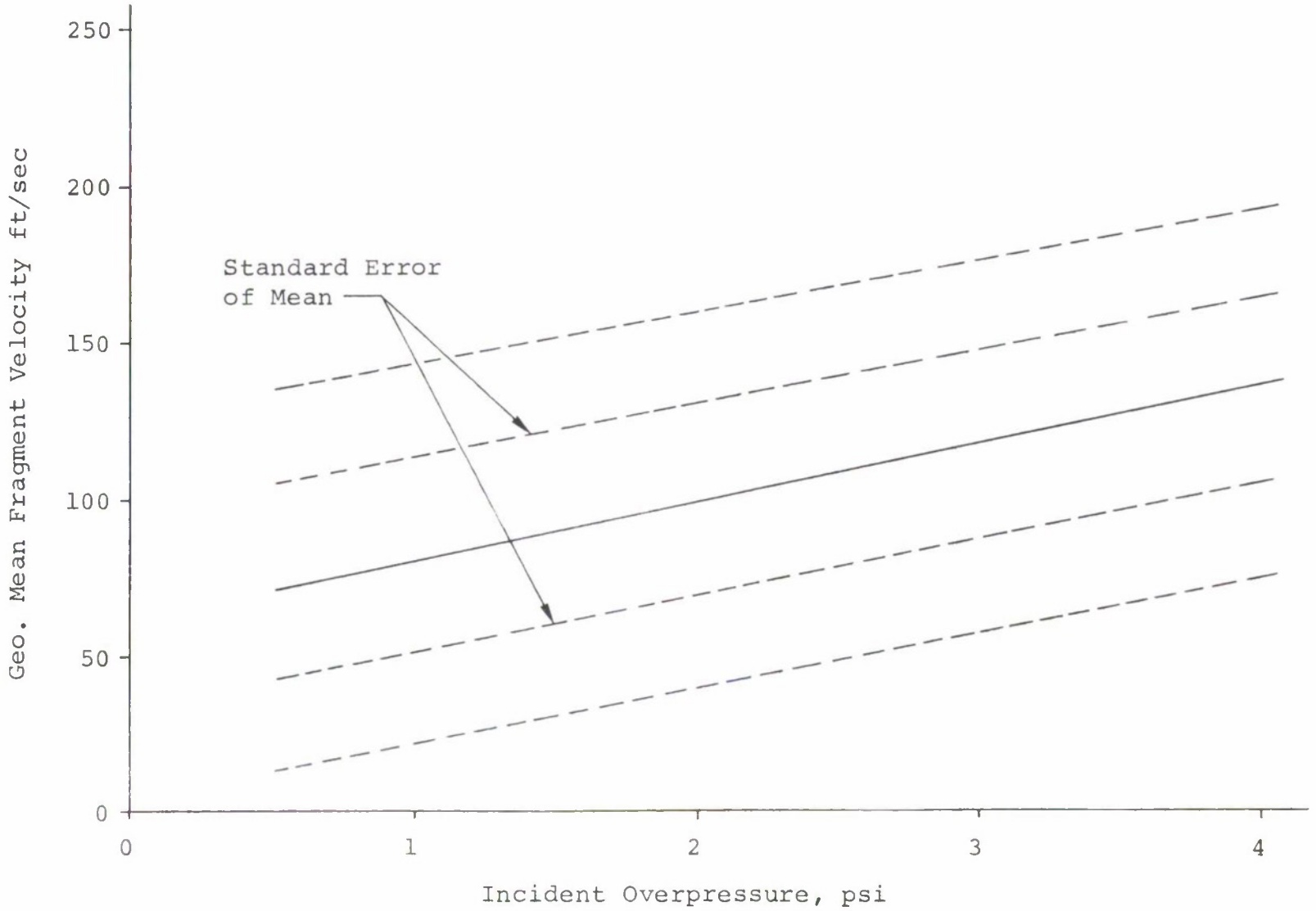

Figure 7. Glass Fragment-Velocity Relationship for Increasing Pressure Levels

overpressure and impulse parameters. Of those analytical approaches based on overpressure-impulse, two, which seem most realistic, are discussed in the following paragraphs.

1. Sewell's Approach

R. Sewell, Naval Weapons Center [89], has developed a blast effects prediction criterion based on achieving a "critical impulse within a critical period". This premise is that if a blast wave impinging upon a structural surface creates a velocity in the elements of the structure, relative to fixed points on the surface, greater than a "critical working velocity", then permanent deformation of the structure will result. A further assumption is that this critical velocity must occur within one-quarter period of the fundamental resonant frequency of the structure, $\gamma/4$.

Since the critical working velocity is not known for most materials, Sewell utilizes the known critical impact velocity, i.e., that velocity causing tensile failure in the material, in the formulation. Since this criterion of blast damage effectiveness is based on achieving a "critical impulse in a critical time period", it takes both the contribution of pressure and impulse into account in that the delivery time limitation requires that the pressure be relatively high in order to produce the necessary impulse within the time limit. Additionally, the characteristics of the target are given consideration in that the critical time is a function of the resonant frequency of the target and the critical impulse is expressed as a function of target characteristics.

The impulse in the critical period achieved by a fixed charge size at the target is a function of the charge-target distance D. An impulse, based only on the incident pressure, greater than I_{D_1} will occur for all charge-target distances less than D_1. Within the distance D_1, a fixed charge will create a sufficient incident pressure to achieve a critical impulse in a critical time and thus rupture the target material. The impulse, achievable by the full reflected pressure of the blast wave in the critical period, which is equal to the calculated critical impulse I_c, is associated with a charge-target distance, D_2, beyond which no significant target damage can occur. Therefore, at charge-target distances greater than D_2, the probability of generating a critical impulse is zero.

Sewell suggests that for a fixed charge size, a linear interpolation in the target kill probability can be made for all charge-target distances for which $D_2 \geq D \geq D_1$.

Criteria for establishing the unity and zero target kill probabilities may be derived for a fixed charge size and charge-target distance. These are:

$$\text{if} \qquad I_{D_1} = \int_0^{\gamma/4} p_o(t)\, dt \geq I_c, \text{ then } P_k = 1, \tag{14}$$

$$\text{and if} \qquad I_{D_2} = \int_0^{\gamma/4} p_r(t)\, dt \leq I_c, \text{ then } P_k = 0, \tag{15}$$

where:

$p_o(t)$ = incident or side-on overpressure function

$p_r(t)$ = full reflected overpressure function (equation (16)), and

$\gamma/4$ = quarter period of the fundamental resonant frequency of the target.

It is assumed that the reflected pressure on a surface decays in the same manner as the incident pressure; thus, the generally accepted approximation for the reflected overpressure function $p_r(t)$ becomes

$$p_r(t) = P_r\left(1 - \frac{t}{\tau}\right) e^{-\frac{t}{\tau}} \tag{16}$$

where P_r is the peak reflected pressure. This approach takes the contribution of both pressure and duration into account in that the delivery time limitation ($\gamma/4$, the one-quarter period of the fundamental resonant frequency), requires the pressure to be relatively high in order to produce a critical impulse with the specified time limit. Specifically, the critical unit impulse is expressed as

$$I_c = V_c \rho_T \delta \ , \tag{17}$$

where:

V_c = critical velocity

ρ_T = density of the target (slugs/in^3)

δ = thickness of the target.

The application of Sewell's approach is best applied to nonbrittle targets, since it implies that greater degrees of deformation in a structure accompany higher impulses imparted to the structure. However, the basic premise of having to achieve a critical impulse within the first one-quarter of the fundamental frequency of any type of target is thought to be valid regardless of the stress-strain relationship of the target.

The use of a critical working velocity for metallic panels is, in effect, an extrapolation of the fundamental research reported by Rinehart and Pearson [83] and Von Karman and Duwey [101]. In the latter paper, the dependence of brittle tensile fracture in long metallic wires on the critical impact velocity V_c is defined by

$$V_c \geq \int_0^{\varepsilon_u} \frac{\sqrt{\frac{d\sigma}{d\varepsilon}}}{\rho} \, d\varepsilon \, , \qquad (18)$$

where:

$\frac{d\sigma}{d\varepsilon}$ = instantaneous slope of the stress-strain curve for a specific metal

ρ = mass density of the metal

ε_u = ultimate strain of the metal.

In a later research paper by Clark and Wood [22] an excellent correlation with test data was established.

In the evaluation of prediction techniques in comparison with existing empirical results, it is generally necessary to make several assumptions and approximations in order to obtain the necessary input data. Certain assumptions were made in order

to conduct a comparative analysis of the predictions obtained through the use of Sewell's criterion and the actual aluminum cylinder damage data experimentally obtained by Schuman [87]. The calculated critical impulse of the aluminum cylinders used in the BRL tests was 5.38 psi-ms. This result was derived using (17) where the critical velocity of aluminum is assumed to be 300 fps.

To determine the critical time, which is considered to be one-quarter period of the resonant frequency, it was assumed that the lowest natural frequency of a short thin walled cylinder is associated with a vibration about the axis similar to that of a vibrating ring. With this assumption the expression for frequency of a vibrating ring as given by Timoshenko is applicable [95]. This equation is given as

$$p_i = \frac{1}{2\Pi} \sqrt{\frac{Eg}{\gamma} \frac{I}{Ar^4} \frac{i^2(1-i^2)^2}{1+i^2}} \qquad (19)$$

where:

p = frequency

i = mode

γ = specific weight

A = cross section area

r = radius

g = acceleration due to gravity.

Since the cylinders were plugged at each end, and thereby stiffened appreciably, a higher frequency than that calculated in this manner would be expected. Assuming a factor of three for this correction, a frequency of 200 cycles per second was obtained for the cylindrical shells utilized as targets. Thus, a quarter period of 1.25 milliseconds was taken as the critical time.

With these values for critical impulse and critical velocity, plots of the probability of achieving an observable deformation in the cylinder, versus distance for varying charge sizes

were made. These functions were derived using equations (14) and (15) and the assumption of linearity. Figure 8 presents two of these curves for two charge sizes employed in the BRL study. In the case of the 8.3-pound charge, an observable deformation, excessive deformation in fact, was obtained at a distance of 16 feet. This distance is well within the distance of 22 feet at which the probability of a permanent deformation is predicted to be a certainty. For the 115-pound charge, an observable deformation was obtained at 70 feet. From the graph, it is seen that the predicted probability of such an event is approximately 0.70. Therefore, it would appear, for these examples, there is reasonable agreement between the experimental results and the "critical impulse in a critical time period" criterion.

2. Critical Stress Approach

In the analyses made in this study, Sewell's premise of having to achieve a critical impulse within the one-quarter fundamental resonant frequency of a structure is used extensively. In the treatment of wood structures, most of the accepted levels of damage considered in this study are based on simply cracking, but not completely breaking, a particular wood member. Therefore, the elastic phase of deflection, up to and including the yield point, is of primary interest. In the application of Sewell's criterion to wood structures, it is assumed that a critical impulse must be imparted to the wood structure so that it will deflect beyond its yield point within one-quarter of its natural period.

To illustrate, a wood beam, simply supported and uniformly loaded will be considered; its natural frequency is

$$p = \Pi^2 \left(\frac{EI}{m\ell^4} \right)^{1/2} \text{ radians/second} \qquad (20)$$

where:

m = mass of the beam per unit length (usually lbs/in)

ℓ = length of the beam.

The quarter period, or critical period C_p, is given by

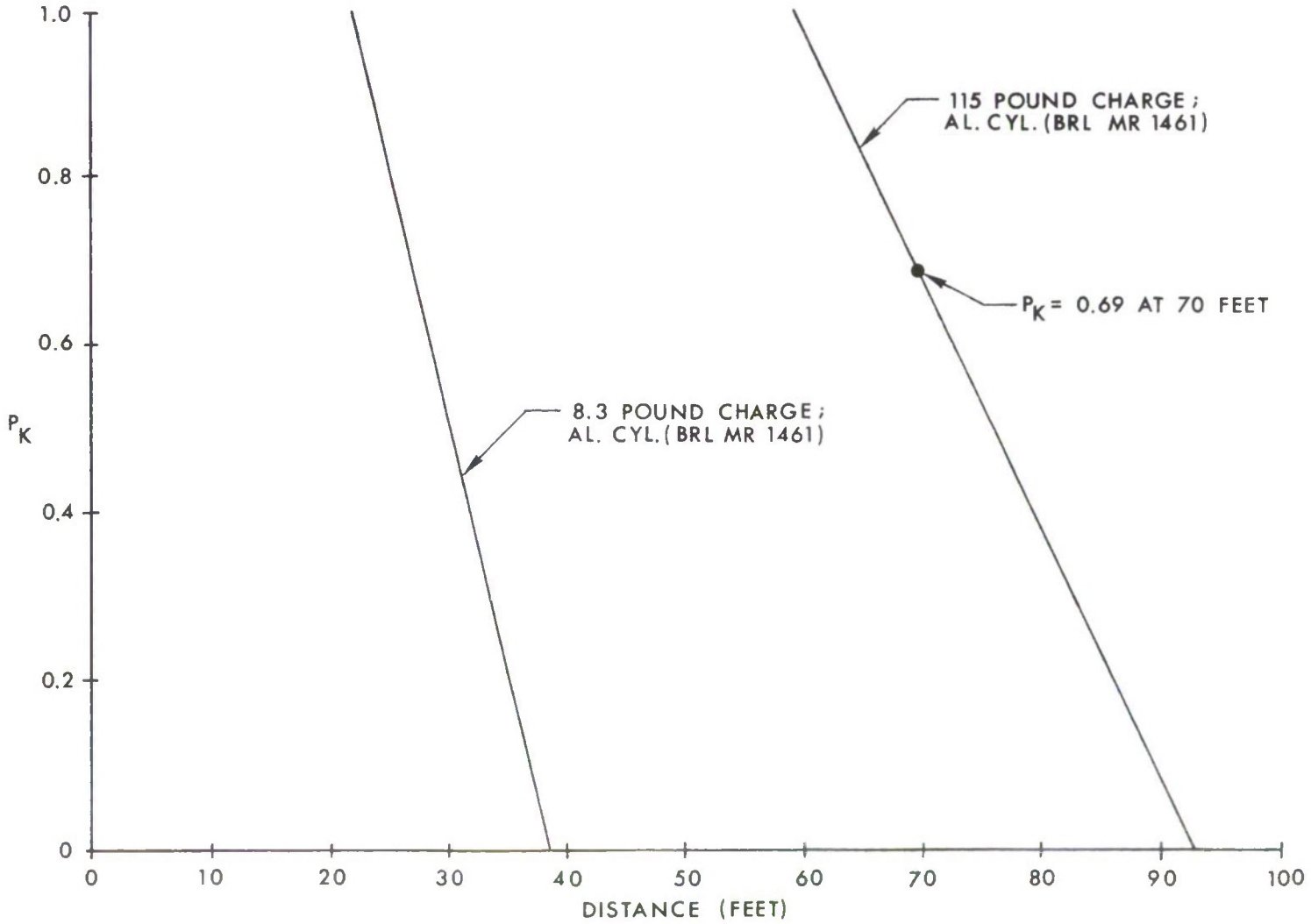

Figure 8. Probability of Damage Versus Distance for Aluminum Cylinders

$$C_p = \frac{1}{4} \cdot \frac{2\Pi}{p} \text{ seconds} \tag{21}$$

The critical impulse, I_c, which must be delivered to the beam is that impulse which deflects the uniformly loaded beam beyond its point of maximum elastic deflection within C_p seconds.

The calculation of the deflection of a loaded beam is based on the deflection of a loaded spring. The energy, U, stored in a deflected linear spring is

$$U = P \cdot \frac{\Delta}{2} \tag{22}$$

where P is the force required to cause the deflection Δ. In order to use equation (22) with a beam, an expression for Δ must be obtained. If the load function f(w) and sufficient boundry conditions are known, this can be obtained from a successive integration of

$$EI \frac{d^4\Delta}{dx^4} = f(w)$$

where:

Δ = deflection

x = distance along the beam.

If the shear V is known, Δ can be obtained from a triple integration of

$$EI \frac{d^3\Delta}{dx^3} = V .$$

In the most common situations (the analysis of a simply supported, uniformly loaded beam), the bending moment equation, M, can be easily written and Δ obtained from

$$EI \frac{d^2\Delta}{dx^2} = -M . \tag{23}$$

The equation thus obtained for Δ will involve a load, w. To find the maximum permissible value for w, w_o, a maximum tensile fiber stress, σ_{max}, is obtained and substituted in the equation

$$M_{max} = \frac{\sigma_{max} I}{C} \tag{24}$$

The M_{max} thus obtained is substituted for M in the bending moment equation along with an x that corresponds to the location along the beam of maximum moment. In the case of the uniformly loaded beam of length ℓ

$$M = \frac{\ell}{2} wx - \frac{wx^2}{2}$$

The maximum moment occurs when $x = \ell/2$, so that

$$M_{max} = \frac{\ell}{2} w \frac{\ell}{2} - \frac{w}{2} \frac{\ell^2}{4} = \frac{w\ell^2}{8}$$

$$w_o = \frac{8 M_{max}}{\ell^2} = \frac{8}{\ell^2} \cdot \frac{\sigma_{max} I}{C} \tag{25}$$

The internal energy, U, is determined by integration of equation (23) over the length of the beam, where

$$p = w_o \, dx \tag{26}$$

In this case, the following simple expression is obtained

$$U = \frac{w_o^2 \, \ell^5}{240EI} \tag{27}$$

The necessary unit impulse, I_c, to provide this required energy is then computed from

$$I = \frac{1000 \cdot (2Um)^{1/2}}{(\text{area of the beam } (in^2))} \text{ psi-msec} \tag{28}$$

Equation (28) assumes that the resisting forces developed during the application of the impulse are negligible.

E. ESTABLISHMENT OF QUANTITY-DISTANCE STORAGE REQUIREMENTS

As a final step in this study, analytical criteria have been formulated with which to determine minimum separation distances for all designated explosive quantities and types of civilian targets. Minimum distances have been established with respect to minimizing the risk that blast damage resulting from an explosive detonation will exceed a predetermined acceptable level. The incident overpressures and incident impulses associated with the derived distances have been presented, in part, in a method analogous to that formulated by O. T. Johnson [52], Ballistic Research Laboratories.

His empirical approach is based on the derivation of a relatively simple relationship which characterizes all combinations of explosive weights and charge-target separation distances which produce one identifiable damage level to a target. Specifically, if a charge of given size and separation distance produces a specific damage level such as window glass breakage, then all other combinations of charge size and separation distance which produce no more severe damage can be reasonably well approximated using his criterion.

Considering a broad range of explosive weights, Johnson notes that if a division between all plotted combinations of pressure and impulse values which cause less damage than an indicated level and those which cause excessive damage were made, then that division would be a hyperbolic function as illustrated in Figure 9. In this figure, the relative relationship of two different damage levels is indicated. This illustration could well indicate the relationship of, say, window glass breakage (Damage Level No. 1) to exterior wall frame cracking (Damage Level No. 2).

Johnson notes that for any designated damage level, combinations of P and I below the curve will cause less than the indicated damage, whereas values above it will cause excessive damage. The curve can be assumed to be hyperbolic and can be expressed as $(P - P_{critical})\ (I - I_{critical}) = C$, a parameter whose value depends on many conditions such as target characteristics, type and shape of the explosive charge, environment, etc. It is noted that as $(I - I_{critical})$ approaches infinity (i.e., as weight, W of the explosive increases) then damage is a function solely of overpressure and in this instance

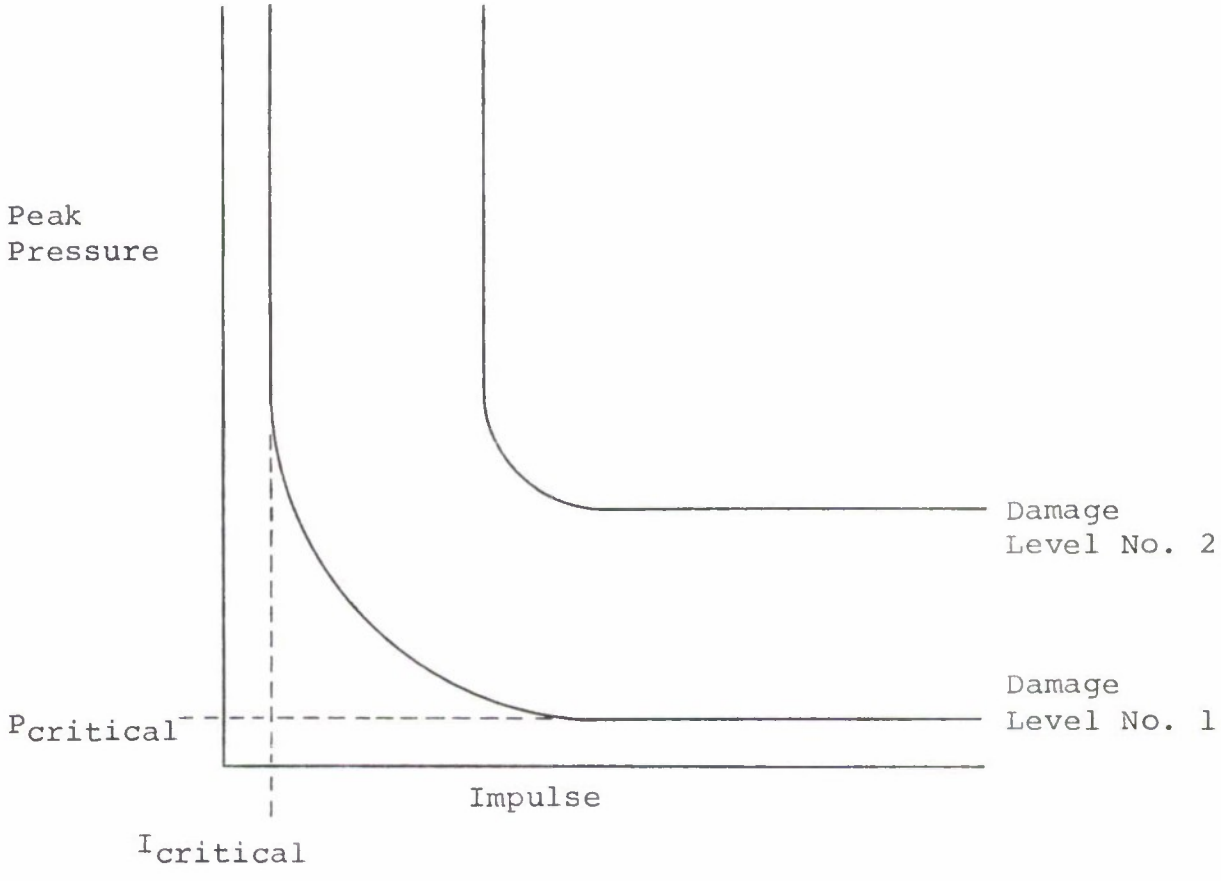

Figure 9. Pressure-Impulse Relationship

$P \rightarrow P_{critical}$. Conversely, if W decreases the damage relates with a critical value of impulse, $I_{critical}$. Since P and I can be uniquely determined from the parameters of explosive weight (W) and distance (R), one can resort to this relationship to determine explosive weight and distance for any arbitrary level of damage or response. Using a large body of experimental data Johnson concluded that for a number of basically different targets the ratio of the distance, R_{100}, needed to do damage for the selected weight, say 100 pounds, to the distance, R_W for some other explosive weight causing similar damage or response can be displayed parametrically, i.e.,

$$\frac{R_{100}}{R_W} \simeq C_W \ . \tag{29}$$

The value of the parameter C_W essentially is constant for a given weight of explosive.

A least square fit of the functional form $C_W = aW^b$, which becomes

$$C_W = 7.64W^{-.435} \tag{30}$$

was determined using the experimental data. The standard deviations for a and b in the above equation are 0.219 and 0.010 respectively.

In order to derive P-I curves, as shown in Figure 9, it is of course, necessary to determine at least one charge size and distance for which the blast forces cause the designated damage level to the target of interest. In the analysis of each target in this study, these distances for five charges, in the 1,000- to 9 million-pound range, were determined for each designated damage level. Because of ease and the desire for comparable values, the computer-programmed models for each target were used to generate the minimum separation distances for all five charges, for each designated damage level. This approach was taken instead of computing a specific separation distance for one charge and using equation (30) to derive the distances for the other charges. Comparisons between these two types of approaches are shown in the Results Section (V) of this report.

F. SHOCK WAVE PARAMETERS

The blast wave parameters resulting from detonation of an explosive charge of given size and orientation have been studied as a function of scaled charge-target separation distances by many agencies. These values are, of course, necessary in applications of any analytical approach to target response predictions. Probably the most extensive of these is the publication by the U. S. Naval Ordnance Laboratory [71]. Their charts and graphs display the properties of explosive material and detail the effects of their detonation in air, underwater, and on metal. In many cases, the data are given in nomograph form which allows effect predictions from the geometry, weight, and composition of the explosives.

C. Kingery [57], Ballistic Research Laboratories, has also summarized experimentally derived values for these parameters for a TNT surface burst (hemispherical charges) as shown in Figure 10. Through use of conversion factors, other types of explosives can be related to these parameter values. Values from these two sources were used in this study.

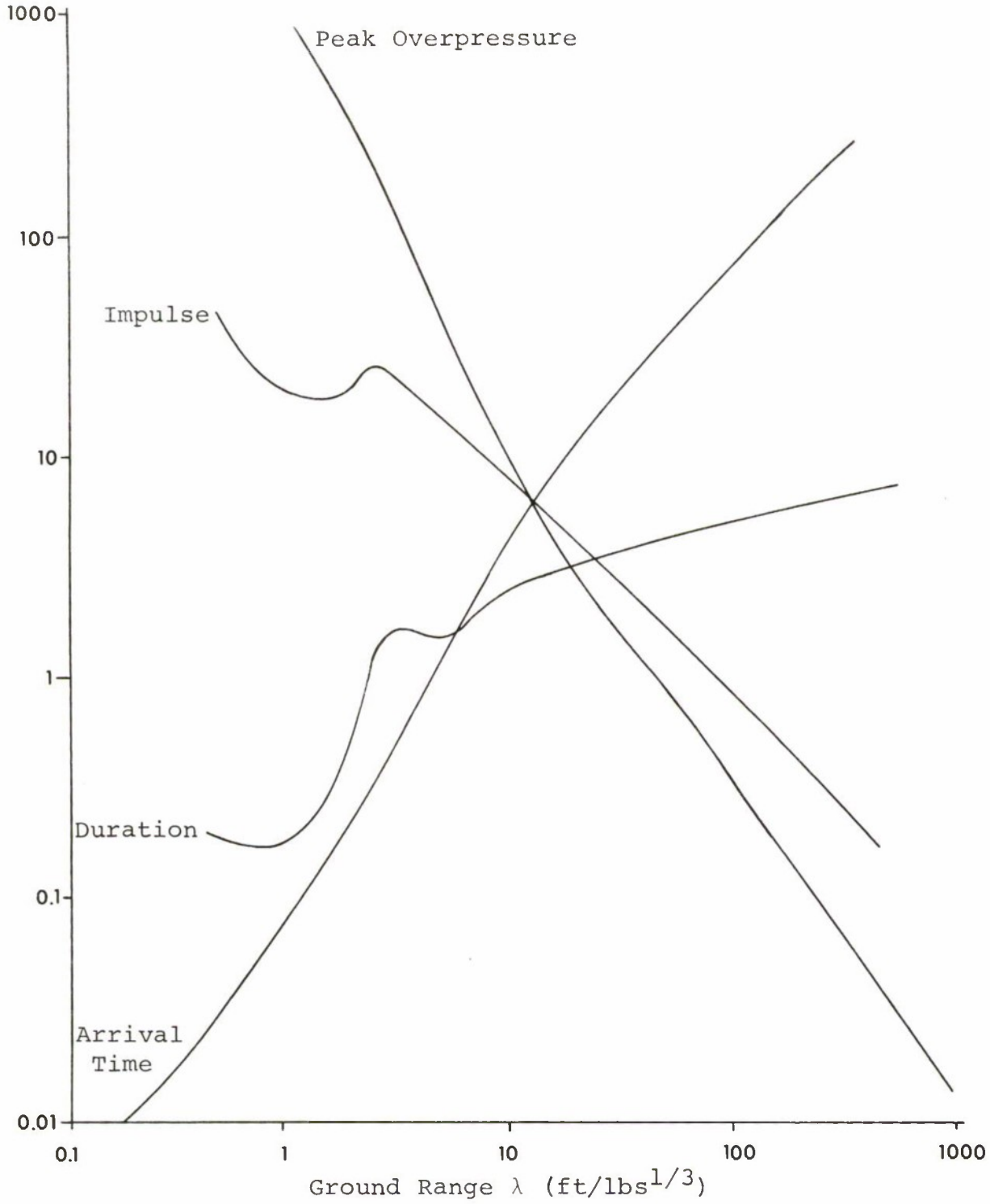

Figure 10. Blast Wave Parameters versus Scaled Distance for TNT Surface Burst (Hemispherical Charges)

IV. ANALYSIS

A. SPLIT-LEVEL HOUSE

The selected generic split-level house is considered to be constructed as shown in Figure 11. The house roof is composed of 2- by 8-inch Douglas fir rafters on 16-inch centers with a total length of 17 feet. The rafter lower ends are notched (8-inch overhang) and nailed to a double 2- by 8-inch plate bolted to the brick wall. Their upper ends are nailed to a 2- by 8-inch ridge board. They are covered with 4- by 8-foot sheets of 1/2-inch plywood, 30-pound tar paper, and 250-pound asphalt shingles. There are no collar beams or knee braces, or any sort of trusswork.

The brick wall is 8-inch solid brick with a common header band every sixth course. There is no reinforcing. There are several steel sash windows 6 feet 2 inches wide by 5 feet 4 inches high containing a 3- by 4-foot 2-inch piece of polished plate glass and 14 9-inch by 12-1/2-inch panes of single strength glass in most brick wall sections. However, there are also large sections of brick wall with no windows or other openings.

The frame wall consists of 8-inch bevel siding, 4- by 8-foot by 3/4-inch fiberboard sheeting, 2- by 4-inch by 7-foot 6-inch studs on 16-inch centers, and 1/2-inch plasterboard on the inside. There are 2-foot 8-inch by 4-foot 6-inch windows both singly and in pairs within an average section of frame wall, the distance between them being about 8 feet.

Three exterior surfaces are considered as possible vulnerable components in the blast damage assessment model for this house: the roof, a portion of the brick wall containing no openings, and the frame section containing window and door openings. For all of the components, the risk level, or unacceptable damage, is defined as structural collapse. Therefore, damage levels which structurally degrade each component but do not cause their structural collapse have been defined. For the roof and frame wall sections, this damage is regarded as the cracking, but not complete severence, of one or more of the main 2- by 8-inch rafters or 2- by 4-inch wall support members. For the brick wall, a deflection of

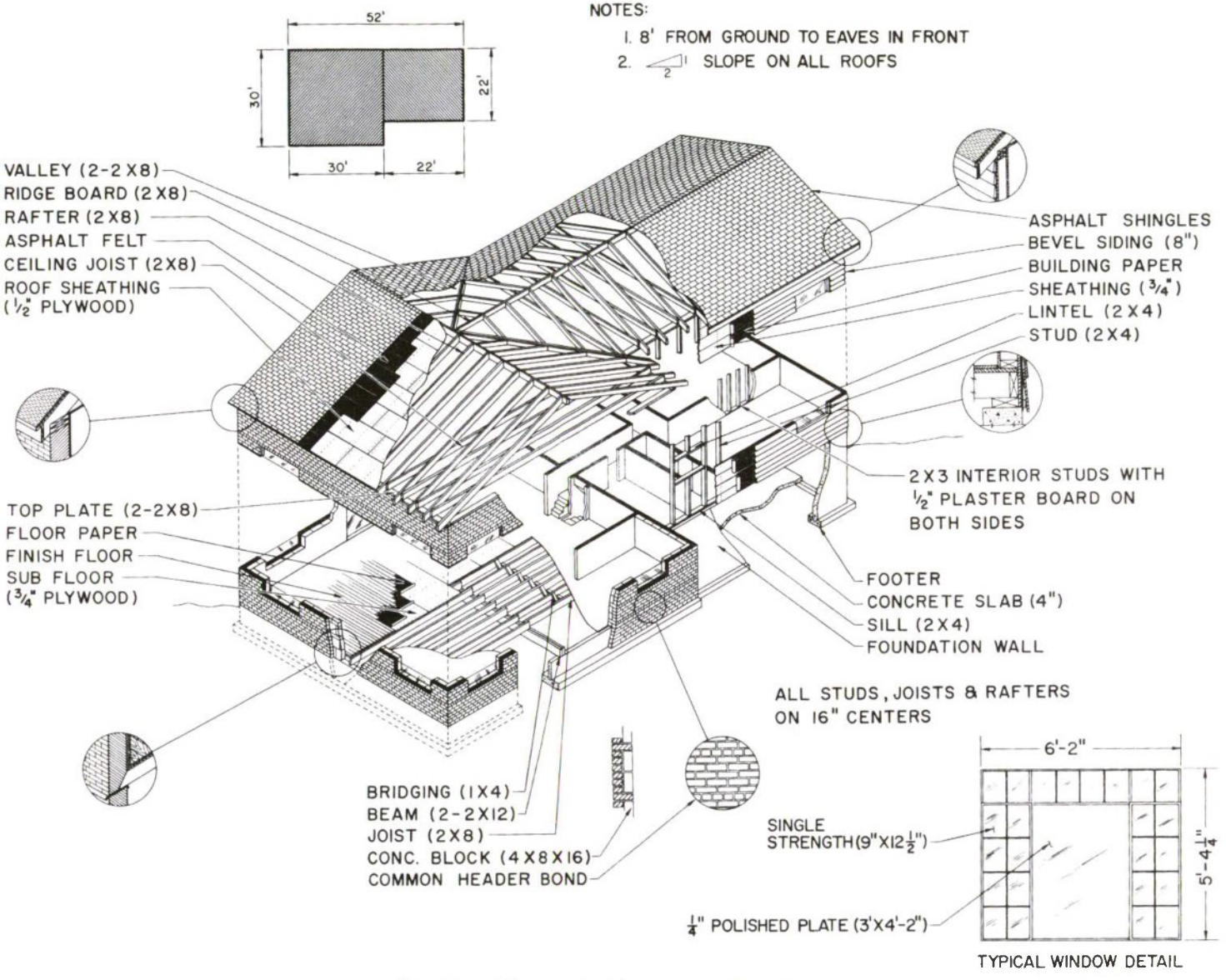

Figure 11. Split-Level House

approximately 5 inches at its center is considered sufficient to seriously damage the wall through extensive cracking, but not to cause partial or complete collapse.

In the computer-programmed methodology, the minimum distance for each specific charge size which relates to the first-to-occur of the above three criteria is determined. Then the required impulse and calculated impulse achieved at this specified distance is determined for all parameter variations considered for each of the other structural components, in order to insure that this truly is the minimum distance.

1. Analysis of the Roof Section

a. Calculation of Critical Period and Critical Impulse

A typical 17-foot long 2- by 8-inch roof rafter is analyzed as a uniformly loaded, simply supported beam, with a dead weight determined from its own weight and the weight of the 16-inch roof section it supports. Using equations (20) and (21), its critical period is computed from

$$C_p = \frac{1000}{4} \cdot \frac{2\Pi}{p} \text{ msec,}$$

where $$p = \Pi^2 \, (EIg/w\ell^4)^{1/2}$$

b. Strength Properties of Wood

The strength and elastic properties of Douglas fir vary, depending largely on the geographical location in which it was grown. Thus, in the above equation, the parameters E (Young's modulus) and w (the weight supported per inch of rafter) are known only within a range of values. Additionally, in the calculation of critical impulse using equations (24) through (28), σ_{max}, the modulus of rupture (defined for wood structures as the fiber stress at the proportional limit) must also be regarded as an indeterminate value.

In Reference 110 the strength properties of some important commercially available woods grown in the United States are given. An extract from that publication is given in Table III.

TABLE III. Strength and Elastic Properties of Douglas Fir Lumber

Type		σ_{max} Modulus of Rupture (psi)	E Modulus of Elasticity (psi x 10^6)
Coast:	Green	7,600	1.57
	Dried	12,200	1.95
Intermediate:	Green	6,800	1.35
	Dried	11,200	1.64
Rocky Mountain:			
	Green	6,400	1.18
	Dried	9,600	1.40

From large samples containing relatively clear test specimens of both green and dried wood, average values of $\sigma_{max} \cong 11{,}000$ psi and $E \cong 1.3 \times 10^6$ psi were obtained. The range of representative roof weights (including the rafter) is estimated to be from 8 to 10 lbs/ft^2 or from 10.64 to 13.30 lbs per lineal foot of rafter. Based on these values, three values of each unknown parameter were considered in the computer model and the critical period and critical impulse calculated for each set. The selected values and computed C_p and I_c appear in Table IV.

It is seen in Table IV that for the parameter values considered most typical (i.e., E = 1.3 million psi, W = 11.97 lbs per foot of roof section, and σ_{max} = 11,000 psi), a critical impulse of 42.71 psi-msec must be delivered within 39.14 msec.

c. Blast Loading Models

Several widely used models for calculating the blast loading on different types of simple structures involve the net loading concept [96]. For a closed rectangular structure, for

TABLE IV. Critical Period and Critical Impulse for House Roof

E (psi x 10^6)	Weight, w (lbs/ft)	σ_{max} (psi x 10^3)	Critical Period, C_p (msec)	Critical Impulse, I_c (psi-msec)
1.1	10.64	9.5	40.12	37.80
1.1	10.64	10.0	40.12	39.79
1.1	10.64	11.0	40.12	43.77
1.1	11.97	9.5	42.55	40.10
1.1	11.97	10.0	42.55	42.21
1.1	11.97	11.0	42.55	46.43
1.1	13.30	9.5	44.85	42.27
1.1	13.30	10.0	44.85	44.49
1.1	13.30	11.0	44.85	48.94
1.3	10.64	9.5	36.90	34.77
1.3	10.64	10.0	36.90	36.60
1.3	10.64	11.0	36.90	40.27
1.3	11.97	9.5	39.14	36.88
1.3	11.97	10.0	39.14	38.83
1.3	11.97	11.0	39.14	42.71*
1.3	13.30	9.5	41.26	38.88
1.3	13.30	10.0	41.26	40.93
1.3	13.30	11.0	41.26	45.02
1.5	10.64	9.5	34.35	32.37
1.5	10.64	10.0	34.35	34.08
1.5	10.64	11.0	34.35	37.09
1.5	11.97	9.5	36.44	34.34
1.5	11.97	10.0	36.44	36.14
1.5	11.97	11.0	36.44	39.76
1.5	13.30	9.5	38.41	36.19
1.5	13.30	10.0	38.41	38.10
1.5	13.30	11.0	38.41	41.91

*Representative case.

example, the loadings on the front and back surfaces are determined, and, if desired, that portion of the back face loading which occurs during the positive duration of the shock wave (as measured at the front face) is subtracted to yield the net loading on the structure.

A closed rectangular structure may be represented by a parallelepiped having length L, height H, and width WD. The maximum blast loading resulting from a normally impinging shock wave striking the flat surface is that exerted by the reflected pressure. The peak reflected pressure P_r, occurring at time t = 0, is given by

$$P_r = 2P_o\left[\frac{7P_{amb}+4P_o}{7P_{amb}+P_o}\right] , \qquad (31)$$

where:

P_o = peak incident overpressure

P_{amb} = ambient air pressure (14.7 psi at sea level).

(1) Loading on the Front Surface. The front surface loading by a normally impinging shock wave can be considered to occur in two phases. The first results in the "diffraction loading" wherein the peak overpressure of the reflected wave predominates. During this phase the reflected pressure will decrease from its peak value, P_r, essentially linearly until the stagnation pressure is attained. The time to decay to stagnation pressure, t_s, can be approximated by

$$t_s = 1000 \cdot \left(\frac{3S}{V}\right) , \text{ msec} \qquad (32)$$

where:

S = the smaller target dimension of H or WD/2

V = the shock front velocity.

The second or "dynamic loading" phase occurs after the overpressure attains its stagnation pressure value. In this latter phase, the dynamic pressure on the target surface is a significant factor. The drag coefficient on the front face

is unity; thus, the drag pressure during the second phase is equal to the dynamic pressure. Therefore, the stagnation pressure P_s is

$$P_s = p_o(t_s) + q(t_s) \ , \tag{33}$$

where $p_o(t_s)$ and $q(t_s)$ are the incident overpressure and dynamic pressure function, respectively, evaluated at time t_s.

The incident overpressure function $p_o(t)$ is assumed to obey the exponential form, so that

$$p_o(t) = P_o \left(1 - \frac{t}{\tau}\right) e^{-\frac{t}{\tau}} \tag{34}$$

where τ is the positive duration of the shock wave. The dynamic pressure function is also exponential in form,

$$q(t) = Q \left[1 - \frac{t}{\tau}\right]^2 e^{-\frac{2t}{\tau}} \tag{35}$$

where Q is the peak dynamic pressure derived from $Q = 2.5 [P_o^2/4P_{amb}+P_o]$.

The general pressure-time variation function pertaining to the front face, p(t), can be expressed as

$$p(t) = P_r - \left[\frac{P_r - P_s}{t_s}\right] t, \text{ for } 0 \leq t \leq t_s,$$

$$p(t) = P_o \left[1 - \frac{t}{\tau_F}\right] e^{-\frac{t}{\tau_F}} + \tag{36}$$

$$Q \left[1 - \frac{t}{\tau_F}\right]^2 e^{-\frac{2t}{\tau_F}}, \text{ for } t_s \leq t \leq \tau_F,$$

where τ_F is the positive duration of the shock wave (as measured at the front face).

(2) Loading on a Top Surface. Blast loading on the top surface commences immediately after the blast wave strikes the front face; however, the average pressure on this surface

rises linearly to a maximum at time t = L/V msec. The maximum average pressure, P_a, occurring at this time is determined as

$$P_a = p\left(\frac{L}{2V}\right) + C_d\, q\left(\frac{L}{2V}\right)$$

$$= P_o\left[1 - \frac{t}{\tau}\right] e^{-\frac{t}{\tau}} + \tag{37}$$

$$C_d\, Q\left[1 - \frac{t}{\tau}\right]^2 e^{-\frac{2t}{\tau}},$$

$$t = L/2V \text{ msec},$$

where C_d is the drag coefficient (see [80, p. 184] for appropriate value).

The average pressure decays exponentially from t = 2/LV to $t = \tau + L/2V$ msec, as

$$p(t) = p_o\left(t - \frac{L}{V}\right) + C_d\, q\left(t - \frac{L}{2V}\right), \tag{38}$$

$$\frac{L}{V} \leq t \leq \tau + \frac{L}{2V}.$$

(3) Loading on the Rear Face. The pressure loading on the back face of the structural member is also determined in discrete time phases. The shock front requires a time L/V msec to arrive at the back face. During the subsequent time interval, the pressure on the back face increases linearly from zero to a maximum value P_b, at time t = (L+4S)/V msec, where S is as previously defined. The overpressure then decays exponentially with a time delay of L/V msec, so that the pressure-time variation on the back face after stagnation may be expressed as

$$p(t') = p_o(t') + q(t')$$

$$= P_o \left[1 - \frac{t'}{\tau_B}\right] e^{-\frac{t'}{\tau_B}} +$$

$$C_D\, Q \left[1 - \frac{t'}{\tau_B}\right]^2 e^{-\frac{2t'}{\tau_B}}$$

$$\text{for } t' = t - \frac{L}{V}, \quad \frac{L+4S}{V} \leq t \leq \tau_B + \frac{L}{V} \tag{39}$$

where τ_B is the positive duration as measured on the back surface.

The pressure-time variations on both the front and rear faces are graphically illustrated in Figure 12. The net pressure loading function $P_n(t)$, $0 \leq t \leq \tau_B + L/V$, is then determined as the difference between front and rear surface loadings. This result is illustrated in Figure 13. Such net loading models are useful in describing the net blast loading on wall sections as well as larger rectangular structures. If, of course, the net loading concept is not desired, then the independent loading and corresponding impulses on all faces can be obtained.

d. Nonnormal Angles of Incidence

The blast loading model for the house roof must indicate the nonnormal angle of incidence of the roof; thus, some modification to the top surface loading model must be made before it is applied. The peak reflected pressure for nonnormal surfaces may be calculated as a function of the incident overpressure from information supplied by the Defense Atomic Support Agency, shown in Figure 14. The values shown in this figure, for the lower range incident overpressures, indicate appreciably different reflected overpressures for the house roof than would be calculated using equation (31).

In a series of blast loading studies conducted by M. L. Merritt [66], the efficiency of coupling between the blast wave and structure surfaces oriented at nonnormal incident angles was examined. His studies were conducted with a large structure, with gage readings taken at numerous locations on the front, top, and rear surfaces. Eight tests were conducted with TNT

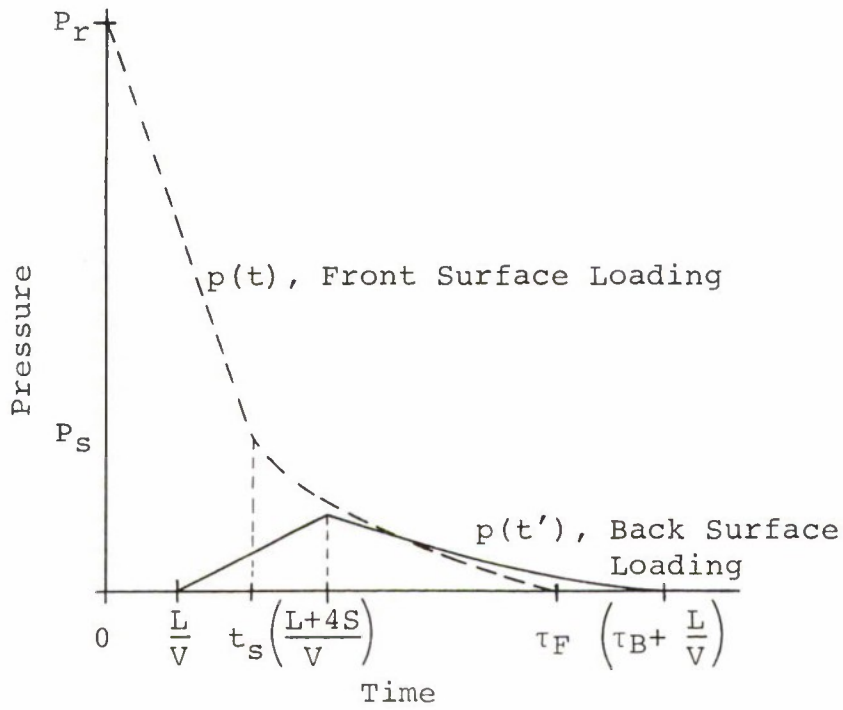

Figure 12. Pressure-Time Variations on Front and Rear Surfaces

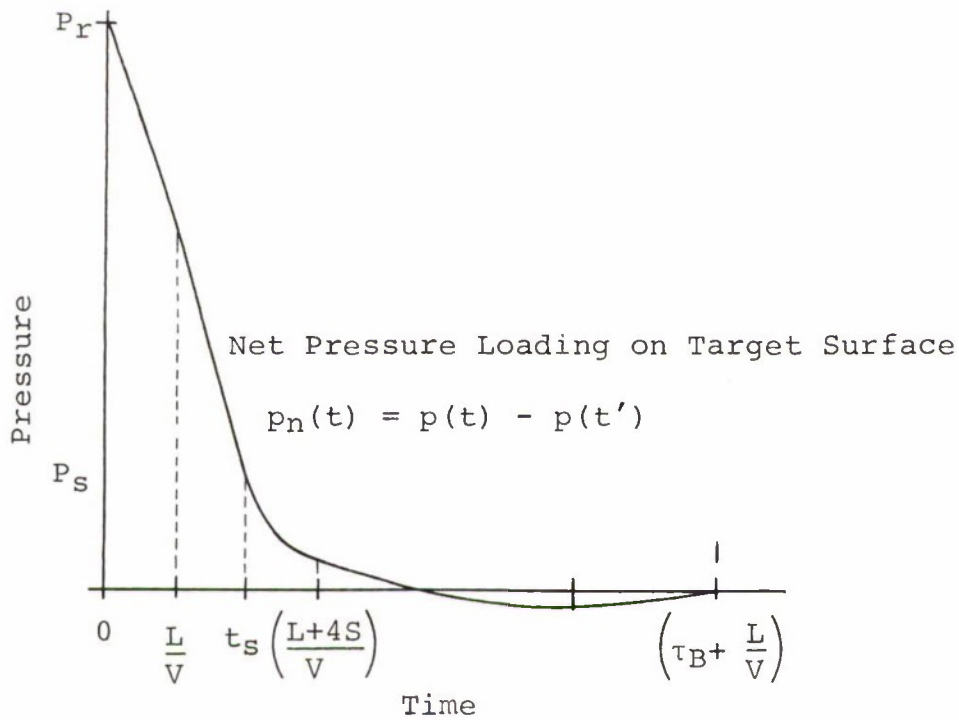

Figure 13. Net Pressure Loading Function.

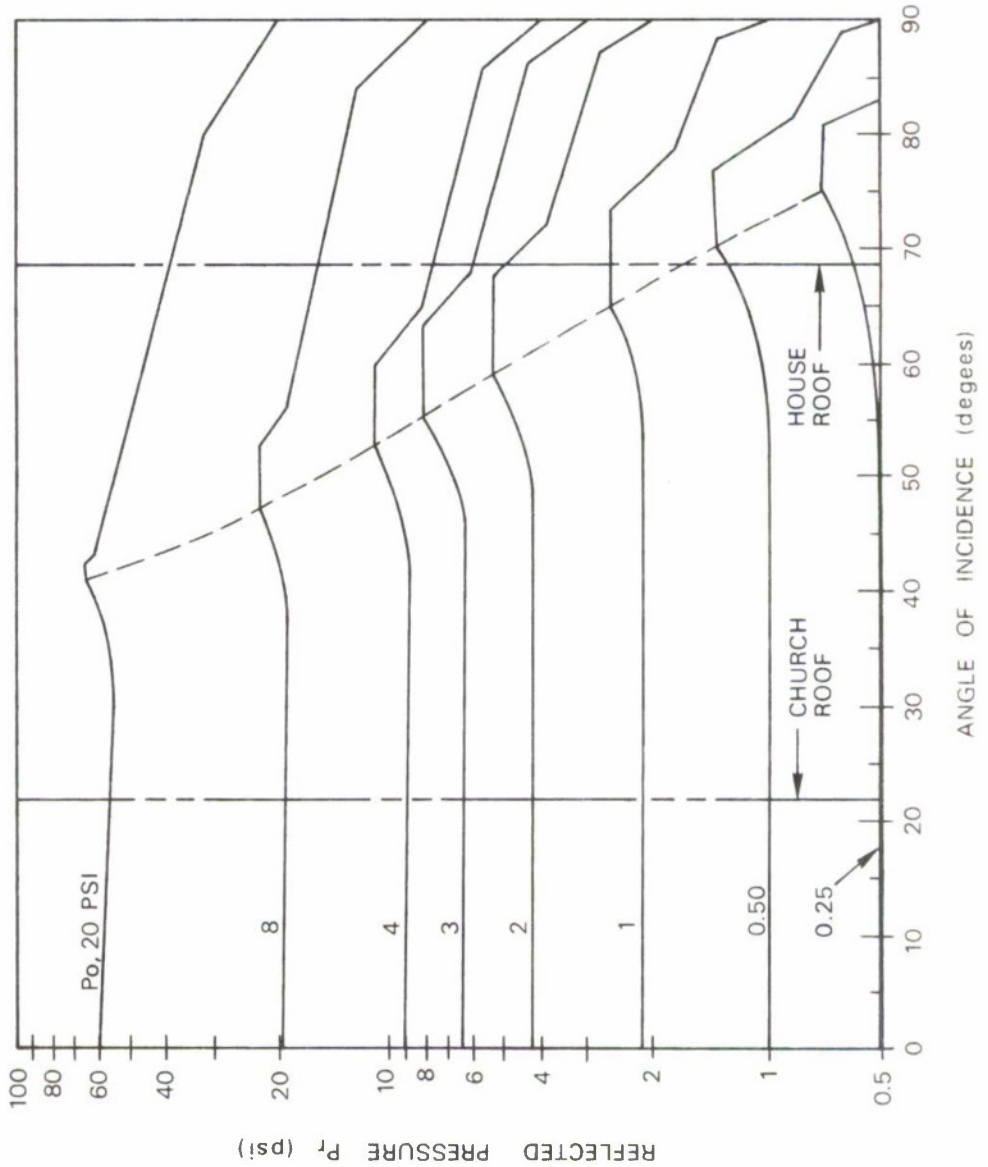

Figure 14. Peak Reflected Overpressures for Different Surface Orientations

charges having weights ranging between 50 and 8,960 pounds, which resulted in about 20 records of the pressure variation with time at different points on the surface. Using his data, it can be concluded that the average reflected overpressure on a surface oriented between 50 and 80 degrees from the normal can be approximated reasonably well with equation (37), provided the peak incident overpressure P_o is replaced with the peak reflected pressure P_r obtained from Figure 14. To illustrate, with a test using 3,200 pounds of TNT and an orientation angle of 60 degrees from the normal, a maximum average pressure of 6.1 psi at a time of 3 msec was measured on the surface, for the 3 psi incident overpressure wave in Merritt's study. Using the data from Figure 14, a reflected overpressure of 7.8 psi is obtained and when used in equation (37), the predicted maximum average overpressure of 6.5 psi is obtained. In light of the close agreement, this method of approximation was used in the treatment of nonnormal incident surfaces.

e. Computed Impulse

The top surface blast loading model was used with the modifications mentioned to determine a minimum separation distance for the house roof for each charge size and combination of parameter values described above. At each of these specified distances, similar calculations were made of the reflected impulse imparted to the house brick wall and the frame portion. Comparative values are discussed following a presentation of the analysis of the frame section and brick wall.

2. Analysis of the Frame Wall Section

a. Calculation of Critical Period and Critical Impulse

The typical 2- by 4-inch Douglas fir wall support member is analyzed as a uniformly loaded, simply supported beam. Its dead weight is determined from its own and the weight of the 16-inch section of plasterboard--fiberboard sheeting--wood siding wall it supports. In the formulation of its critical period and impulse, values of E, w, and σ_{max} are considered in the ranges of 1.3 to 1.5 x 10^6 psi, 18.30 to 20.00 lbs/ft of wall, and 10,000 to 11,000 psi, respectively. The calculated stud, critical periods and critical impulses for the resulting sets of parameter values are presented in Table V.

TABLE V. Critical Period and Critical Impulse Values for Frame Wall

E ($psix10^6$)	Weight, w (lbs/ft)	σ_{max} ($psix10^3$)	Critical Period (msec)	Critical Impulse (psi-msec)
1.30	18.30	10.0	27.02	34.86
1.30	18.30	11.0	27.02	38.34
1.30	20.00	10.0	28.25	36.44
1.30	20.00	11.0	28.25	40.09
1.50	18.30	10.0	25.16	32.45
1.50	18.30	11.0	25.16	35.70
1.50	20.00	10.0	26.30	33.93
1.50	20.00	11.0	26.30	37.32

b. Blast Loading Model

In determining the net blast loading on the frame wall, the loading on the outside wall is computed using equations (31) through (36) with the exception that S is replaced with S′ in equation (32). The quantity S′ is the average distance (for the entire front face) from the center of the wall section to the edge of an opening. It represents the average distance which rarefaction waves must travel over the front face to reduce the reflected pressures to the stagnation pressure. S′ is taken as 3.2 feet in this case. The overpressure on the inside of the front face starts rising at impact because the blast wave immediately enters through openings. It is assumed to rise linearly until a maximum average pressure, P_b, is reached at time t = 2L/V msec. Further, the dynamic overpressure is assumed to be negligible on the interior of the structure. Therefore, P_b is determined as

$$P_b = P_o \left(1 - \frac{t}{\tau}\right) e^{-\frac{t}{\tau}} \text{, for } t = \frac{2L}{V} \text{ msec.} \qquad (40)$$

The average overpressure function is assumed to decay exponentially after reaching P_b so that

$$p(t) = P_o \left(1 - \frac{t}{\tau}\right) e^{-\frac{t}{\tau}} \text{, for } \frac{2L}{V} \leq t < \tau \text{ .} \qquad (41)$$

These two functions are integrated from time = 0 to the critical period and this impulse is subtracted from that calculated on the front face of the wall in order to assess the net reflected impulse imparted to the frame wall within the critical period.

3. Analysis of the Brick Wall Section

The resistance functions and the unit impulse required to severely crack the brick wall are computed using equations (1) through (9). For a simply supported 8-inch thick brick wall, a steady pressure of approximately 0.5 psi is required to cause tensile bond failure in the mortar; thus, in this analysis, a requirement for an average reflected overpressure of at least 0.5 psi throughout a time interval equal to its calculated critical period is stipulated. It is further assumed that when the overpressure decays to a low level, the latter part of the decay process is of little consequence to the effective impulse imparted to the target. URS Corporation [109] indicate that this value of overpressure is probably in the range of 0.1 to 0.3 psi. As a consequence, the calculation of reflected impulse on brick walls is determined in the study by integrating the overpressure function from time t = 0 to a time at which the overpressure function decreases to 0.1 psi.

a. Calculations of Critical Period and Critical Impulse

A 1-inch wide column of wall may be analyzed as a uniformly loaded beam so that its critical period is given by equation (21). Two values of E were considered, 1.3 and 1.5 million psi, whereas the tensile bond failure stresses treated were 50 and 70 psi. The weight of a brick wall is usually taken as 120 lbs/ft^3. Using these parameter variations, the following critical periods were established for the 8-foot high brick wall: for $E = 1.3 \times 10^6$ psi, $C_p = 6.19$ msec; for $E = 1.5 \times 10^6$ psi, $C_p = 5.76$ msec.

b. Blast Loading Model

The blast loading on the house brick wall is modeled by equations (31) to (36) which reflect no openings in a perpendicular wall. Critical impulse requirements for the wall vary with

the assumed tensile bond failure stress and the value of P_v used in equations (2) through (5). P_v includes the blast loading forces on the roof which, of course, change with variations in separation distances. Assuming that the house brick wall supports one-half of the blast loading imparted to the front half of the roof, the blast loading on the 1-inch brick column may be calculated using the maximum average pressure on the roof, P_a (see equation (37)). P_v is then derived as the sum of one-half of the contribution of P_a to the brick beam and the roof weight it supports.

In the computer program output, a unit impulse for the brick wall, based on the blast loading on the roof for each given charge and separation distance, is indicated for each set of parameter variations considered for the brick wall.

4. Sample Set of Computed Values

The computer output for the house analysis is arranged so that the computed critical periods and impulses are printed for the house roof (Table IV), the frame section (Table V), and the brick wall section, in sequential order. Then, for each set of parameter variations for the house roof, the five charge sizes are considered in order to determine a minimum separation distance for each, with respect to the roof. As each of these values is determined, the incident overpressure, peak reflected pressure and positive duration of the charge is noted and a probabilistic statement concerning the likelihood of glass fragment injury to occupants, is made. The other two house components are then considered at this distance. The required, or critical, impulse and the reflected impulse achieved at this distance are printed for every set of values considered for these two components. Table VI displays a typical printout for a set of representative parameters of the house roof and a charge size of 10,000 pounds.

Table VI indicates that at the minimum separation distance of 289.9 feet for the 10,000-pound charge, the calculated reflected impulses on the frame portion and the brick wall of the house at this distance are far less than the necessary critical impulse values computed for the different sets of parameter variations considered. The eight sets of comparative values given for the frame section above, relate to the eight sets of parameter values given in Table V.

TABLE VI. Computed Output for One Set of House Roof Parameters

MINIMUM DISTANCE FOR E = 1,300,000 psi; WEIGHT = 11.97 lbs/ft of roof; Mod of Rupture = 11,000 psi
CHARGE WEIGHT = 10,000 lbs; SEPARATION DISTANCE = 289.9 ft
INCIDENT OVERPRESSURE = 1.79 psi; PK. REF. OVERPRESSURE = 3.76 psi; DURATION = 39.4 msec

HOUSE FRAME SECTION:
Probability of Glass Fragment Injury:
For P_o = 1.79 psi, Probability of Serious Wounds = 0.

REQUIRED AND CALCULATED IMPULSES:

REQUIRED IMPULSE (psi-ms) =	CALCULATED IMPULSE (psi-ms) =
34.86	18.50
38.34	18.50
36.44	18.54
40.09	18.54
32.45	18.43
35.70	18.43
33.93	18.47
37.32	18.47

House Brick Wall:
Required and Calculated Impulses:

Required Impulse (psi-ms) =	Calculated Impulse (psi-ms) =
128.79	43.44
128.94	43.44
128.76	43.44
128.89	43.44

House roof damage was the first to occur in the 1,000 to 100,000-pound charge sizes; however, brick wall damage occurs first with the larger, longer duration charges. The minimum quantity-distance criterion is established for the house target with respect to both types of damage. Plots of the pressure-impulse relationship for the five charge sizes are presented in the Results section, along with plots of the separation distances resulting from the variation-of-parameters method of analysis.

5. Prairie Flat Frame House Test

A comparison of the predicted results using the house model described above can be made using experimental results obtained from the Prairie Flat Test [33]. A two-story frame house 33 feet 4 inches long by 24 feet 8 inches wide with a roof constructed from similar materials, but using 2- by 6-inch rafters, and having the same roof angle of inclination was used in this test. It was exposed to the blast overpressures from a one million-pound TNT detonation at 4,000 feet distance. The front of the house contained four large windows, one small window, and one door. Two of the large windows contained two large panes each of 3/32-inch thick glass, and had no mullions. The most serious damage observed in this test was the cracking of 19 of the 26 wood 2- by 6-inch wood rafter members. Plaster cracks were found throughout the house; especially predominant were shear cracks on the side near the windows, but, for the most part, these were minor. The front door and one bathroom door were torn from their hinges and two other door latches were torn out, but these doors stayed on their hinges. Based on these observations, it was concluded that the damage done to this house represents the threshold damage for which the minimum separation distance criterion can be derived.

The 2- by 6-inch rafter members in this house are also Douglas fir; thus, the same range of strength properties apply as is shown in Table IV. Using these values and the model for blast loading on the roof described above, a range of minimum separation distances between 3,400 and 4,500 feet is predicted. The close agreement in these observed and predicted results lends credence to the use of a "critical impulse within a critical period" criterion.

B. A-FRAME CHURCH BUILDING

The church roof is supported by laminated Douglas fir wood beams 7.6 inches by 16 inches by 39 feet long spaced on 15-foot centers. They are bolted to a matching beam at the top and are securely bolted to a concrete footing at the bottom. Both ends are considered simply supported and the effects of support at the junction of the sidewall are assumed to be negligible. The upper 32-foot beam section supports the decking while the lower 7-foot section supports no loading.

The 4-inch thick, 8-inch wide double tongue and groove decking is random length end-matched. For this analysis it was considered to be simply supported on 15-foot centers rather than run continuous across the beams. The decking is covered with asphalt roofing and has a total combined weight of 13 lb/ft. There is no additional insulation or inside finish.

Excluding the windows, the large (90-foot long) roof is considered the only vulnerable component of this church. The risk level or unacceptable damage is again defined as structural collapse of the roof. Of concern, then, is whether the laminated beams crack prior to failure of the decking members.

1. Analysis of the Laminated Beams

The 39-foot laminated beam and the section of roof it supports was analyzed as a step-wise uniformly loaded, simply supported beam with a dead load determined from its weight and that of the 15-foot wide section of decking and roofing materials. Parametric values considered for Young's modulus, the weight supported per foot of beam, and the modulus of rupture are presented in Table VII along with the calculated critical period and impulse values. Equations (22) through (28) are used in the derivation of impulse values.

a. Blast Loading Model

The church roof has an angle of inclination of approximately 23 degrees from the vertical; the peak reflected pressures for this angle are seen from Figure 14 to be very nearly equal to these values calculated from equation (31). Using the calculated value of P_r, the average blast loading as a

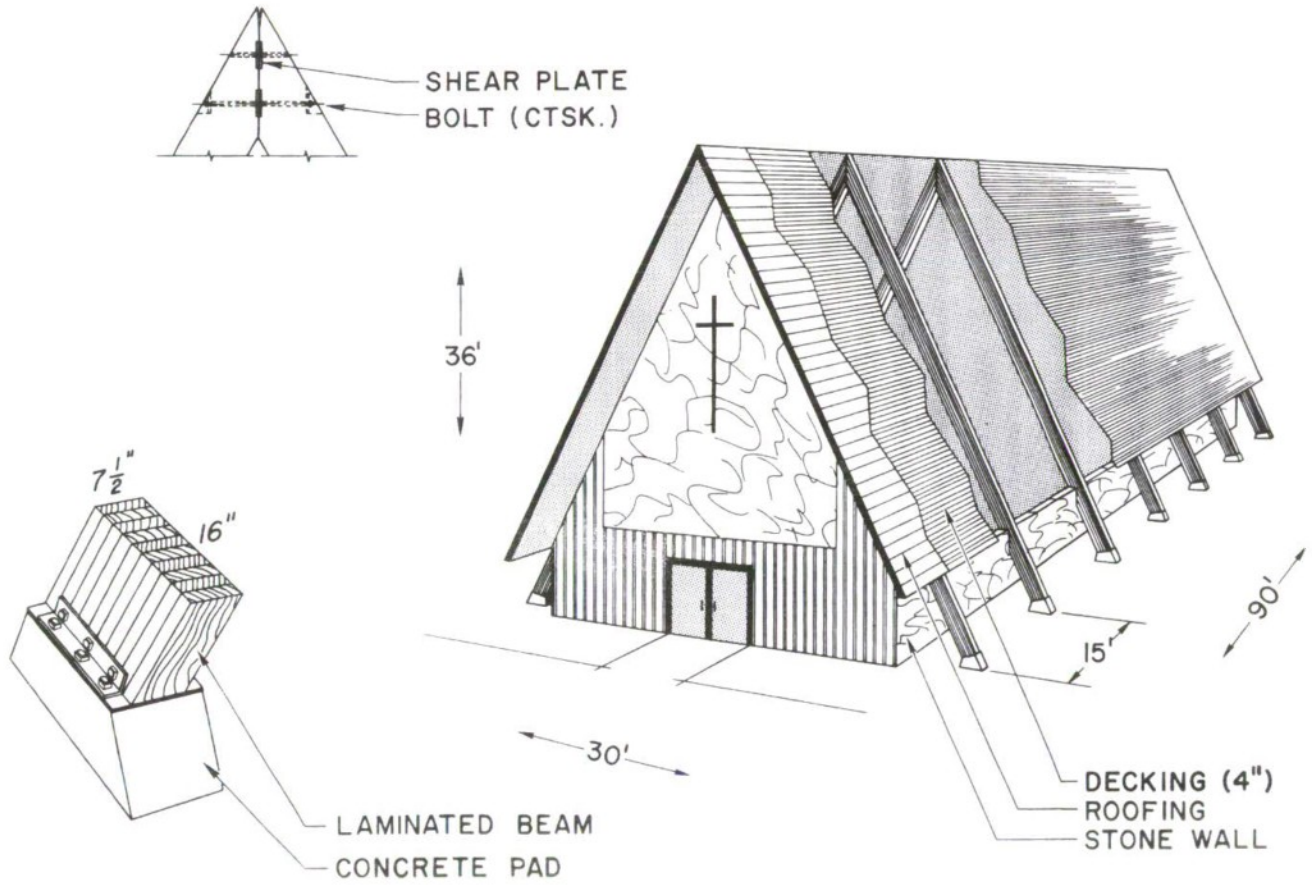

Figure 15. Typical Modern Church

TABLE VII. Critical Period and Critical Impulse for Church Beams

E ($psix10^6$)	Weight, w (lbs/ft)	σ_{max} ($psix10^3$)	Critical Period (msec)	Critical Impulse (psi-ms)
1.1	200.00	9.5	117.62	44.37
1.1	200.00	11.0	117.62	51.37
1.1	200.00	12.0	117.62	56.04
1.1	215.00	9.5	121.95	45.97
1.1	215.00	11.0	121.95	53.22
1.1	215.00	12.0	121.95	58.06
1.1	230.00	9.5	126.13	47.51
1.1	230.00	11.0	126.13	55.01
1.1	230.00	12.0	126.13	60.02
1.3	200.00	9.5	108.19	40.81
1.3	200.00	11.0	108.19	47.26
1.3	200.00	12.0	108.19	51.11
1.3	215.00	9.5	112.18	42.28
1.3	215.00	11.0	112.18	48.96
1.3	215.00	12.0	112.18	53.41
1.3	230.00	9.5	116.02	43.70
1.3	230.00	11.0	116.02	50.61
1.3	230.00	12.0	116.02	55.21
1.5	200.00	9.5	100.72	37.99
1.5	200.00	11.0	100.72	43.99
1.5	200.00	12.0	100.72	47.99
1.5	215.00	9.5	104.43	39.36
1.5	215.00	11.0	104.43	45.58
1.5	215.00	12.0	104.43	49.72
1.5	230.00	9.5	108.01	40.69
1.5	230.00	11.0	108.01	47.11
1.5	230.00	12.0	108.01	51.39

function of time can be calculated in the same manner as was used with the house roof (with equations (37) and (38)). In comparing the house roof and the church roof (Tables IV and VII), it is seen that the critical periods for the church beams are much longer, yet their critical impulse values are not much greater. Thus, with a much longer time to receive a relatively equal critical impulse, the church beam is a much more vulnerable structural component.

2. Analysis of the Church Decking

a. Calculation of Critical Period and Critical Impulse

The 4-inch thick, 8-inch wide, 15-foot long decking members are also laminated Douglas fir and therefore have similar strength properties to the wood members previously discussed. A typical decking member is also analyzed as a uniformly loaded beam. The parameter values considered and the critical period and impulse values calculated are shown in Table VIII.

TABLE VIII. Critical Period and Critical Impulse for Church Decking

E ($psix10^6$)	Weight, w (lbs/ft)	σ_{max} ($psix10^4$)	Critical Period (msec)	Critical Impulse (psi-ms)
1.3	13.00	1.1	32.22	114.28
1.3	13.00	1.2	32.22	124.66
1.3	13.33	1.1	32.63	115.74
1.3	13.33	1.2	32.63	126.23
1.5	13.00	1.1	29.99	106.39
1.5	13.00	1.2	29.99	116.05
1.5	13.33	1.1	30.38	107.77
1.5	13.33	1.2	30.38	117.54

b. Blast Loading Model

It was indicated previously that the peak reflected pressure on the roof may be computed from equation (31), even though it has a nonnormal angle of inclination. The

blast loading model on a perpendicular surface utilizes equations (32) through (36) with no back pressure on the interior side of the decking.

c. Comparative Results

In all cases, the church laminated beams were assessed to crack prior to failing of the roof decking. The calculated minimum separation distance for church roof beam for the 10,000-pound charge is 1,184.9 feet, when the representative set of parameters $E = 1.3 \times 10^6$ lbs/in^2, $w = 215.0$ lbs/ft of beam and $\sigma_{max} = 11{,}000$ lbs/in^2 is used. The calculated reflected impulse on a typical decking member at this distance is approximately 33 psi-ms, which is far less than the required impulses for any of the sets of parameter values given in Table VIII. Plots of the pressure-impulse relationships related to church beam failure for the five charges are given in the Results section.

C. FLAT ROOF SCHOOL BUILDING

The roof of the elementary school is supported on 3- by 14-inch by 28-foot long Douglas fir beams on 2-foot centers. These are toenailed at each end to 2- by 8-inch top plates securely bolted to the top of the 10.5-foot stone walls. The roofing is of built-up tar and gravel construction placed on top of 1-inch structural insulating board. A light tile ceiling is placed directly on the bottom of the rafters. The total roof weight is approximately 20 lbs/ft^2 (including beams).

The end wall is 8 inches thick with stone mortared together with no reinforcing. It is 10 feet 6 inches high and contains no windows. It has the same simple support conditions as the house brick wall.

The windows in the front wall vary somewhat in size, the maximum being approximately 3 feet 6 inches by 5 feet. All windows are 1/4-inch plate glass supported by aluminum frames.

The school roof and stone wall are the most likely structural components to collapse under a given blast loading. The windows, of course, will fracture and present an appreciable

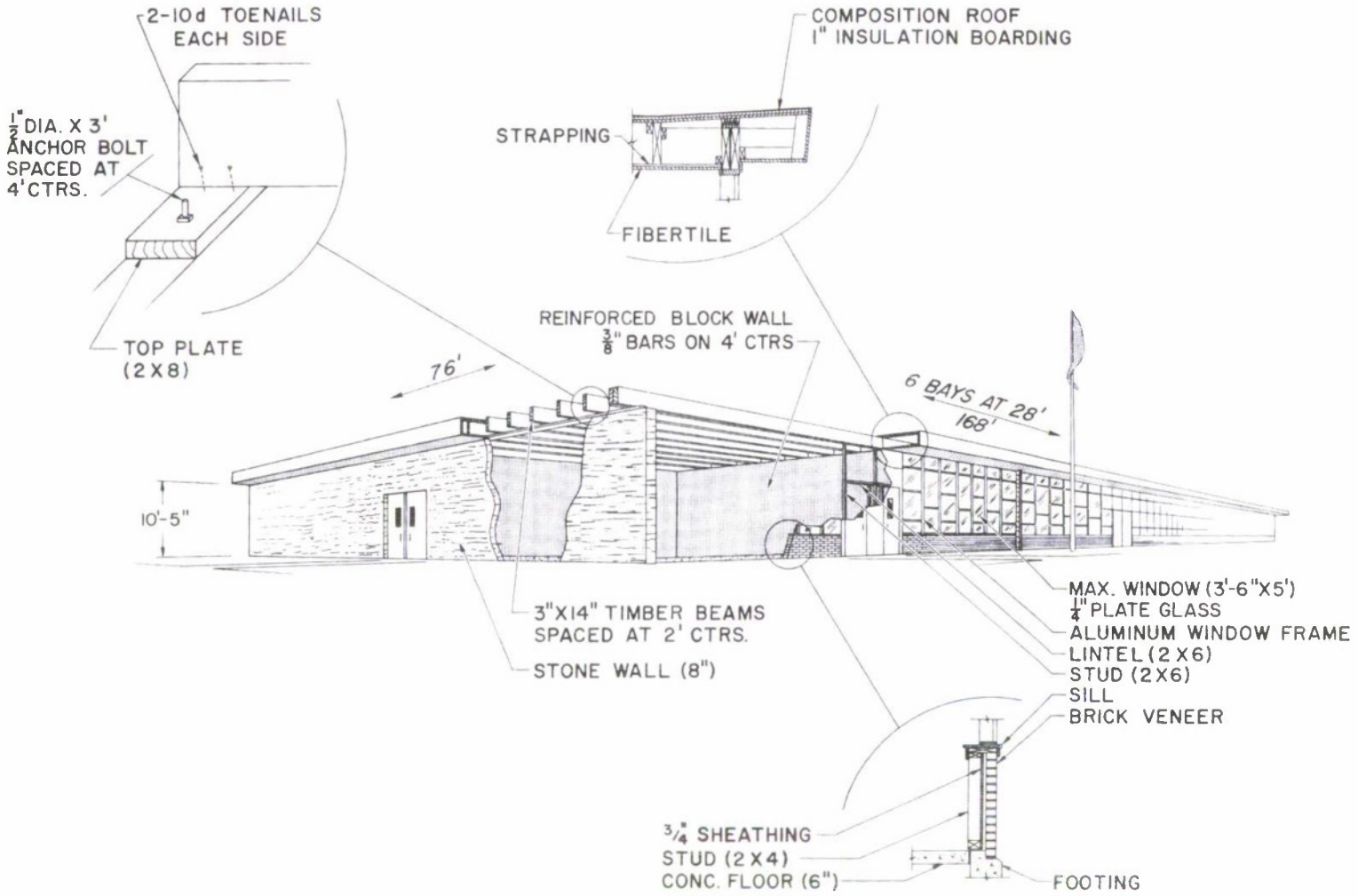

Figure 16. Typical Elementary School

glass fragment hazard; however, the loss of the windows and window frame portion of the front wall will not cause collapse of the roof because of the orientation of the roof support beams. The unacceptable risk levels, then, have been defined as structural collapse of the roof or the stone wall section. Blast damage levels corresponding to cracking the roof rafters and/or severely cracking the stone wall therefore have been defined as acceptable criteria on which to establish minimum separation distances. To reemphasize, a deflection of the center of the 8-inch stone wall of approximately 5 inches is considered sufficient to seriously crack the wall but not to cause partial or complete collapse.

1. Analysis of the Stone Wall

The resistance functions and the unit impulse required to severely crack the stone wall were computed using the model for masonry walls, equations (1) through (9). As in the treatment of brick and concrete walls, a steady pressure of approximately 0.5 psi was assumed to be required to cause tensile bond failure in the mortar. In the programmed analytical model, then, a requirement of at least a 0.5 psi average overpressure throughout a blast loading interval equal to the calculated critical period was stipulated. As in the analysis of the other types of wall section, the effective reflected impulse was estimated as the integral of the overpressure function from time t = 0 to a time at which the overpressure level decreases to 0.1 psi.

a. Calculation of Critical Period and Critical Impulse

Equations (20) and (21) were used to obtain the critical period for a 1-inch wide column of stone wall, analyzed as a uniformly loaded beam. Three values each of Young's modulus and the tensile bond failure stress for mortar were considered. These sets of parameter values and the computed critical periods are shown in Table IX.

b. Blast Loading Model

The lack of openings in the stone wall prevents back pressure from building up on the inside of the stone wall; thus, the blast loading on the front face of the wall is the only

TABLE IX. Critical Periods for the School Stone Wall

E ($psix10^6$)	Tensile Strength (psi)	Critical Period, C_p (msec)
1.2	30.0	12.63
1.2	50.0	12.63
1.2	70.0	12.63
1.3	30.0	12.14
1.3	50.0	12.14
1.3	70.0	13.15
1.4	30.0	11.70
1.4	50.0	11.70
1.4	70.0	11.70

consideration. It is modeled using equations (31) to (36). As indicated in the treatment of the other wall sections, the critical impulse requirements vary with the assumed tensile bond failure stress (30 to 70 lbs/in^2) and the blast loading on the roof which is reflected in the parameter P_v used in equations (3), (4), and (5). Under the assumption that the stone wall supports one-half of each roof section, an estimate of the blast forces per inch of stone wall can be obtained using the calculated maximum average pressure on the roof, P_a. P_v becomes the sum of one-half the contribution per inch of wall of P_a and the weight of the roof section which the increment of wall supports.

2. Analysis of the School Roof

a. Calculation of Critical Period and Critical Impulse

The school roof beams are analyzed as being uniformly loaded. Their critical period calculations are straightforward using equations (20) and (21). Values of Young's modulus are estimated as 1.3 and 1.5 x 10^6 psi; the weight per foot of beam as 30 and 40 pounds; and the modulus of rupture as 1.1 and 1.2 x 10^4 psi. Critical impulse values for the uniformly loaded beams are obtained using equations (22) through (28). The corresponding values for C_p and I_c, for the eight sets of parameter values, are given in Table X.

TABLE X. Critical Period and Critical Impulse for School Roof

E ($psix10^6$)	Weight, w (lbs/ft)	σ_{max} ($psix10^3$)	Critical Period (msec)	Critical Impulse (psi-ms)
1.3	30.0	1.1	52.88	81.44
1.3	30.0	1.2	52.88	88.85
1.3	40.0	1.1	61.06	94.04
1.3	40.0	1.2	61.06	102.59
1.5	30.0	1.1	49.23	75.82
1.5	30.0	1.2	49.23	82.71
1.5	40.0	1.1	56.84	87.55
1.5	40.0	1.2	56.84	95.51

3. Comparative Values

Because the roof section is parallel to the direction of flow of the impinging blast wave, the top surface model to determine the blast loading on the exterior of the roof, presented as equations (37) and (38), are directly applicable. Since the blast forces will also act on the interior surface of the roof, a net loading model must be used. With diffraction of the blast wave through window openings, the average pressure on the interior of the roof section rises linearly to a maximum value, P_t, at time t = 2L/V msec. The maximum average pressure at this time is given by

$$P_t = p\left(t - \frac{L}{2V}\right)$$
$$= P_o\left[1 - \frac{t'}{2V}\right]e^{-\frac{t'}{2V}} \qquad t' = \frac{2L}{V}\ \text{msec} \tag{42}$$

For the time interval $2L/V<t<\tau + 2L/V$, the average overpressure function on the inside of the roof is assumed to decay exponentially in accordance with the above expression.

Computed net reflected impulse values on the school roof are smaller than the impulses required to crack the stone wall, but because of the normal incident orientation of the roof to the shock front, they are much harder to achieve. A comparison is made in the following.

For the 10,000-pound charge, a separation corresponding to cracking of the stone wall is determined as 180 feet. The critical impulse required at this distance is 111.15 psi-msec. The reflected impulse achieved on the school roof at this distance is approximately 28.5 psi-msec for all eight combinations listed in Table X. This value is far less than the range of reflected impulse required to fail the roof (81.4 to 102.6 psi-ms).

In all cases, the school stone wall was judged to fail first under blast loading, therefore, it has been used as criterion for establishing P-I curves and the distance plots shown in the Results section.

D. OFFICE BUILDING

The office building walls are relatively inexpensive curtain walls composed of 8- by 8- by 16-inch concrete blocks, unreinforced, laid using normal brick wall construction procedures to construct an 8-inch thick wall. In the segments of block walls having windows, the solid portion is approximately 4 feet high. Windows, composed of 4- by 4-foot by 1/4-inch plate glass in aluminum frames, are placed on top of the walls. The vertical aluminum frames offer some resistance or support to the wall in that they must be buckled and the aluminum sill bent in order to critically deflect the block wall portion.

The solid concrete block wall portions are assumed to be mortared in on all sides between the inflexible concrete columns. Thus, an arching action must take place in order to deflect this wall. The wall is obviously much more resistant to blast forces than simply supported masonry walls because the arching action requires a considerable amount of mortar crushing prior to failure.

In the analysis of this civilian target, it must be determined which of these two wall sections fails first at given quantity-distance specifications. As in the treatment of other masonry walls, failure is defined as the severe cracking accompanying an approximate 5-inch deflection of the center of the wall.

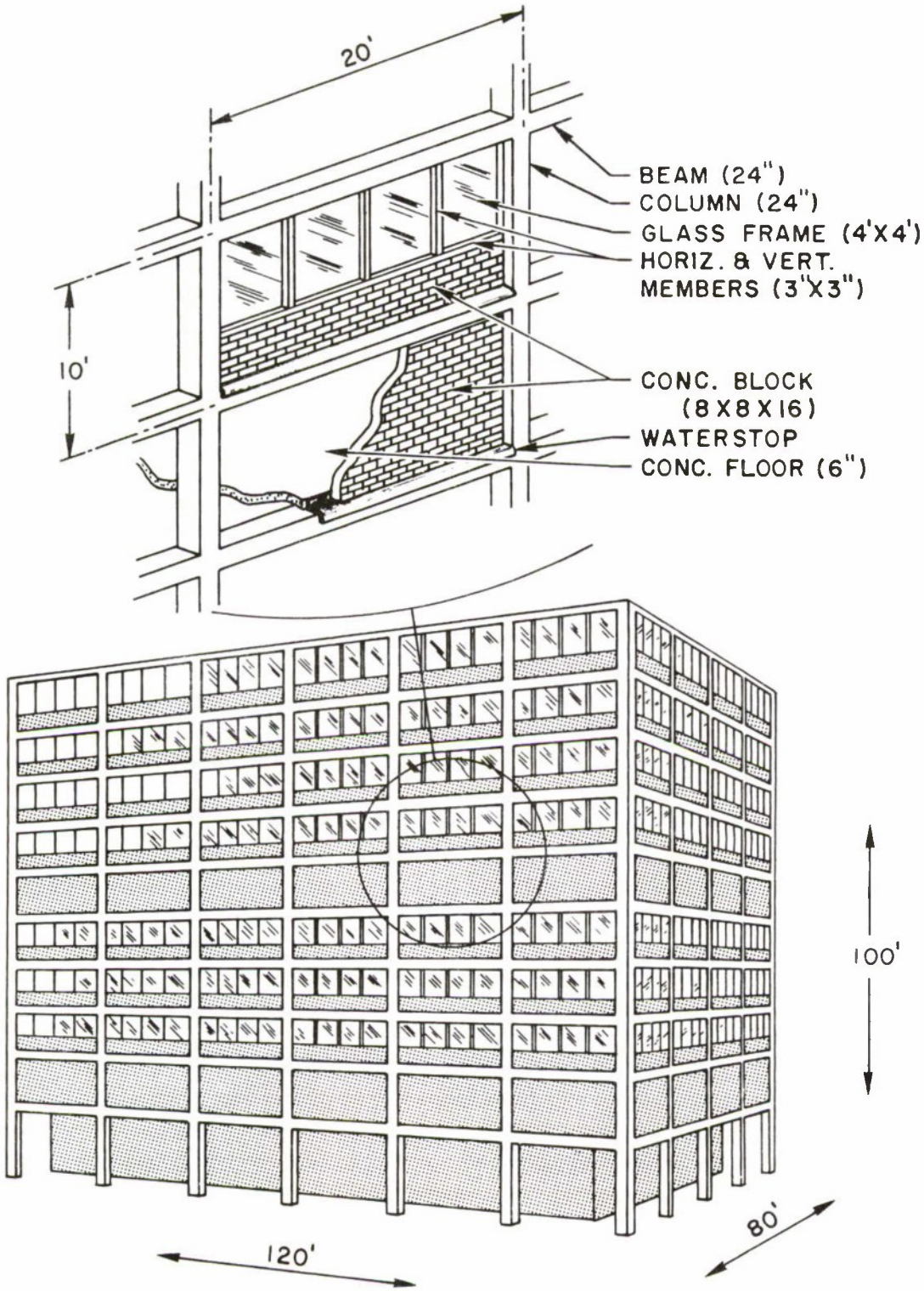

Figure 17. Multi-Story Building

1. Critical Periods of the Office Building Walls

The techniques used in the calculation of the critical periods, and the assumptions under which the critical impulse for the half wall are computed, are the same as those used in the treatment of other types of walls previously discussed. However, because all ends of the full wall are held relatively secure by the inflexible concrete columns, its critical period is determined from the analysis of a uniformly loaded beam with fixed ends. The combination of parametric values and the critical periods calculated for both types of walls are given in Table XI.

TABLE XI. Critical Periods of the Office Building Walls

E ($psix10^6$)	Tensile Strength (lbs/in^2)	Critical Period, (msec)
Half Wall:		
1.2	30.0	15.00
1.2	50.0	15.00
1.2	70.0	15.00
1.3	30.0	14.41
1.3	50.0	14.41
1.3	70.0	14.41
1.4	30.0	13.89
1.4	50.0	13.89
1.4	70.0	13.89
Full Wall:		
1.2	30.0	4.60
1.2	50.0	4.60
1.2	70.0	4.60
1.3	30.0	4.43
1.3	50.0	4.43
1.3	70.0	4.43
1.4	30.0	4.27
1.4	50.0	4.27
1.4	70.0	4.27

The office half wall supports only the window frames which will not transmit blast forces to the wall; thus, the blast loading contribution to P_V in equations (37) and (38) is very minor. The critical impulse value for all sets of parametric values approximates 75 psi-msec.

2. Analysis of the Full Wall

The approach to estimating the resistance forces set up in the deflection of a masonry wall, under conditions in which it is constrained under essentially rigid supports, is the "arching action theory" presented in several references (see [105] for several of these). The assumed mode of response of the wall is as follows.

The wall is idealized as a beam of solid, uniform, rectangular cross section, constrained between rigid supports on two opposite edges. The masonry material is assumed to have no tensile strength. Therefore, immediately on loading, cracks develop on the tension side and extend to the centerline. During subsequent motion, each half of the beam is assumed to remain rigid and rotate about its end support and the center. This rotation is resisted by a force couple developed as a result of the two halves being wedged between the rigid supports, thus causing crushing at the ends and center. This rotation continues until either the load is removed or the resisting couple vanishes, in which case the wall collapses. The magnitude of the resisting couple is seen to depend on the magnitude of the compressive forces developed at the ends and center, and on the moment arm between these forces. Both of these values, in turn, depend on the stress-strain properties of the masonry material. Various assumptions have been made for these stress-strain properties.

A number of these and the resultant models for determining the resistance forces are discussed in [105]. The method used in this study is based on a "linearized elastic-plastic" stress-strain relationship presented originally in [73]. Essentially, this method assumes a linear relation between the mid-span deflection and the strain along the contact area, up to a yield strain that corresponds to the crushing stress of the material. The derivation of this theory and that for calculation of the resisting moment are not repeated herein because of their length.

Using the approach outlined above, the total work associated with the integration of the resistance-deflection curve up to a 5-inch deflection is calculated as 708 in-lbs/in of wall. This value, then, was used in equations (6) through (9) to determine a critical impulse, for this arching type wall, of 140.5 psi-msec.

3. Blast Loading Models for the Office Walls

The front surface loading model (equations (31) through (36)) is applicable to the full wall, since it has no opening through which to allow shock wave diffraction. Based on mortar sample crushing tests, a steady pressure of approximately 5 psi must be maintained for a significant period so that sufficient crushing action of the mortar at the top and bottom of wall may take place. Therefore, it is assumed in the calculation of the effective impulse imparted to the wall, that an average pressure of 5.0 psi must be maintained over a time interval equal to its calculated critical period.

The net loading concept is used in measuring the net reflected impulse to the half wall. As the blast wave diffracts over the top of the wall, a counteracting force is built up on the rear face of the wall in accordance with equation (39).

In comparing the two sets of minimum separation distances for the different walls, it was found that the separation distance is the greatest for the 10,000-pound charge for the office half wall, is approximately equal for the 1,000- and 100,000-pound charge for the two walls, and is shortest for the office full wall for the larger 1- and 9-million-pound charges. The minimum separation distance criterion for the office building, therefore, must take into account the blast responses of both walls. Pressure-impulse curves and relative distance plots for the office building are given in Section V.

E. PASSENGER BUS

The prevention of overturning is the basis on which acceptable damage criteria have been established for the vehicular targets--the passenger bus, camper-pickup unit, and the mobile home. The pressure-impulse requirements to overturn these targets are therefore determined in this analysis, and the

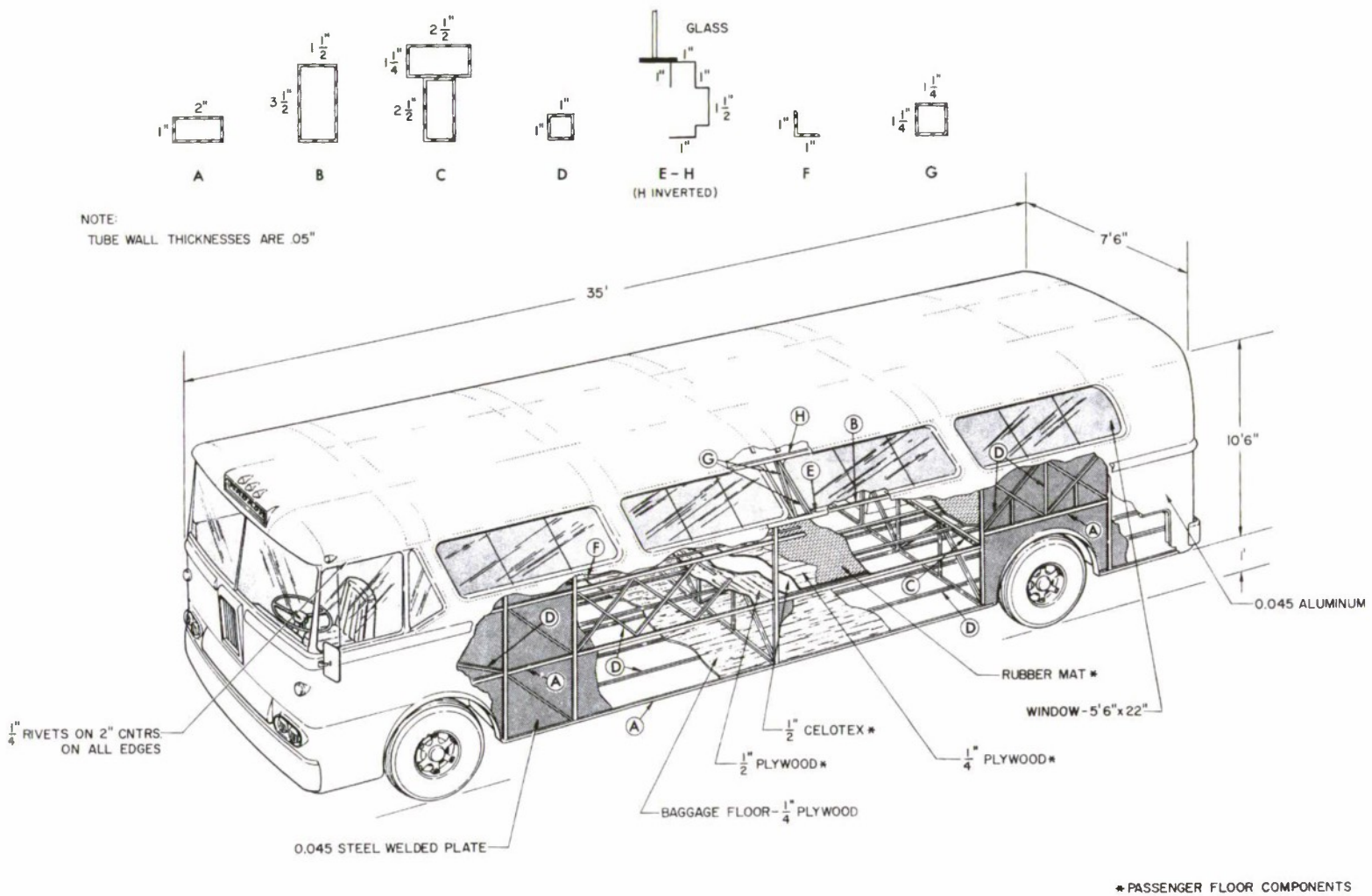

Figure 18. Passenger Bus

acceptable damage level arbitrarily established as being that damage associated with 80 percent of the reflected impulse necessary to overturn each vehicle. With such forces imparted to the vehicle, some deformation of the exposed sidewalls, window breakage, and the dislocation of some internal fixtures will probably occur, especially for the smaller charges. These effects, however, should not present an unacceptable hazard to the occupants.

Preliminary investigation with available experimental data indicates that all of these vehicular targets will overturn prior to experiencing any substantial degree of sideways displacement, at least on dry asphalt or concrete. These results were determined using a coefficient of friction of approximately 0.7.

1. Analysis of the Passenger Bus

The bus analyzed is a rather standard intercity highway bus made by Mack. The external skin sections of the bus are attached to a rather light but extensive space frame composed of many small members, primarily square or rectangular steel tubing. There is no main frame such as is commonly found in trucks and older cars. The outer skin, either steel or aluminum, and the plywood passenger and baggage floors are rigidly attached to the framework and provide part of the structural strength.

The side of the bus below the passenger floor is extremely resistant to sideways deformation. However, the upper half is considerably lighter and undergoes deformation at reasonably low overpressures. The principal dangers to passengers, however, would come from window breakage or overturning of the bus.

The empty bus weighs approximately 22,000 pounds, and when fully loaded with 40 people and baggage, an estimated weight of about 30,000 pounds is attained. The center of gravity is estimated at about 40 inches from the ground plane.

The reflected impulse needed to overturn a stationary target requires a determination of the mass distribution of the target and the location of the center of gravity. The height of the center of gravity above the point of rotation, A, in

the ground plane is designated as h_g and the distance, in the ground plane, from the center of gravity to the point of rotation as d. The distance, $d_o = \sqrt{d^2+h_g^2}-h_g$, represents the distance the center of gravity must rise so that it is directly above point A, at which point gravitational forces will overturn the target. For most targets, point A is a point in the ground plane directly below the outside surface plane of the vehicle.

The work, W, done in overturning the target is

$$W = d_o \cdot \text{(weight of the vehicle, w)} \tag{43}$$

When a sufficient impulse is applied to the target rapidly, it will give the target an angular velocity, ω, great enough to permit inertial forces to complete the overturning action. The angular velocity will be sufficient when the kinetic energy is greater than the work required from equation (43), where

$$KE = 1/2\ I_A\omega^2 \tag{44}$$

The value I_A is the moment of inertia about point A and is given as

$$I_A = m\left(\frac{b^2+h^2}{12} + c^2\right) \tag{45}$$

where:

m = mass of the target

b = width of the target

h = height of the target

c = the transfer axis distance; $c = d_o+h_g$.

By equating the required work, W, with the kinetic energy and substituting equation (45) into (44), an expression for the required angular velocity, ω, to overturn the target is obtained:

$$\omega = [2W/I_A]^{1/2} = \left[\frac{2\ d_o w}{I_A}\right]^{1/2} \qquad (46)$$

The required unit impulse (psi-ms), H, required to produce this angular velocity is

$$H = \frac{1000 \cdot I_A \cdot \omega}{h_c \cdot \text{(presented area of the target)}} \qquad (47)$$

where h_c represents the height above the ground where the center of the blast pressure is applied.

The computed reflected impulses required to overturn the stationary bus are all well within the present quantity-distance criteria for the five charge sizes considered. The bus therefore was analyzed under more vulnerable conditions, that of being in a 460-foot radius turn at 50 mph.

In order to select a typical turning condition for the bus, it was experimentally determined, that for normal safe driving, the resultant force exerted on a vehicle by the road (composed of the centripetal force applied in the horizontal plane and the weight reaction force applied vertically) would be inclined a maximum of 20 degrees from the vertical. This would occur at different speeds for different radius curves, but at 50 mph is associated with a 460-foot radius curve. The centripetal force corresponding to 20 degrees is $w \cdot \tan 20 \text{ degrees} = .364\ w$. A condition of "unstable equilibrium" can be used which is represented, for a stationary bus, by a tipping to the point where the center of gravity is directly above point A; for a bus in a turn, unstable equilibrium will occur when a blast on the inner side of the curve has tipped the bus such that the sum of the moments about A, of the centrifugal force and the weight, equal zero. Thus, the bus in a 50-mph, 460-foot radius turn is at unstable equilibrium when:

$$.364w\ (\sqrt{d^2+h_g^2} \cdot \sin\theta) - w\ (\sqrt{d^2+h_g^2} \cos\theta) = 0 \qquad (48)$$

$$.364w = \cot\theta$$

$$\theta = 70 \text{ degrees}$$

where θ is the angle between the ground plane and a line connecting the displaced center of gravity with the point of rotation A and d and h_g are as previously defined. Therefore, to reach the unstable equilibrium position, the center of gravity must rise a distance

$$d_o = (\sin\theta\sqrt{d^2+h_g^2}) - h_g.$$

The distance the c. g. moves in the direction of the centrifugal force becomes

$$d_c = \cos\theta \cdot \sqrt{d^2+h_g^2} .$$

The work done by the centrifugal force is therefore

$$W_c = d_c \ (.364 \ w) \ . \qquad (49)$$

The above work is subtracted from the total work requirement calculated with equation (43) to determine the work required only by the blast force to overturn the bus. Using this modified work calculation in equations (44) through (47) results in a determination of the reflected impulse calculation required to overturn the bus moving in the 460-foot radius turn.

a. Critical Impulse Values

The precise weight of the passenger bus and the precise location of its center of gravity are unknown parameters. Three values of each were considered in the calculation of critical impulse. For w, values of 28,000, 30,000, and 32,000 pounds were selected while the c. g. locations were 38, 40, 42 inches above the ground plane. The distance $h_g{}^d$ is taken as 43.2 inches. The calculated reflected impulse values required to overturn this moving bus are presented in Table XIII.

b. Blast Loading Model

The net loading concepts were used in analysis of the vehicular targets. The blast loading on the rear side of the target is subtracted (equation (39)) from the reflected loading on the front surface (equations (31) through (36)) to determine a net loading. Integration of the net loading function then

TABLE XII. Critical Impulses for Passenger Bus

Bus Weight ($lbsx10^3$)	C. G. Location, h_g (inches above ground plane)	Critical Impulse, I_c (psi-ms)
28	38	102.45
28	40	109.77
27	42	117.09
30	38	98.29
30	40*	105.31
30	42	112.34
32	38	94.26
32	40	100.99
32	42	107.72

*Representative case.

determines the net reflected impulse imparted to the target. The pressure-impulse plots for the representative set of parameter values and the relative separation distances obtained for the bus, with respect to the other targets, are presented in the Results section.

F. CAMPER-PICKUP UNIT

The camper-pickup combination is quite sturdy compared to the house trailer. The side walls are composed of a very light, nonstructural, aluminum outer skin; a very irregular glued and stapled framework of 1- by 2-inch, 2- by 2-inch, and 2- by 3-inch wood members with spacing to accommodate the windows, cupboards, etc.; and an inner covering of 1/8- or 3/16-inch plywood glued and nailed to the framework. In the interior there are numerous cupboards, seats, counters, etc., which contribute considerable strength and stiffness to the side walls. The structural detail is illustrated in Figure 19.

1. Method of Analysis

The minimum separation distance for this unit for a specific charge was determined, as previously stated, as the distance at which 80 percent of the reflected impulse required to

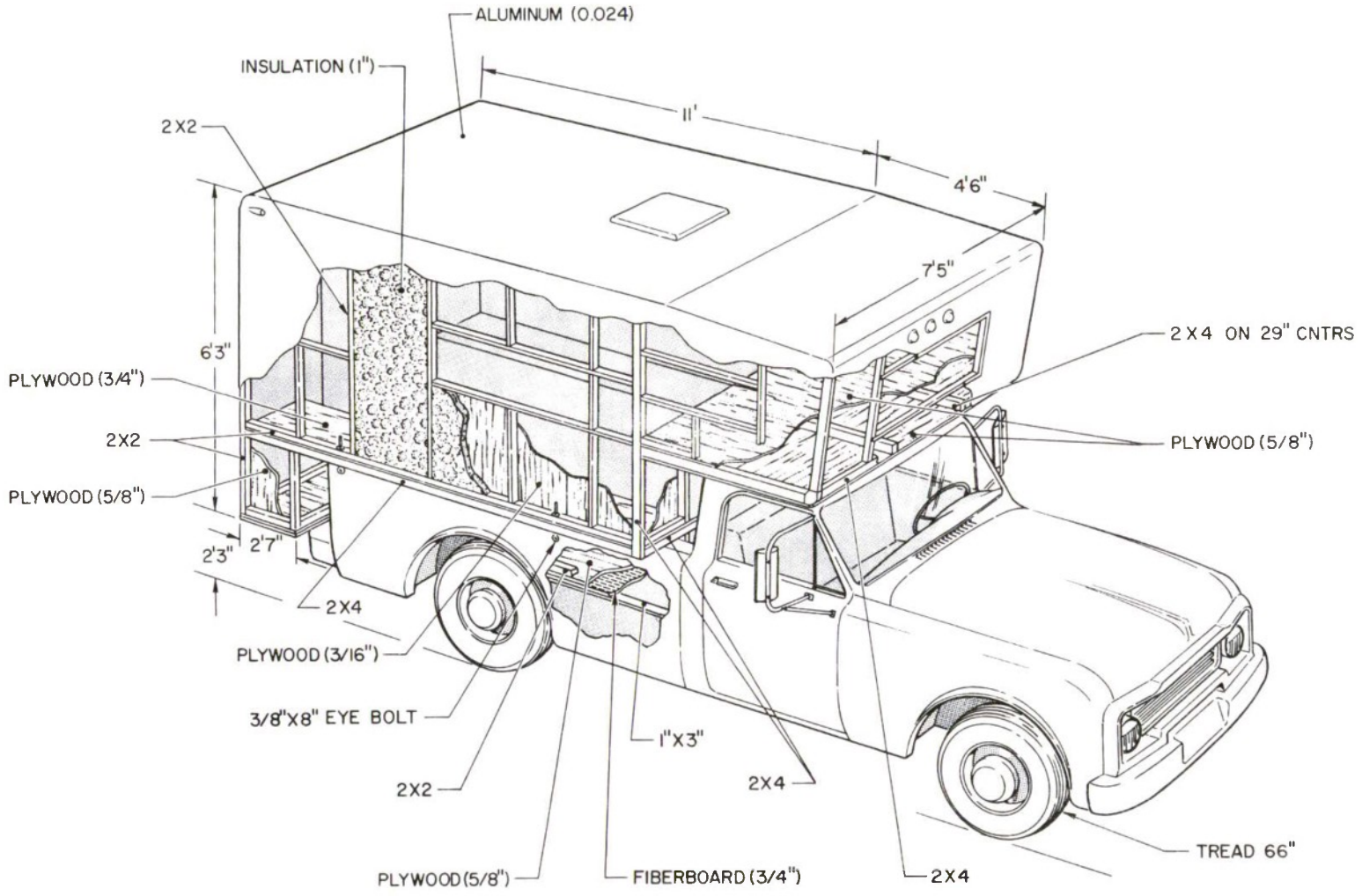

Figure 19. Camper-Pickup

overturn the unit is attained. Again, the permanent deformation of the sidewalls and glass breakage which will occur at this point are considered acceptable.

The reflected impulse required to overturn the camper-pickup unit can be determined through straightforward use of equations (43) through (47) presented in the previous section. Three values of the combined center of gravity of the unit were considered; 41, 43, and 45 inches above the ground plane; while the combined weights considered were 5,600, 5,900, and 6,200 pounds. The distance, d, from point A (the outside edge of the pickup tire) to a point in the ground plane directly below the center of gravity was 33 inches. The computed reflected impulse required to overturn the camper pickup unit for these sets of parameter values are presented below in Table XIII.

TABLE XIII. Critical Impulses for Camper-Pickup Unit

Total Weight (lbs)	Combined C. G. Location, h_g (in. above ground plane)	Critical Impulse, I_c (psi-ms)
5,600	41	78.14
5,600	43	82.35
5,600	45	98.49
5,900	41	76.56
5,900	43*	80.68
5,900	45	96.48
6,200	41	75.05
6,200	43	79.09
6,200	45	94.56

*Representative case.

2. Blast Loading Model

The net blast loading concept was used for the camper-pickup unit and the computed reflected impulse required, computed from the resultant net loading function. The pressure-impulse plot for the representative set of parameter values shown in Table XIII are given in the Results section.

G. MOBILE HOME

The mobile home has a main frame consisting of two light but deep channels, with cross channels welded between these main frame members in the same plane. On top of the cross channels, 2- by 4-inch wood members run lengthwise on 16-inch centers; they are stabilized by 1- by 3-inch wood members placed at right angles, on 24-inch centers. Covering these are 1/2-inch plywood sheeting and nonstructural finish flooring materials.

The sidewalls have a nonstructural outer metal skin, 2- by 3-inch studs on 16-inch centers with several 1- by 2-inch stringers, and an inner covering of nailed and glued 3/16-inch plywood. The various cupboards, partitions, etc., have not been illustrated. The roof has light truss cross members composed of 2- by 2-inch chords and metal web members. There is a 2- by 4-inch wood member running lengthwise through the center of the trusses to stabilize them. The roof is not particularly vulnerable to blast loading because the shock wave is assumed to impinge on the side of the trailer and the reflected pressure on the roof is only very slightly higher than the incident pressure. Other structural detail is given in Figure 20.

1. Critical Impulse

The formulation of the required reflected impulse to overturn the mobile home follows that presented in equations (43) through (47). The values of the height of the center of gravity treated were 70, 72, and 74 inches while the total weights considered were 12,000, 13,000, and 14,000 pounds. The distance d was determined as 44 inches. The critical impulses calculated for these sets of parameter values are shown in Table XIV.

The net loading concept was also used in determining the reflected impulse imparted to the mobile home for a specified quantity-distance combination. For the representative case of parameter values, the pressure-impulse plot is presented in the Results section.

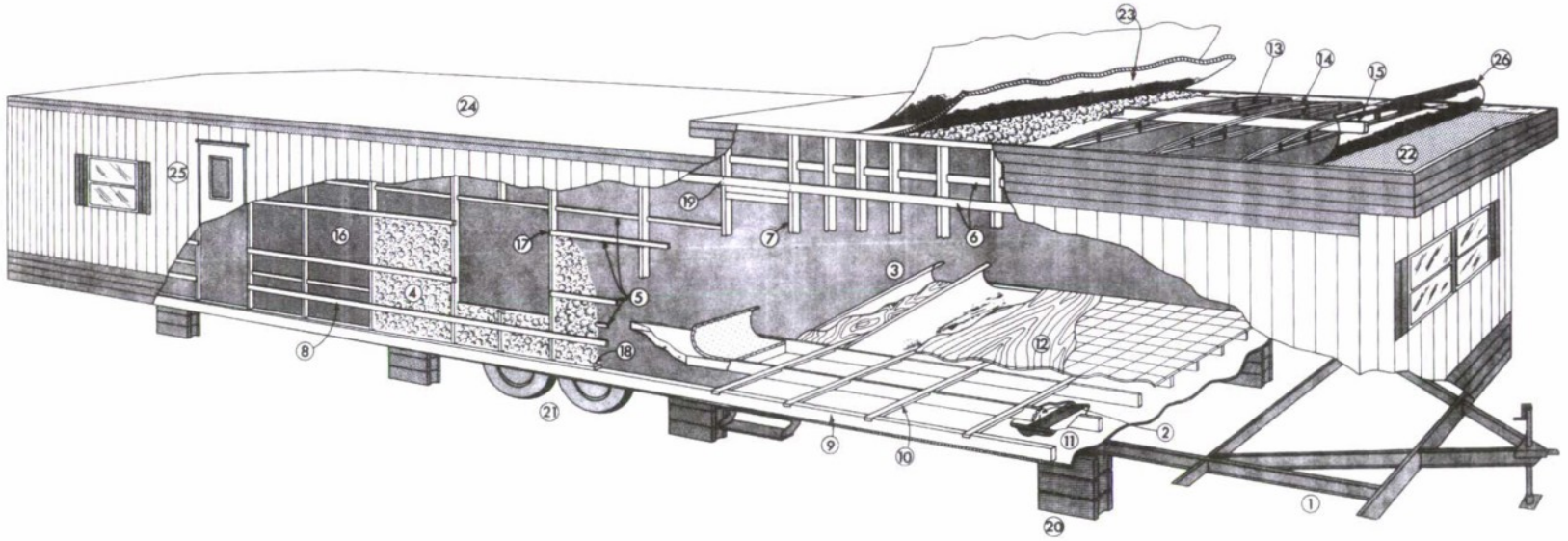

1 8 channel, 8.5 pounds per foot.
2 5/16" dia. x 3" long lag screw thru each cross frame member into each 2x4.
3 Triple floor insulation, surface next to frame is asphalt impregnated board. Blanket of 3.25 high density fiberglass is laid over the insulation board. Polyethylene vapor barrier. Dead air space between vapor barrier and wood flooring.
4 Sidewall insulation, high density fiberglass combined with reflective aluminum exterior. Fiberglass is stapled to prevent sag.
5 1"x2" kiln dried spruce, spaced as needed.
6 1"x3" kiln dried spruce, spaced as needed.
7 2"x3" kiln dried spruce, spaced 16" on center or as needed.
8 1"x3" kiln dried spruce, spaced as needed.
9 2"x4" kiln dried spruce, spaced 16" on center.
10 1"x3" kiln dried spruce, spaced 24" on center.
11 5/8" asphalt celotex.
12 1/2" plywood.
13 2"x2" kiln dried spruce
14 2"x2" kiln dried spruce
15 2"x4" kiln dried spruce
16 3/16" hardwood veneer panels. All wall panels are glued and nailed.
17 Two 6d nails.
18 One 10d nail spaced 8" thru 2x3 plate into floor edge 2x4.
19 Two 8d nails.
20 Concrete leveling blocks spaced 8 places.
21 Tires clear of ground when on concrete blocks.
22 Blanket of fiberglass.
23 3/8" plywood.
24 28 gage steel roof. The roof is coated with aluminized asphalt compound for added sound protection and sealer.
25 .02 inch aluminum side panels with baked on, prefinished color surface. Side walls are made with overlapping seams to insure water tight construction. Fastened with 3/16" by 1" hex head sheet metal screws.
26 Polyethylene vapor barrier attached to ceiling joist.

Figure 20. Mobile Home

TABLE XIV. Critical Impulses for Overturning Mobile Home

Weight (lbsx10^3)	C. G. Location, h_g (inches above ground plane)	Critical Impulse, I_c (psi-ms)
12	70	57.69
13	70	62.49
14	70	67.30
12	72	57.00
13	72*	61.75
14	72	66.50
12	74	56.33
13	74	61.03
14	74	65.72

*Representative case.

H. PERSONNEL

The "standard man" as used in many military target description and vulnerability studies is illustrated in Figure 21. The quantity-distance specification for the personnel target has been established so as to prevent his being violently thrown to the ground, down stairs, or against nearby structures. Lovelace Foundation personnel have studied the levels of overpressure at which man and other objects are translated by large blast forces [19]. They have indicated that the translation velocity at which man would be subjected to the above dangers is approximately 3.5 ft/sec. The criterion for establishing quantity-distance specifications for man, then, has been based on the reflected impulse which results in the translation of the average 168-pound man at a maximum velocity of 3.5 ft/sec.

It was determined in the Lovelace studies that the dynamic overpressure is the main factor in the translation of objects in a blast wave. Therefore, in order to achieve a translation of a 168-pound man, the impulse associated with the integration of the dynamic pressure function must be greater than the product of the mass of the man and his translation velocity or

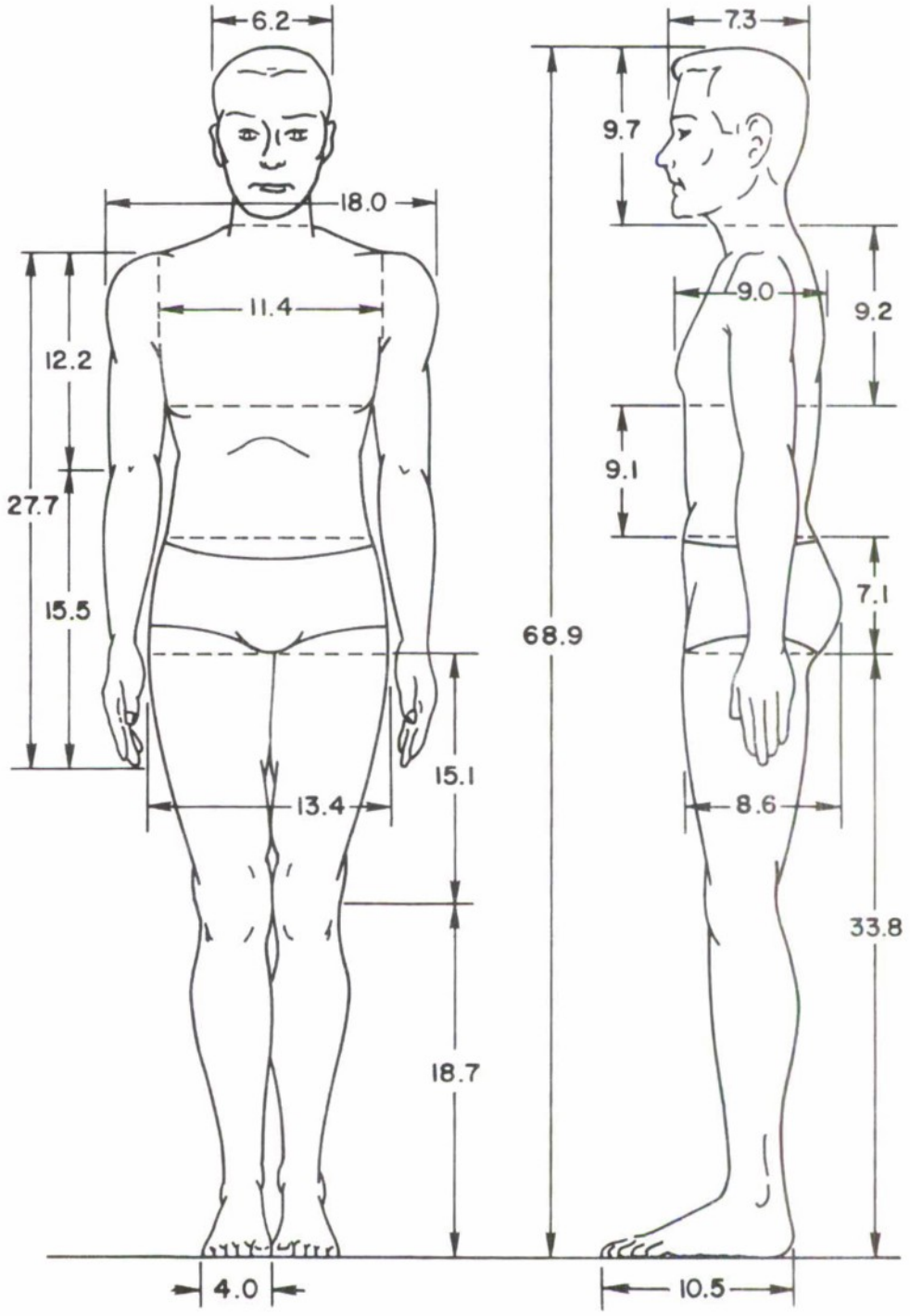

Figure 21. Standard Man

$$PA \cdot \int q(t)dt > m \cdot v \qquad (50)$$

where:

$q(t)$ = dynamic pressure function given by equation (35)

m = mass of the man

v = translation velocity

PA = presented area of the man (inches^2)

The above equation allows velocity to be expressed as a function of time; thus, through an integration of that function, the translation distance associated with a maximum velocity of 3.5 fps can be obtained. Finally, the maximum acceleration a_{mx} over the calculated translation distance becomes

$$a_{mx} = \frac{F_{mx}}{m} \qquad (51)$$

where:

F_{mx} = force given by $Q_o \cdot PA$

Q_o = peak dynamic overpressure.

The critical impulses required to translate the 168-pound man at a maximum velocity of 3.5 fps were computed using three values of presented area. These were 5.5, 6.7, and 8.0 square feet. The latter value represents the presented area of a standing man facing the blast forces.

In the analysis of the personnel target a peak reflected overpressure of 5.0 psi was used as the threshold of ear drum rupture. For the smaller charges it was found that if the peak reflected pressure was below 5.0 psi, the peak dynamic overpressure and thus the dynamic overpressure impulse was not sufficiently large to translate the man to the specified 3.5 fps. In these cases the maximum distance from the explosive charge at which ear drum rupture occurs was designated as the limiting value.

The respective pressure-impulse plot for the 168-pound man with a presented area of 8.0 square feet is given in the Results section.

I. EXPLOSIVE STORAGE IGLOO

Three standard types of explosive storage igloo were examined:

1. The first type is supported by a No. 1 gage corrugated steel arch with a 2-foot minimum earth cover. The igloo has a 13-foot radius and is 59 feet long (inside dimension). The front concrete wall is 12 inches thick with two 5- by 10-foot steel doors opening outward. The outside of the door is covered with 3/8-inch steel plate. Insulation and 16-gage steel plate comprise the inside portions of the door. This igloo construction is shown in Figure 22.

2. A second type of igloo consists of a No. 8 gage corrugated steel arch with a 2-foot minimum earth cover. The igloo has a 5-foot 6-1/2-inch radius plus a 2-foot 4-1/2-inch base wall 68 feet long. The 12-inch thick concrete walls at each end contain two doors similar to the ones shown in Figure 22.

3. Another type contains a concrete arch 14 feet in height with a thickness varying between 6 and 9 inches. It also is covered with a 2-foot minimum earth cover. The front wall is concrete, 1-foot thick, and contains two steel doors covering an 8- by 8-foot opening. The doors are heavier than those used in the other two types and consist of 5/8-inch steel plates plus insulation.

The first type of igloo (SAC type) was chosen for analysis because the large front wall and lighter doors make it most vulnerable. The risk levels were defined as severely cracking the concrete wall so that it structurally collapses or dislodging the doors so that stored munitions might be exposed to fire or other projectiles resulting from subsequent explosions. Based on these definitions, three possible types of failure were considered:

1. Deformation of the door such that the pins pulled from their sockets in the door frame,

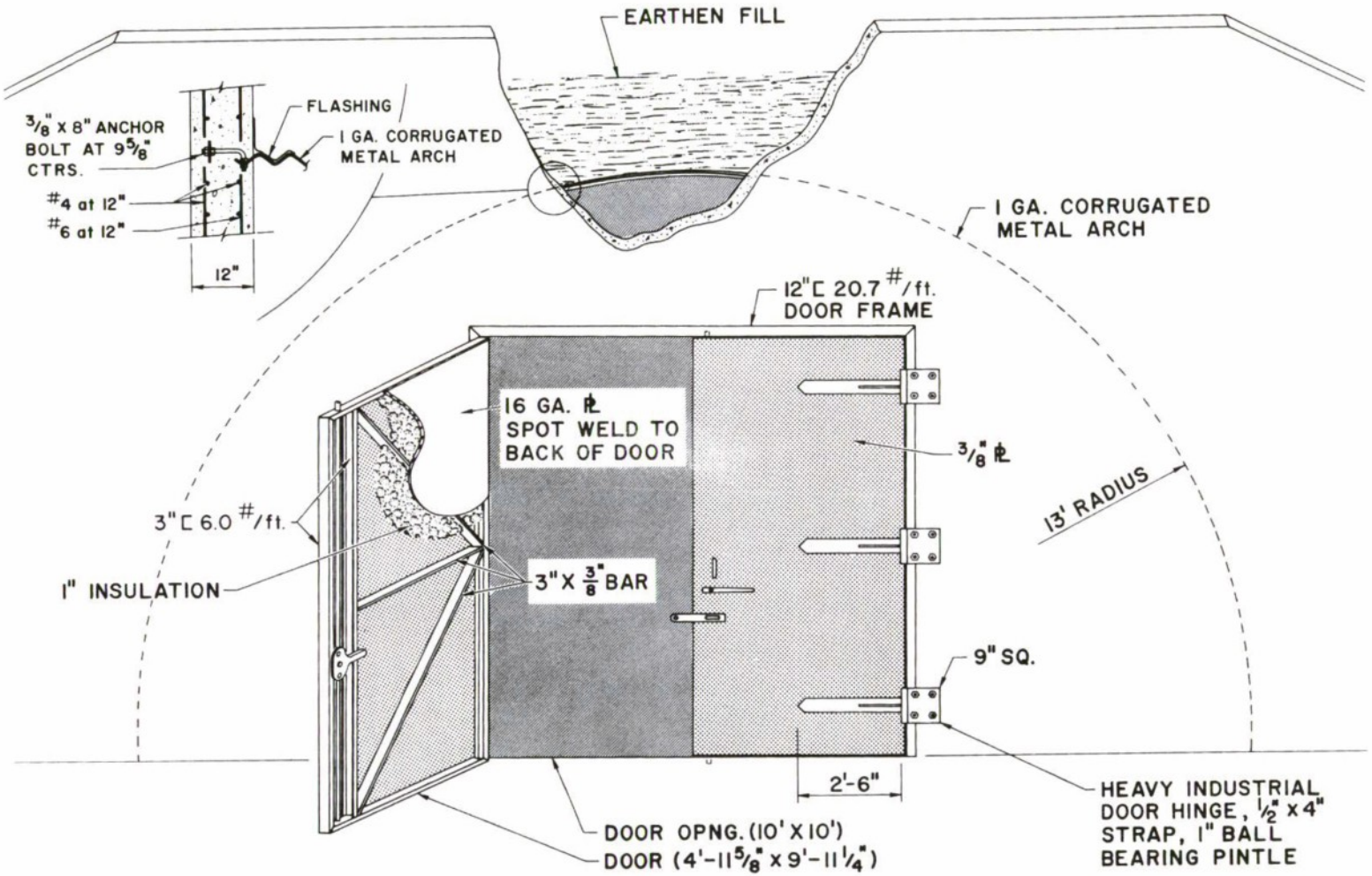

Figure 22. Standard Explosive Storage Igloo, Front

2. Shearing of the pins between the door and the socket, and

3. Failure of the concrete wall around the door.

The 3-inch thick igloo door is composed of a 3/8-inch outer steel plate welded to a 3-inch deep, 6-lb/ft steel channel forming the perimeter of the door. One inch of insulation is glued to the inside of a 3/8-inch plate, and a 16-gage plate is tack-welded on the backside of the channel. The door is held in place by three hinges with 1-inch diameter pins. Pins within the door of 1-3/8-inch diameter extend 1-1/2 inches into reinforced holes in the door frame. The door for modeling purposes was approximated by a 3/8-inch plate 2 feet wide by 10 feet high stiffened by the two 3-inch channels which are near the free edge of the actual door. The simulated door was simply supported top and bottom.

An 8-inch deflection of the door is necessary in order to dislodge the pins from the holes in the door frame. Analyzed as two rigid halves with a plastic hinge in the middle, the work W required to achieve the stipulated deflection becomes $W = M\theta$; where M is the plastic moment needed to deform the central section of the door, and θ is the central deflection angle. The required unit impulse is determined by using equation (28). Using 50,000 psi as yield strength for the steel door, a required impulse of 139 psi-msec was calculated.

Analyses of shear pin failure and of fracturing the concrete wall, by Johansen's yield line theory, indicate that deformation of the door so that the pins are dislodged, will occur first. Therefore, reflected impulses which cause this latter type of damage are used to denote quantity-distance specification in this study. The pressure-impulse plots for distances derived using a yield strength of 50,000 psi are given in the Results section.

J. COMMERCIAL AIRCRAFT

The Boeing 707 aircraft was used as the representative large commercial jet aircraft. Several sections of it are shown in Figures 23 through 29. These indicate the station numbering system and the exterior skin specifications.

The fuselage shell is of the semi-monocoque type with aluminum skin and clad 7075-T6 longitudinal stringers. The shell is

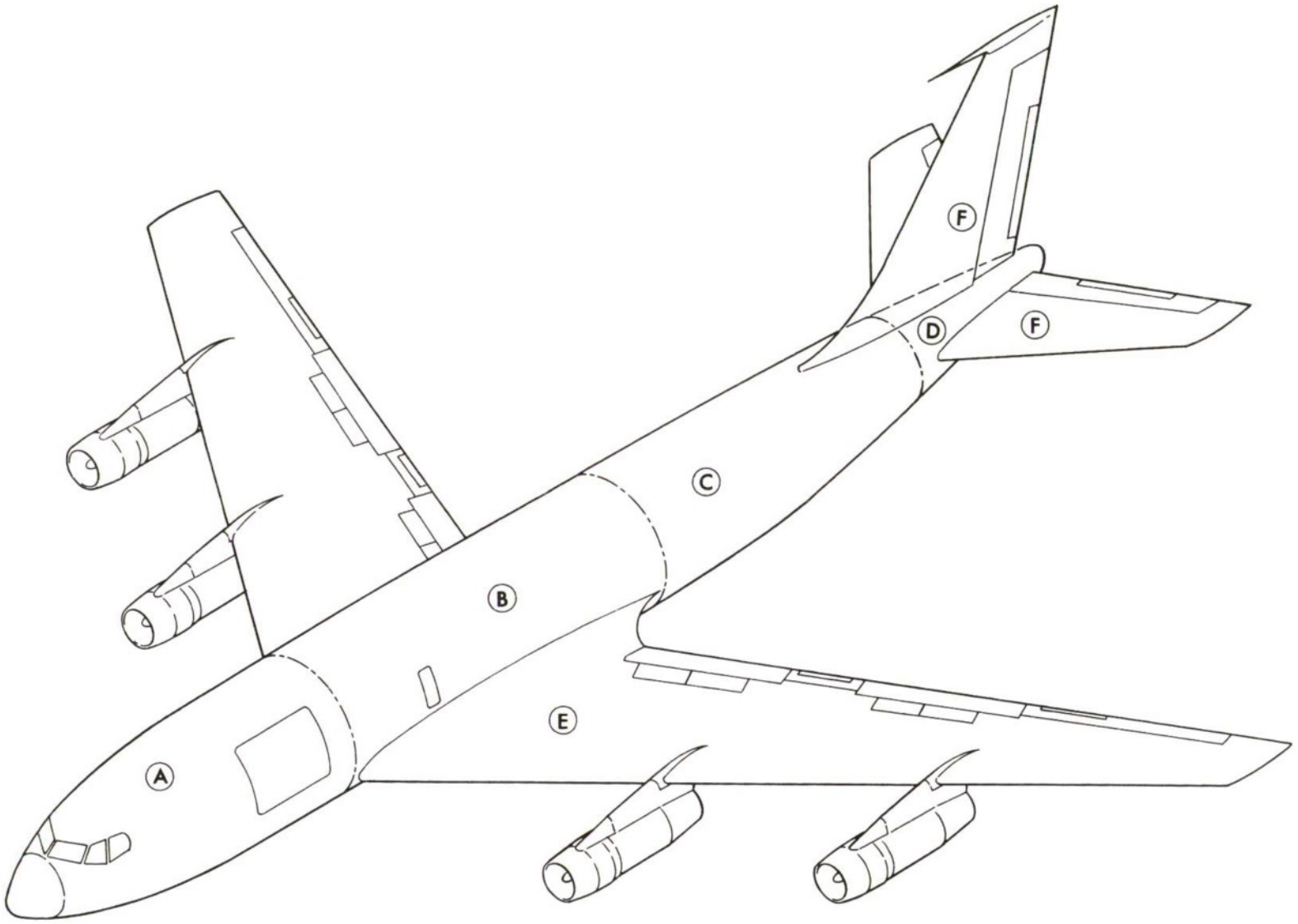

Figure 23. Boeing 707 Aircraft

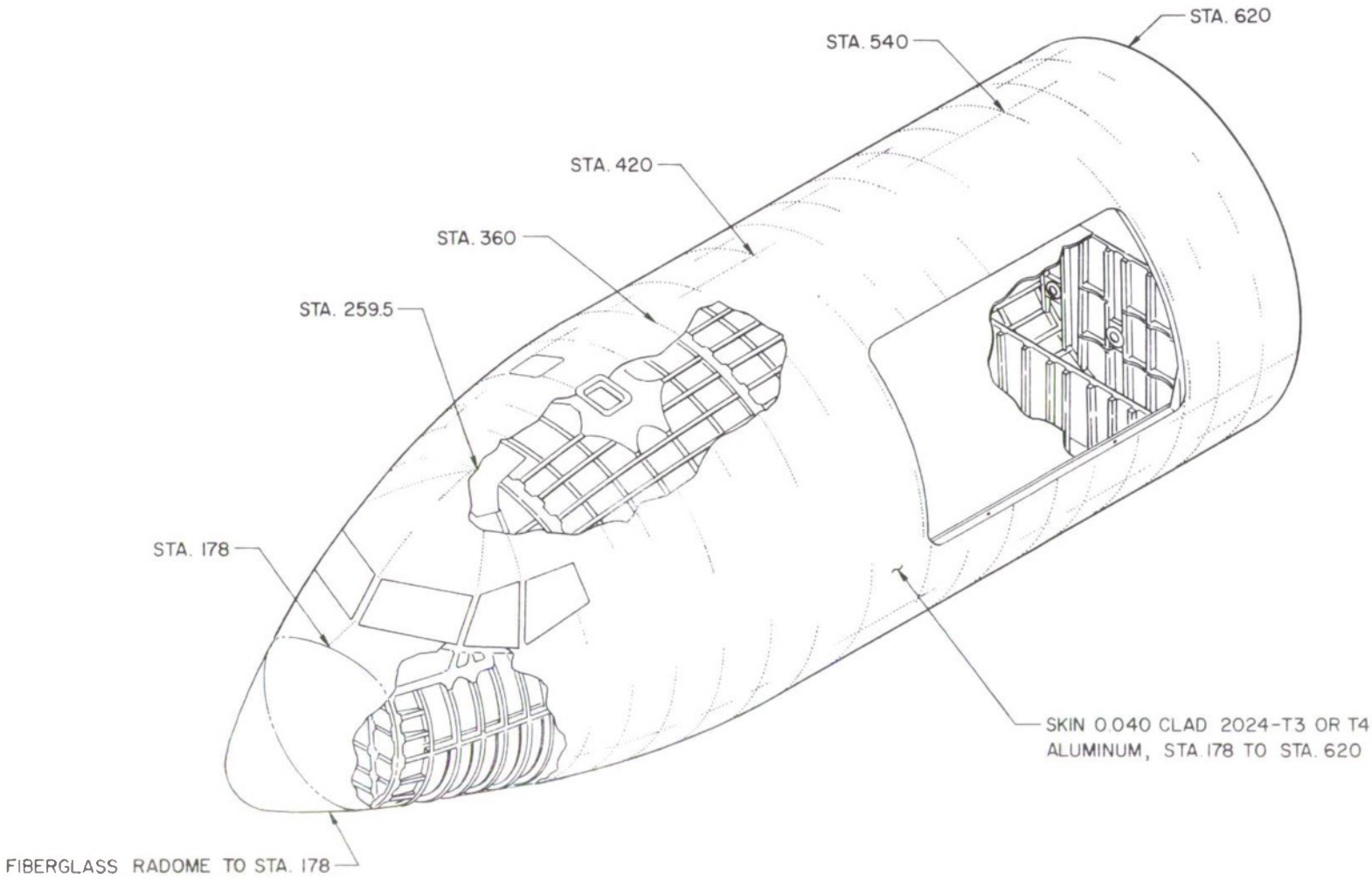

Figure 24. Boeing 707 Aircraft, Forward Fuselage Section A

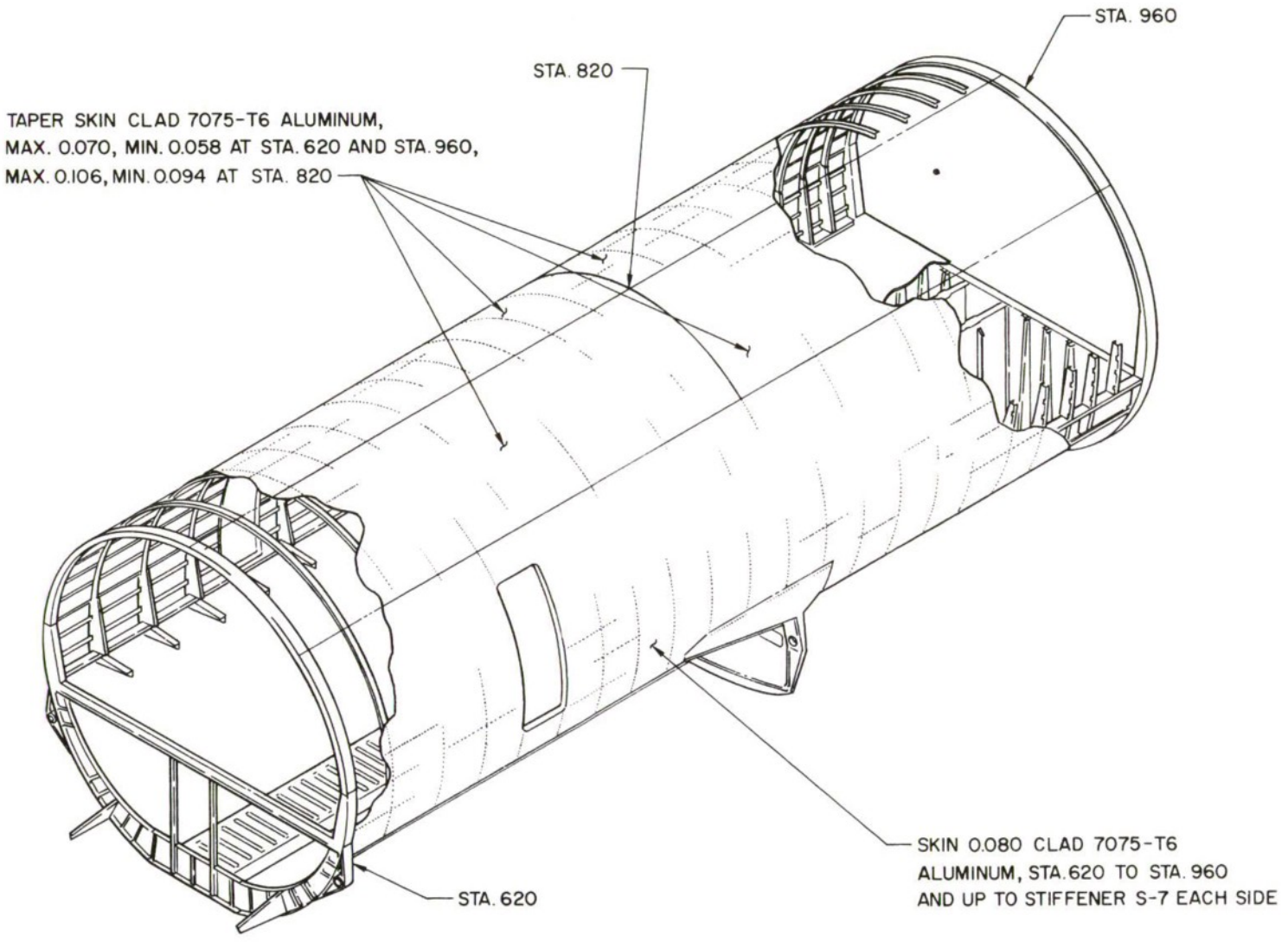

Figure 25. Boeing 707 Aircraft, Central Fuselage Section B

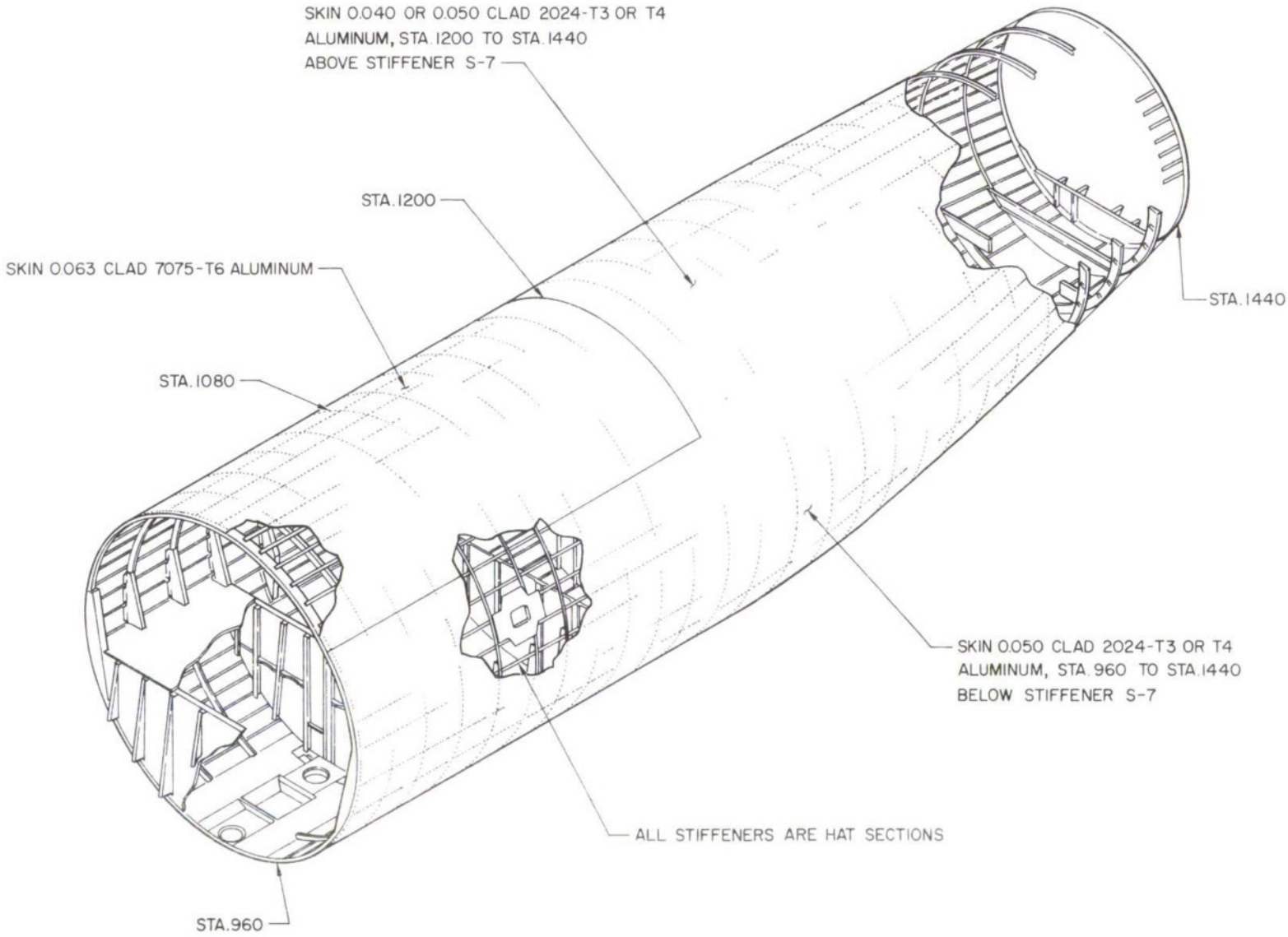

Figure 26. Boeing 707 Aircraft, Rear Fuselage Section C

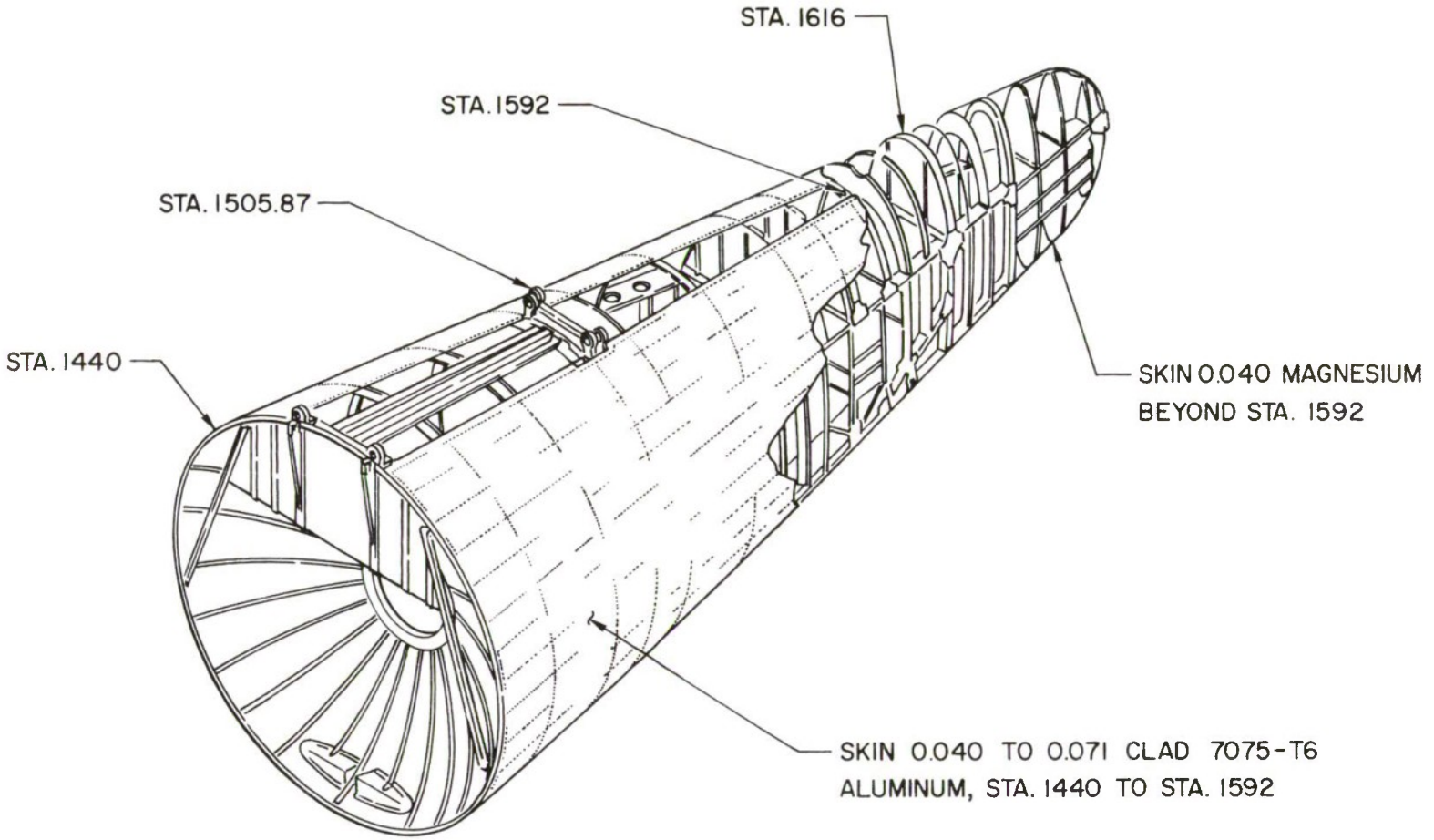

Figure 27. Boeing 707 Aircraft, Tail Fuselage Section D

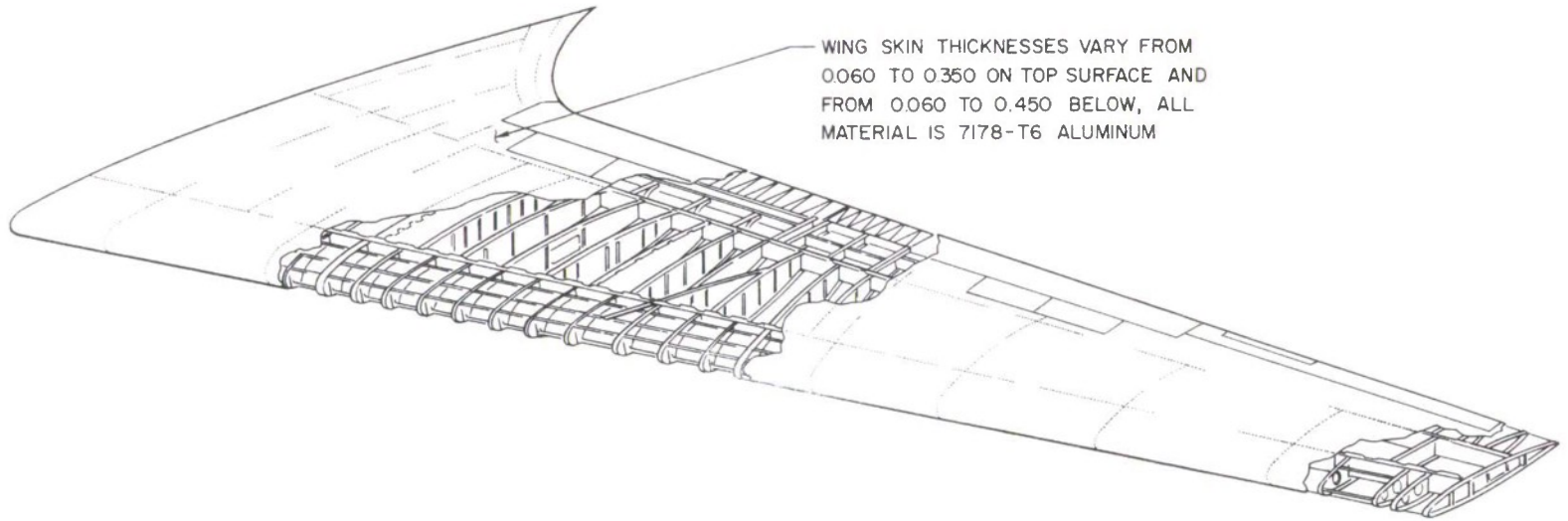

Figure 28. Boeing 707 Aircraft, Wing Structure Section E

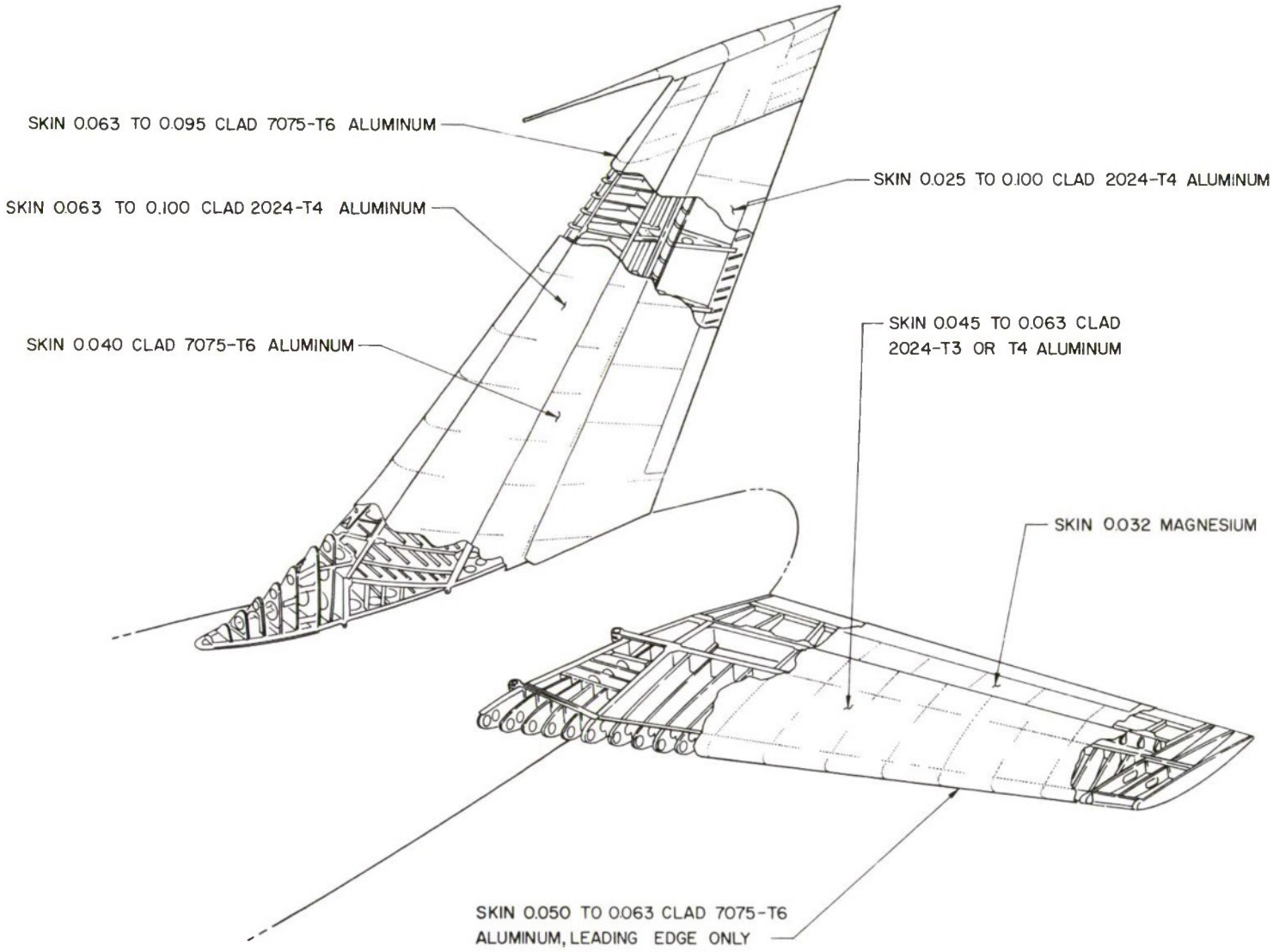

Figure 29. Boeing 707 Aircraft, Rudder and Stabilizer Structure Section F

stiffened circumferentially by bulkheads and 7075-T6 "Z" section frames.

The wing is a full-cantilever, semi-monocoque, cellular structure tapering in both platform and depth. The skin coverings vary in thickness from 0.06 to 0.45 inch.

The horizontal stabilizer and vertical fin of the tail are of two-spar construction. There is no other spanwise stiffening.

The University of Dayton Research Institute has conducted an extensive study of the static and dynamic loadings required to fail the most vulnerable skin panels and other components on this aircraft [88]. The first step in their study was to perform stress analyses on several of the weaker fuselage skin panels. Since the skin panels transmit the blast loading to the internal structure, the location of the critical skin panels gives an indication of areas in which the substructure should be investigated. Complete analyses were conducted on these components. Based on their conclusions, a large fuselage skin panel located between fuselage stations 1060 and 1080 on the underside was shown to be the most critical or vulnerable skin panel. Permanent deformation of this panel occurs under a 2.3 psi reflected overpressure.

The unacceptable damage risk levels for the aircraft have been defined as damage which may cause loss of control of the aircraft. It is probable that the aircraft can undergo substantial deformation of its skin panels without approaching damage which would cause loss of control. Therefore, in this study, initial deformation to the substructure supporting the skin panel sections has been used to establish quantity-distance specification.

In [88], the static loading required to permanently deform the frame section supporting the vulnerable skin panels described above is 7.23 psi. The dynamic response of this panel is described as a function of the ratio of the positive duration of the blast wave to the natural period of the frame member. This relation is shown in Figure 30.

The natural period of the frame member T is given by:

$$T = 2\Pi/\eta \ , \qquad (52)$$

where:

$$\eta = 2.68 \sqrt{\frac{EIg}{A\rho R^4}} \ . \qquad (53)$$

In (53), and as previously defined,

E = Young's modulus

I = cross-sectional moment of inertia

g = gravitation constant

A = cross-sectional area

ρ = density of the frame material

R = radius of the frame.

Three values of Young's modulus for the aluminum frame were considered in the analysis: 10.6, 11.0, and 11.6 million psi. For E = 10.6×10^6 psi, a natural period of 36 msec was calculated for the aluminum frame.

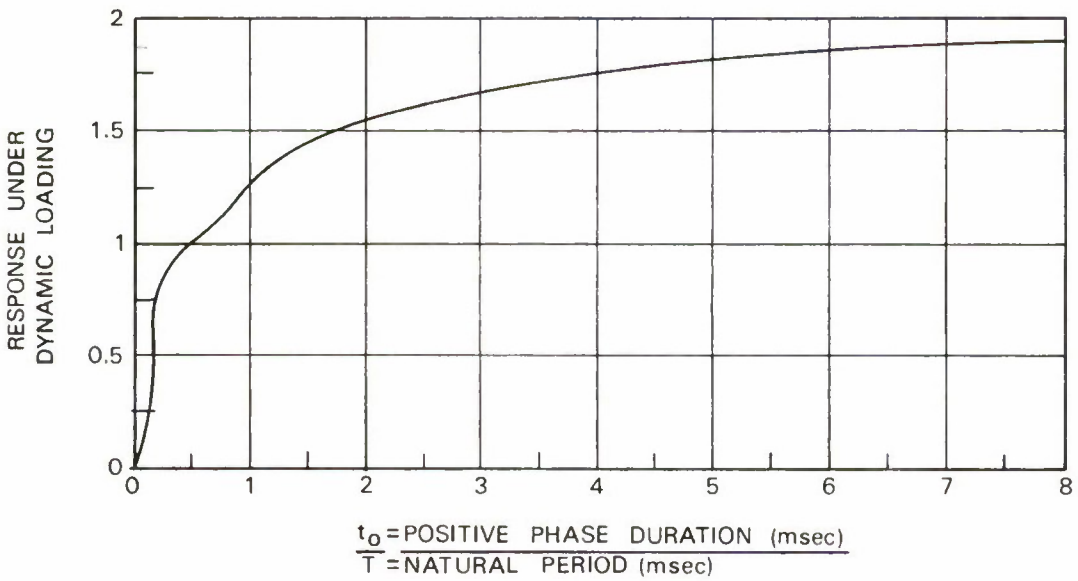

Figure 30. Dynamic Response Versus t_o/T for Free Air Overpressure

A quantity-distance specification for each charge size is computed as the distance at which the incident overpressure, P_o, in (53) satisfies the inequality,

$$D_F \cdot (R_F \cdot P_o) > 7.23 \text{ psi} \qquad (54)$$

where:

D_F = dynamic response factor determined from Figure 30

R_F = reflection factor taken from Figure 14.

For a normal side-on impingement of the blast wave on the fuselage, the reflection coefficient for the panel under investigation is determined from an angle of incidence of 63 degrees.

The plot of the pressure-impulse curve for the aircraft target is presented in the Results section.

V. RESULTS

This project has resulted in additional information which will be of substantial value in the assessment of the potential risks associated with explosive storage in the vicinity of inhabited structures. These results will be presented and discussed in this section of the report.

A. BASIS FOR THE RESULTS

These results have been developed through an extensive review of past test activity and theoretical treatments, plus the use of mathematical models of the behavior of targets in a blast field; these models have been described in earlier sections of this report. The computer program for the implementation of all the models has been prepared in Fortran language and furnished as a deck of program cards, a program statement printout, and a program user's manual.

These results have been developed for the estimation of blast damage only, and are applicable to the specific targets which have been defined. It is recognized that fragments, debris, fire, and other damage mechanisms can represent real hazards to these targets; however, other programs exist for investigating these factors, and they have thus been eliminated from this consideration.

The results are given for charge sizes of 1,000 to 9 million pounds of TNT equivalent explosive under the following conditions: detonated in a single event; located on the surface of the ground; without intervening barricades between the charge and target; and for charge shapes which produce a hemispherical blast wave within a few λ_d (scaled distance) units of the charge. While other charge-target interactions can be modeled with minor adjustments, it is important to understand that the reported results are only for these specific (and most probable) conditions. Further, these results are specific for the targets which have been described and can only be expanded to other apparently similar targets through an understanding of the structural properties of the new target and an application of the computer model to the new requirement. For most cases, the new target dimensions and

structural properties can be used as an input to the program and a new set of values determined directly.

It is important when investigating targets other than the specific ones described for this study to include all of the structural changes and to be sure that the model is applicable. There are types of changes which would require a change in the model as well as a new set of structural properties. For example, the full height office building wall has been analyzed as an 8-inch masonry wall rigidly restrained both at the top and bottom of the panel by 2-foot square reinforced concrete beams. This wall possesses most of its strength due to this rigid restraint. If the wall panel were built with a small space at the top, perhaps filled with calking material, the wall failure mode and strength would change greatly. There are many situations such as this where the construction can appear to be very similar, but in reality is quite different. The user of this model must be cognizant of these real differences.

B. QUANTITY-DISTANCE VALUES

Figures 31 through 35 present the computed acceptable distance requirements for each of the ten targets exposed to blast from 1,000, 10,000, 100,000, 1 million, and 9 million pounds of explosive. The circle represents the distance value computed using the most probable set of structural and physical properties for the target. In many cases a range of values for each parameter has been used as input to the model. Where any combination of these parametric variations produced a change in the distance requirement, it has been noted and the maximum spread of such values shown on the Figures.

The present inhabited building distance limitations as well as other applicable distances from [28] are shown on each figure for comparison purposes.

These results indicate that the present inhabited building distance requirements may be somewhat conservative for the 1,000-pound quantity if only blast hazards are considered. All inhabited targets fell within the barricaded distance and most were at distances less than 300 feet.

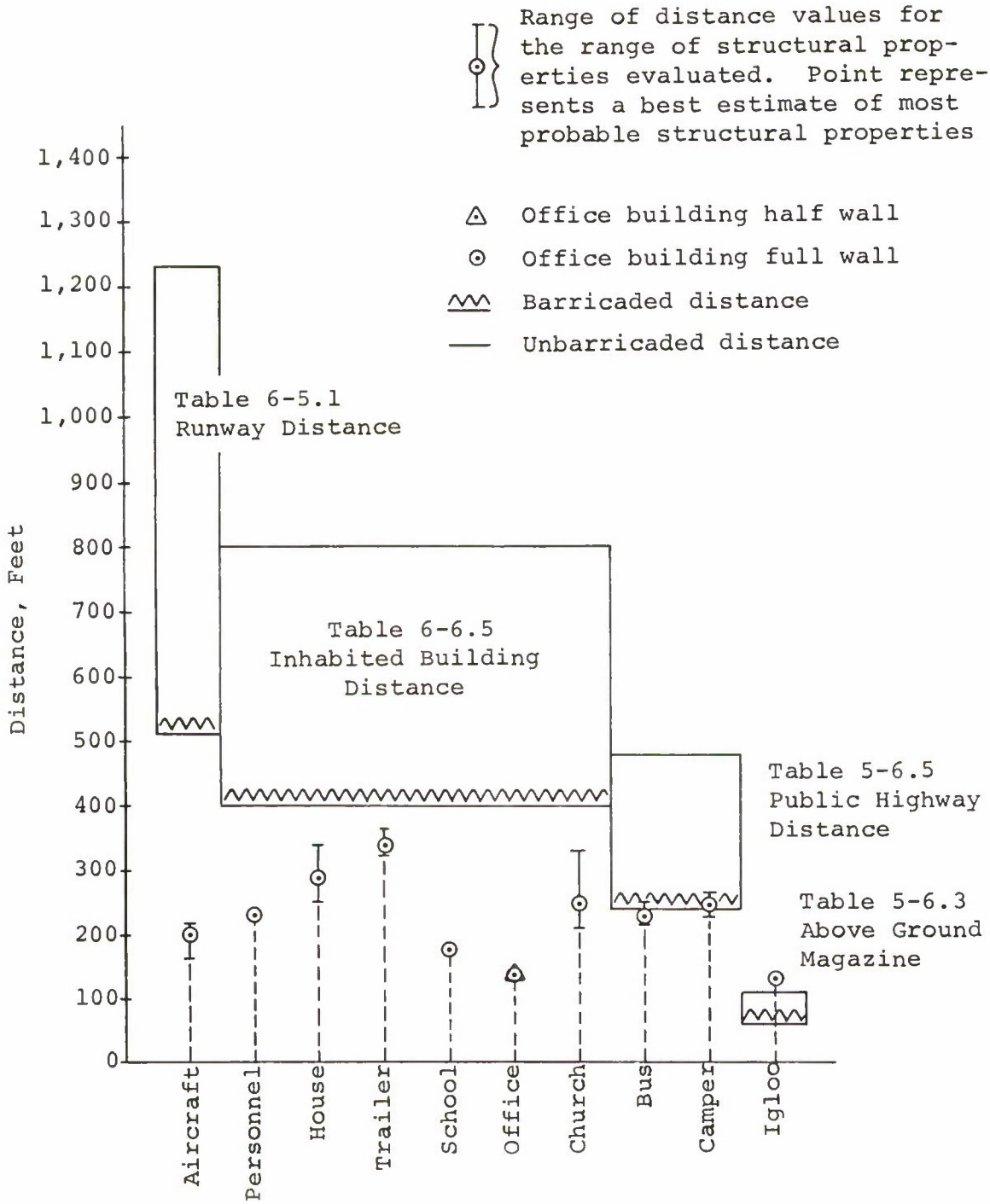

Figure 31. Computed Distance Requirements for Acceptable Damage to Targets Exposed to the Blast From 1,000 Pounds of TNT

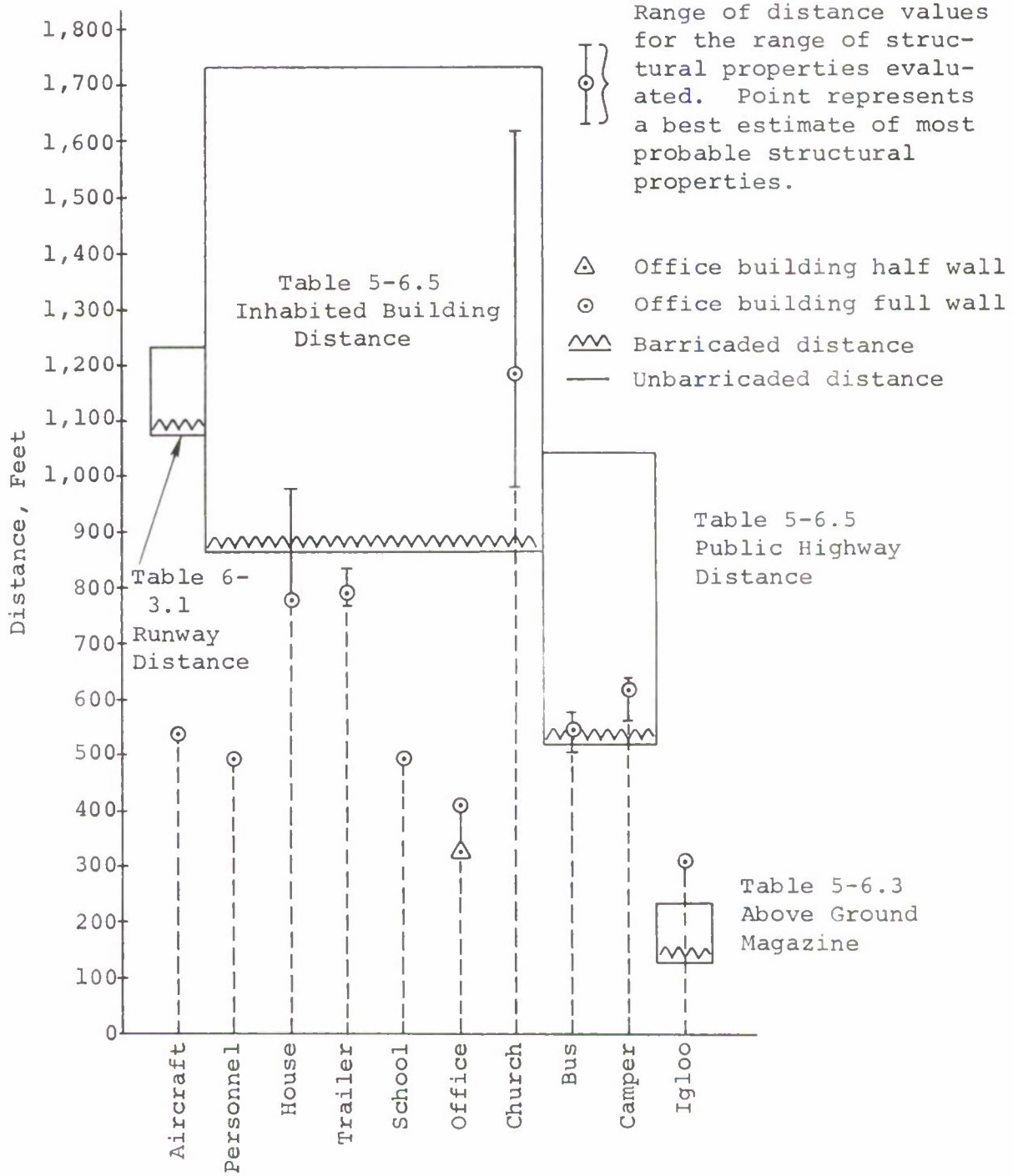

Figure 32. Computed Distance Requirements for Acceptable Damage to Targets Exposed to the Blast From 10,000 Pounds of TNT

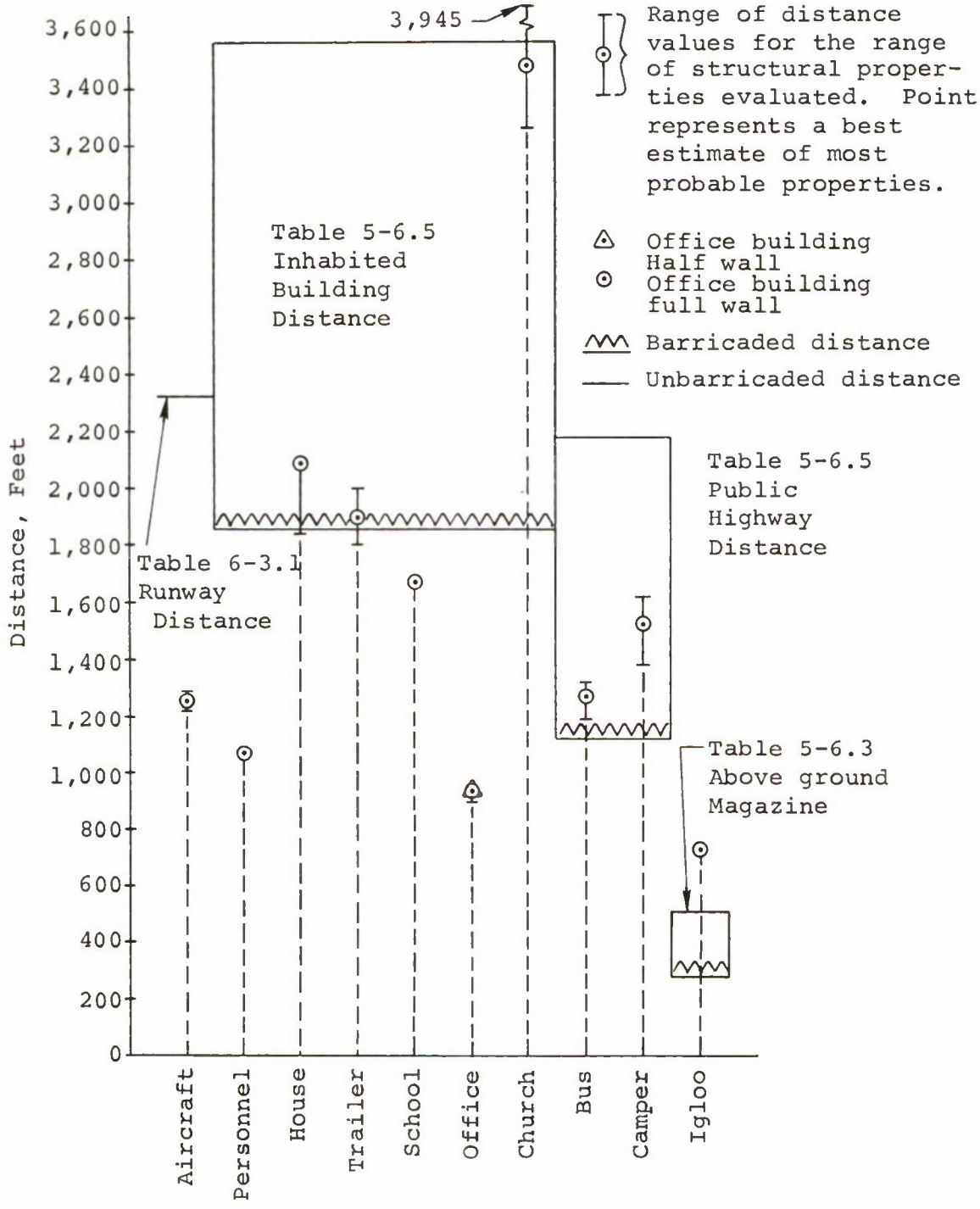

Figure 33. Computed Distance Requirements for Acceptable Damage to Targets Exposed to the Blast From 100,000 Pounds of TNT

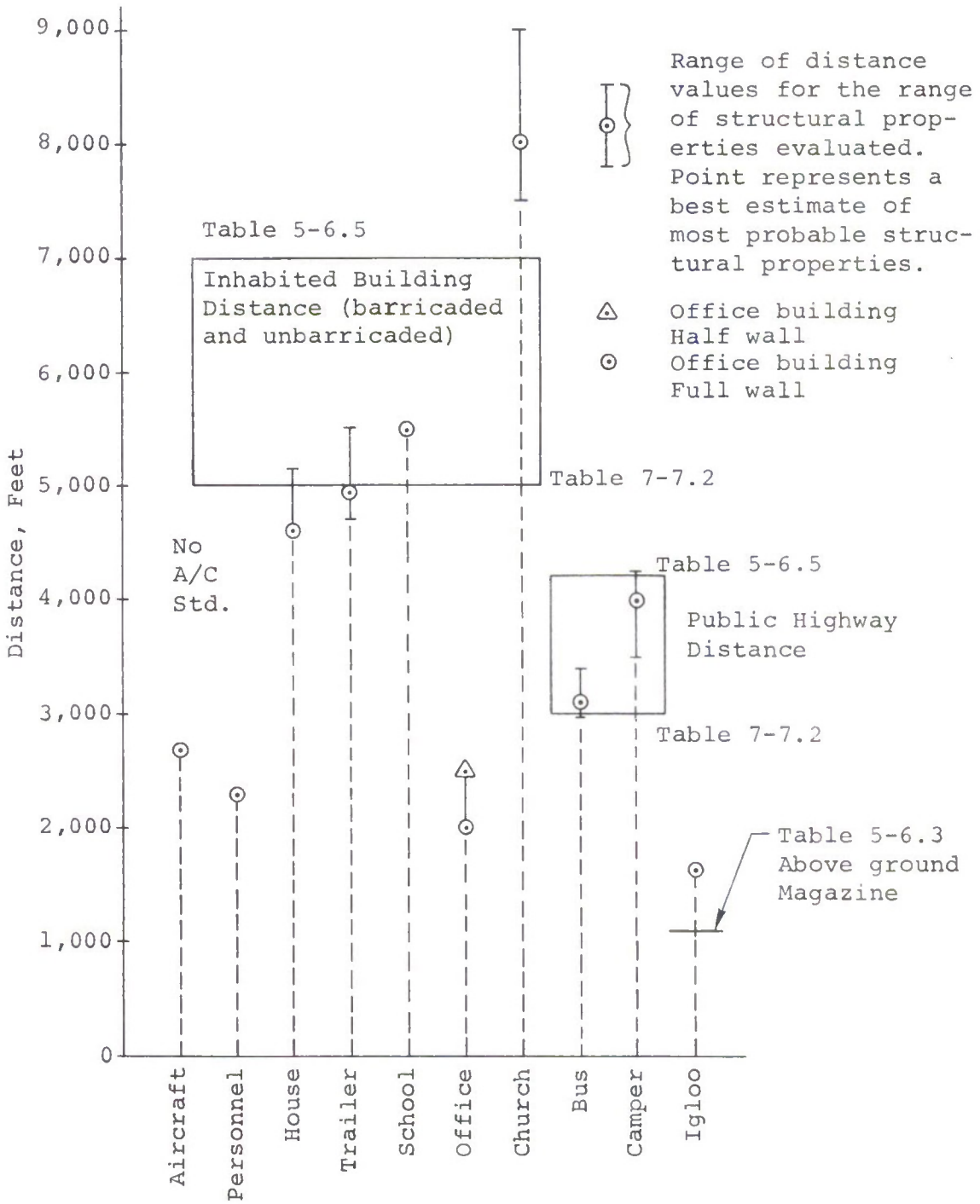

Figure 34. Computed Distance Requirements for Acceptable Damage to Targets Exposed to the Blast From One Million Pounds of TNT

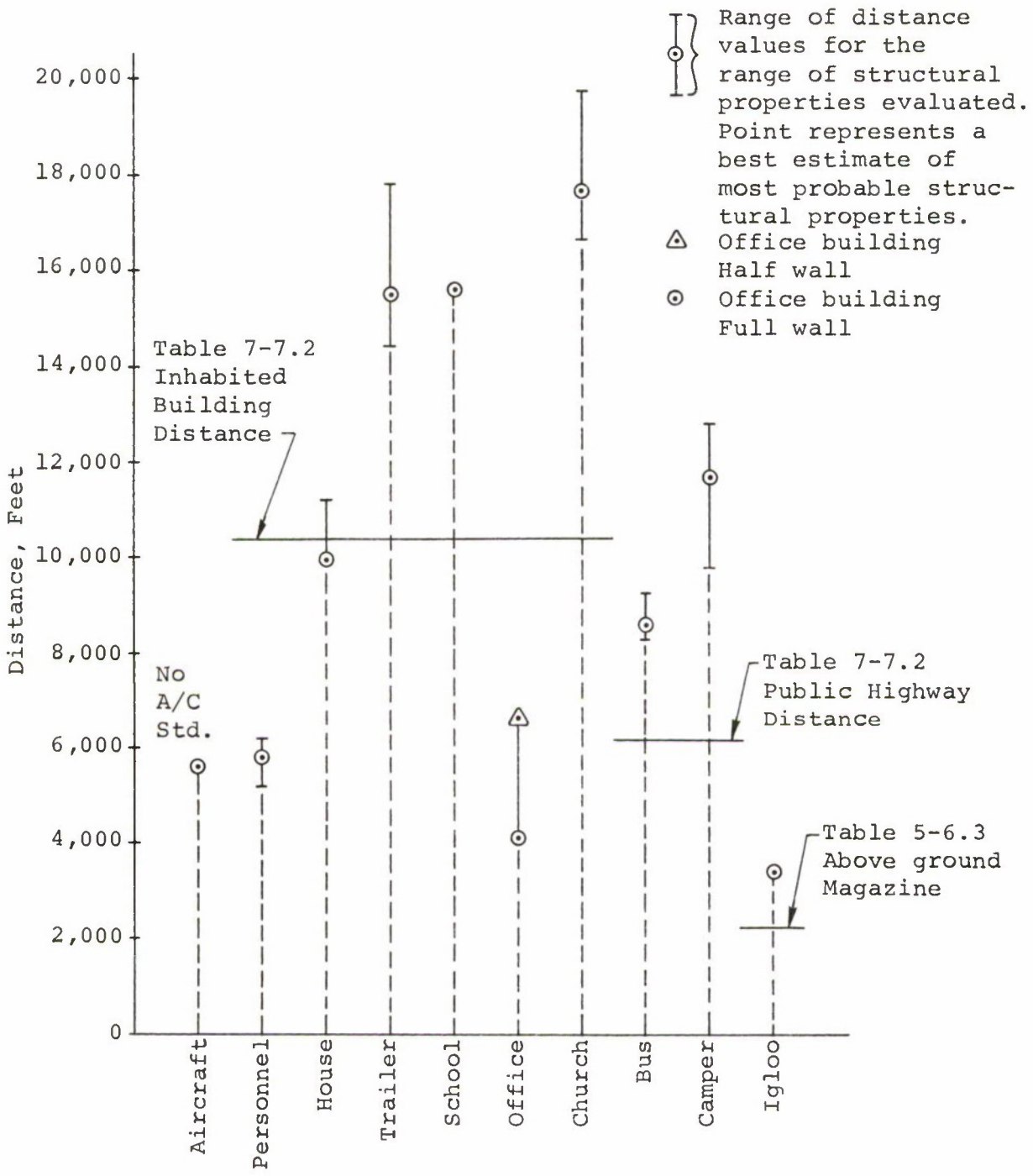

Figure 35. Computed Distance Requirements for Acceptable Damage to Targets Exposed to the Blast From 9 Million Pounds of TNT

The computed distances for the 10,000-pound quantity indicate that the large church roof might be damaged, at the present barricaded limit, to a greater extent than may be acceptable. This large roof surface is a very efficient blast energy collector, and it will be noted that the church target must be expected to suffer unacceptable damage at distances beyond the barricaded storage limit for all of the large explosive quantities.

The computed distances for all other inhabited targets are within or very near the barricaded storage limit for 10,000-pound charges.

There is good experimental verification from the China Lake tests [98] for the house exposed to a 10,000-pound blast. The frame house exposed at 865 feet in these tests suffered only minor structural damage.

The results from the set of computations for a 100,000-pound charge are similar to the 10,000-pound results in that only one target, the church roof, would be expected to suffer extensive damage at the present barricaded limit. Two other targets, the house and trailer fall very near the present limit but might not be damaged unacceptably. Other inhabited buildings are within the present requirement.

The million-pound limitation of 7,000 feet appears to be conservative, since only the church roof shows unacceptable damage at this limit. All other buildings fell below 5,500 feet.

There is experimental verification for the house target at this charge size from the Prairie Flat test. A frame house placed at 4,000 feet from the charge suffered significant but acceptable damage in this test. The model would place the Prairie Flat house at between 3,400 and 4,500 feet depending on the values of the rafter strength properties assumed.

For the 9-million-pound charge size, the computed results indicated a substantial hazard to three of the target structures at the 10,400-foot limitation, and significant risk to the two vehicles. It appears that the school, church, and trailer would be unacceptably damaged and that the camper-pickup and bus are near overturning. The other inhabited targets are apparently safe from blast damage at the present limitation. Three of the targets would not suffer unacceptable damage at even much closer distances.

These target distance values are based upon the response of the more vulnerable components of the target to the reflected pressure produced on that component by the blast from a specific quantity of explosive at the computed distance. The effect of target resonant behavior, opposing forces acting on the component, and the incident pressure decay function were all considered where appropriate. The net result of the computation is an incident peak pressure and impulse which is determined to be just sufficient to cause the established failure level to the particular target.

C. PRESSURE-IMPULSE RELATIONSHIPS

Figures 36 through 46 present the functional relationships between incident peak pressure and impulse for the limiting condition for the ten targets. Thus, all points above the curves would exceed the acceptable damage limits established, while those below the curve would be acceptable. Values for the five charge sizes are plotted and shown as points. A smoothed curve has been drawn through the plotted data. These values correspond to the most probable values, shown as circles in the preceding Figures (31 through 35).

These results provide excellent confirmation of the pressure-impulse relationships postulated by O. T. Johnson [52] and given theoretical support by E. E. Hackman [42]. The functions are clearly hyperbolic and are well defined through the regions of greatest interest.

It should be noted that the iterative process employed by the model uses integer values of scaled distance or λ_d units. Thus, the distances determined are within plus or minus 10 feet for the 1,000-pound charge size, plus or minus 100 feet for the million-pound size, etc. In refining the program, this iterative process could be changed to consider smaller λ_d increments, but it would greatly increase the machine running time. The incident pressure and impulse values are sensitive to the distance determined and a reduction of one λ_d unit of distance would increase both the peak pressure and impulse values. Some of the apparent dispersion in pressure-impulse values on these figures may be attributable to the use of interger λ_d increments of distance.

W	R	P	I
1,000	290	1.79	30
10,000	776	1.36	54
100,000	2,089	1.00	92
1,000,000	4,600	0.92	185
9,000,000	9,985	0.92	350

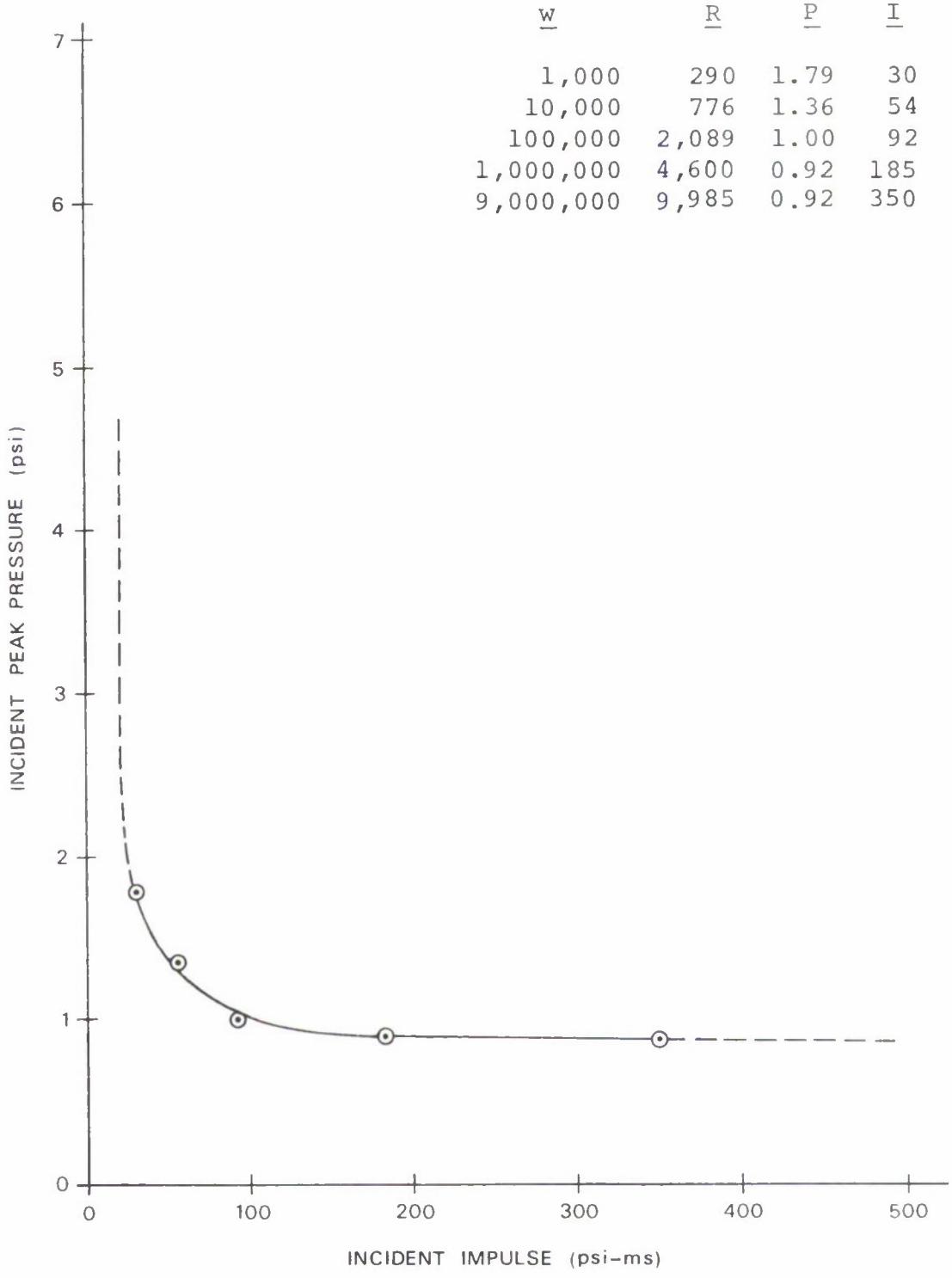

Figure 36. Acceptable Incident Peak Pressure-Impulse Relationship for Constant Damage to the House

W	R	P	I
1,000	180	3.64	48
10,000	496	2.49	84
100,000	1,671	1.36	116
1,000,000	5,500	0.77	155
9,000,000	15,600	0.52	235

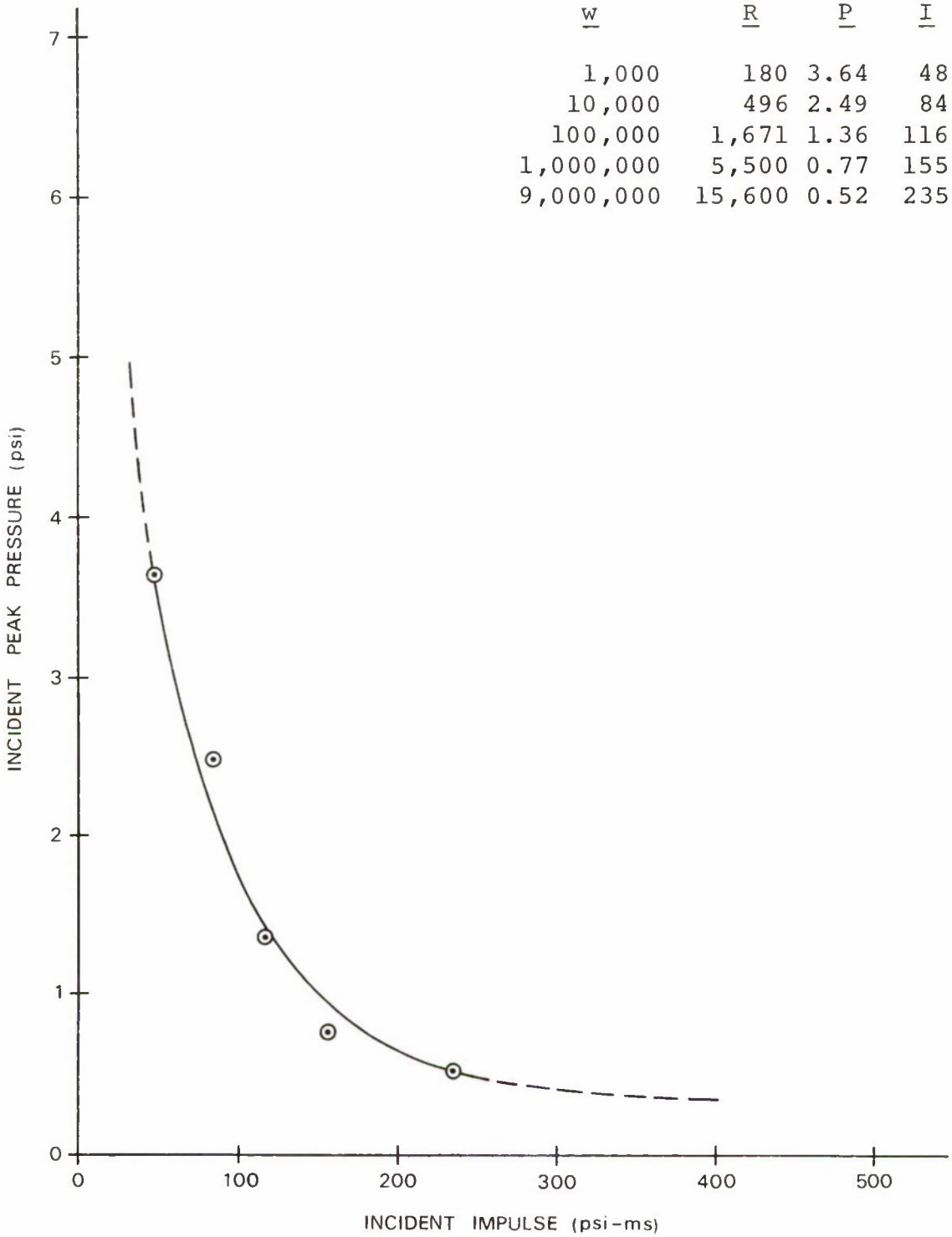

Figure 37. Acceptable Incident Peak Pressure-Impulse Relationship for Constant Damage to the School Wall

W	R	P	I
1,000	140	5.68	61
10,000	323	4.60	128
100,000	928	3.00	205
1,000,000	2,500	2.15	340
9,000,000	6,656	1.58	550

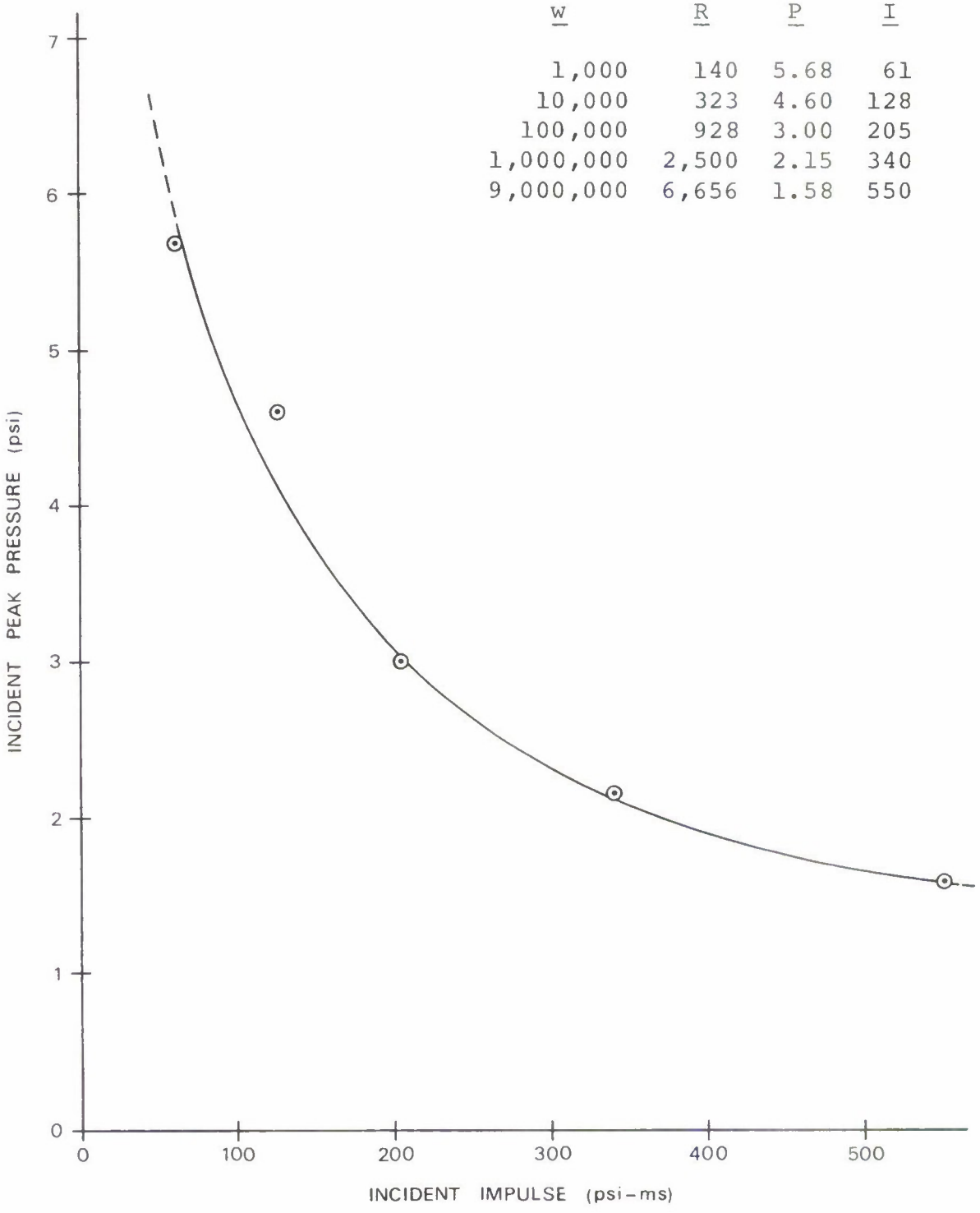

Figure 38. Acceptable Incident Peak Pressure-Impulse Relationship for Constant Damage to the Office Building Half Wall

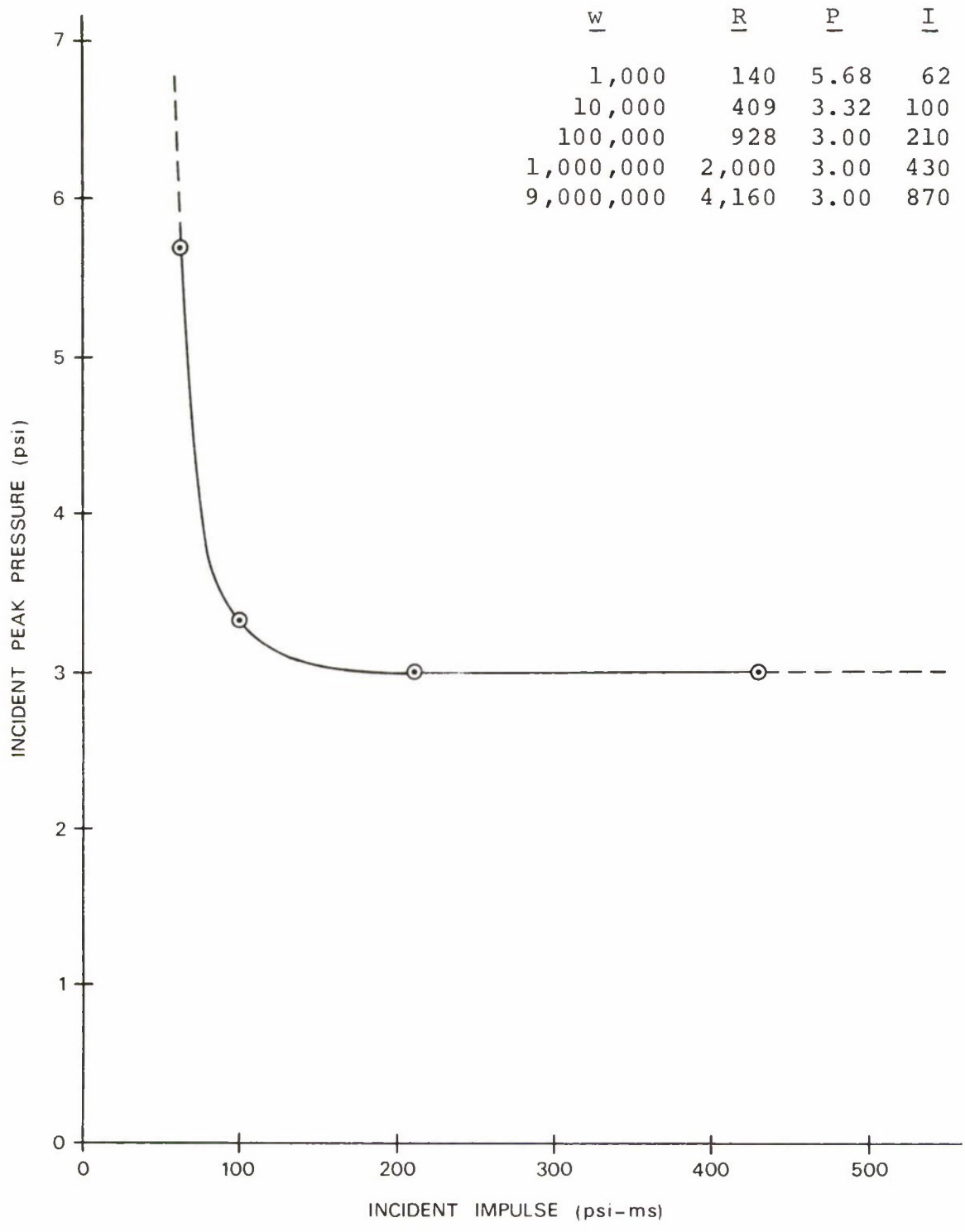

Figure 39. Acceptable Incident Peak Pressure-Impulse Relationship for Constant Damage to the Office Building Full Wall

W	R	P	I
1,000	230	2.5	38
10,000	496	2.5	80
100,000	1,068	2.5	180
1,000,000	2,300	2.5	370
9,000,000	5,824	2.0	630

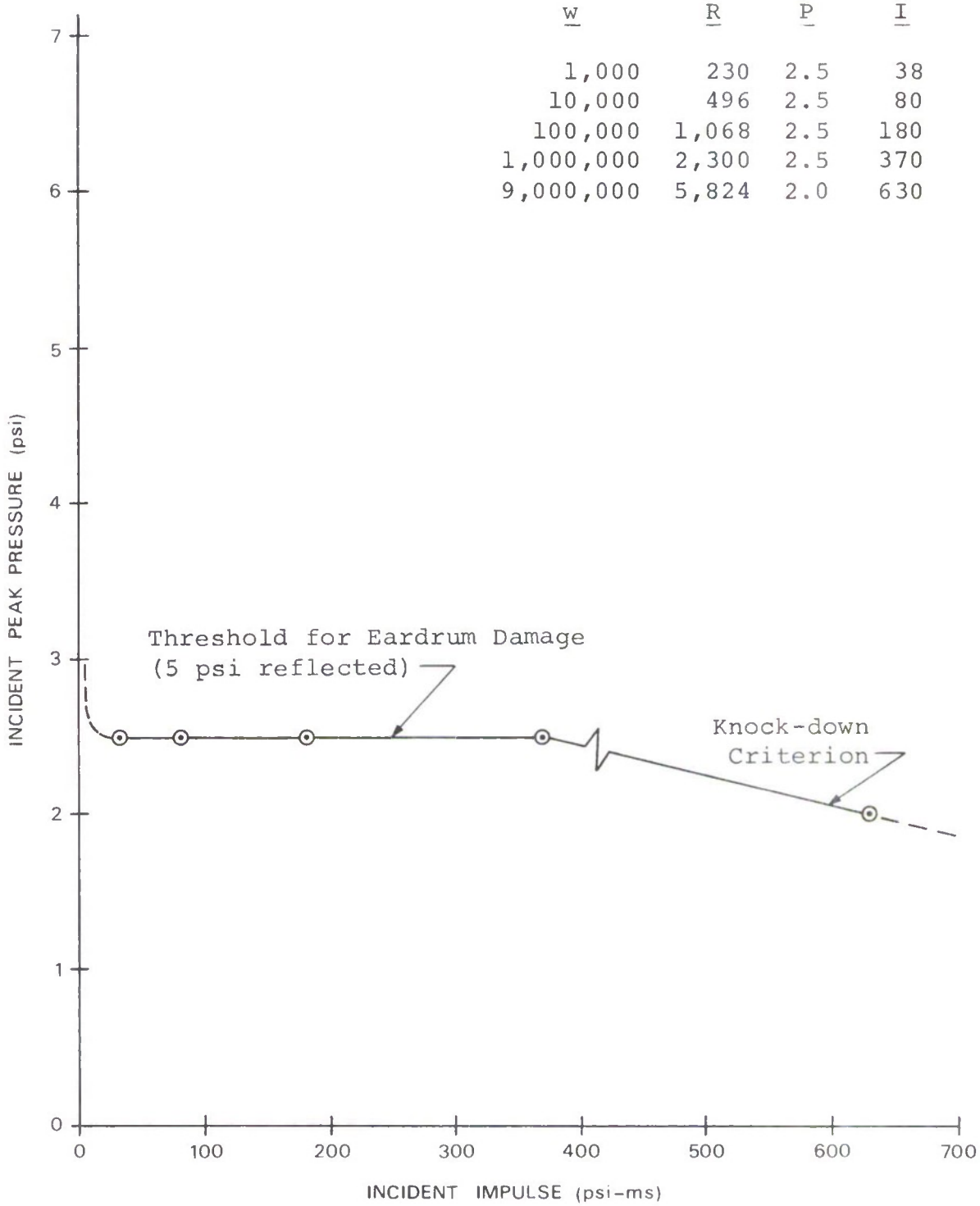

Figure 40. Acceptable Incident Peak Pressure-Impulse Relationship for a 168-Pound Man Exposed to Explosive Blast

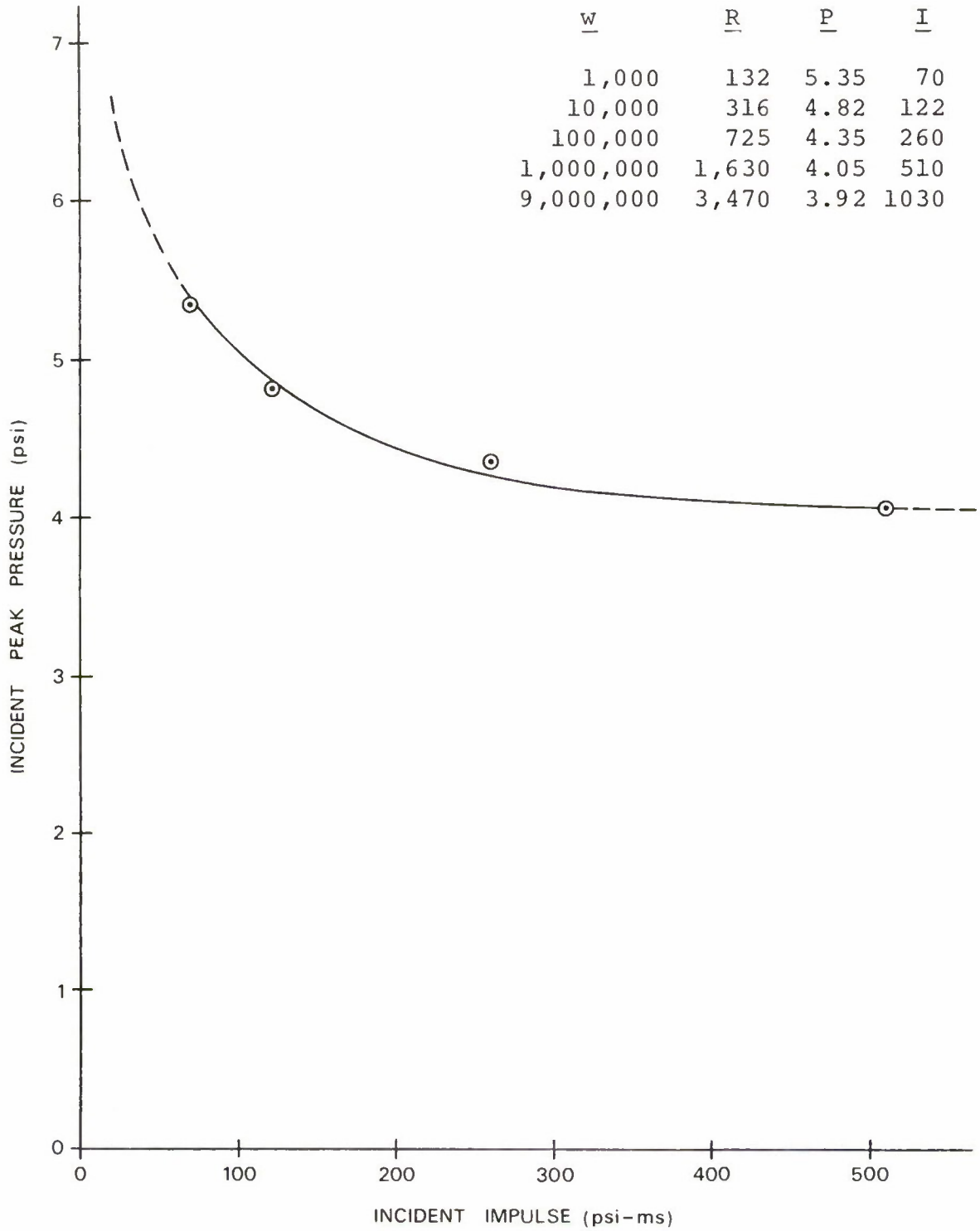

Figure 41. Acceptable Incident Peak Pressure-Impulse Relationship for Igloo Doors Exposed to Explosive Blast

W	R	P	I
1,000	250	2.15	35
10,000	1,185	0.77	35
100,000	3,481	0.52	54
1,000,000	8,000	0.48	106
9,000,000	17,680	0.44	210

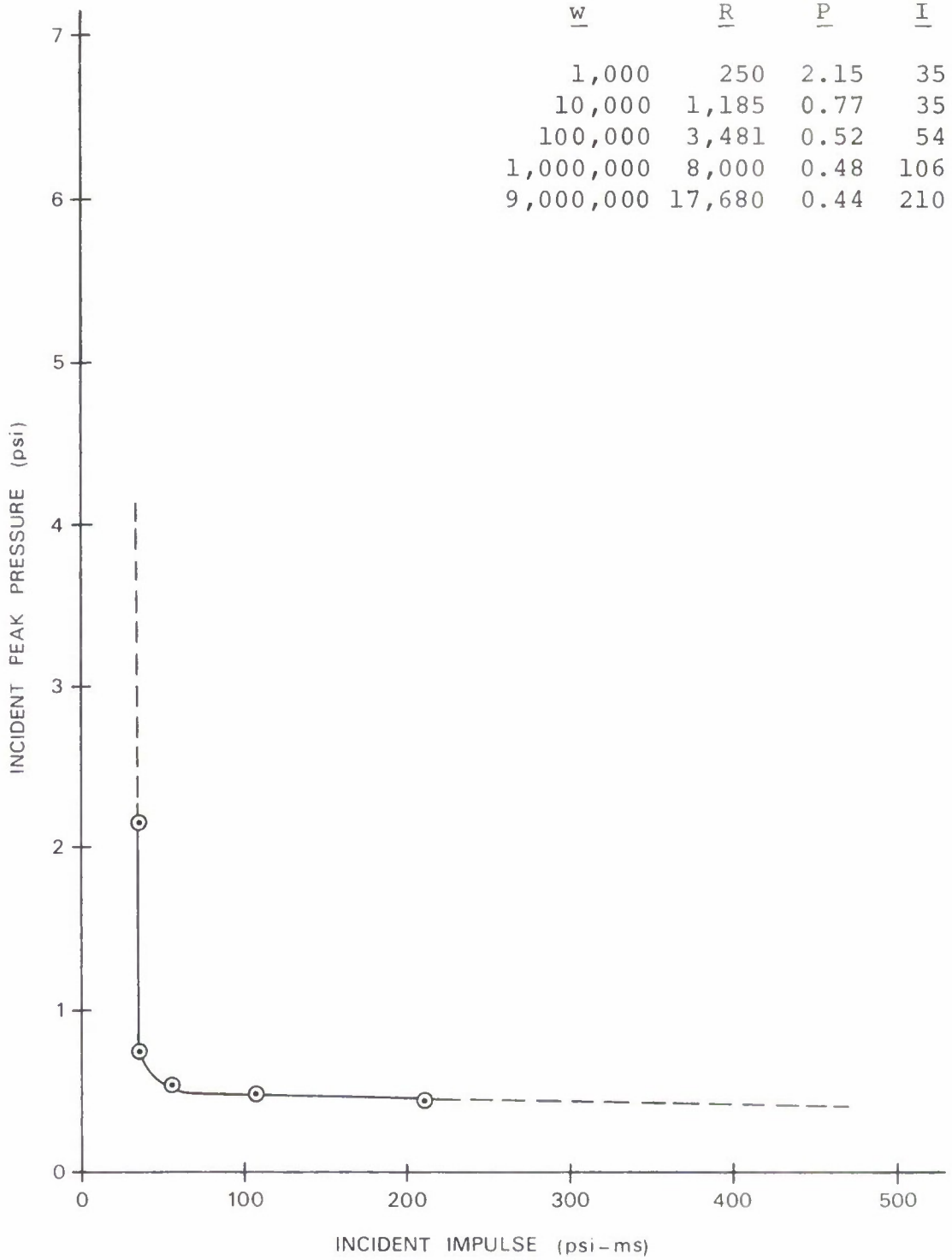

Figure 42. Acceptable Incident Peak Pressure-Impulse Relationship for Constant Damage to the Church Roof

W	R	P	I
1,000	340	1.45	26
10,000	790	1.23	50
100,000	1,900	1.08	102
1,000,000	4,950	0.82	172
9,000,000	15,500	0.49	240

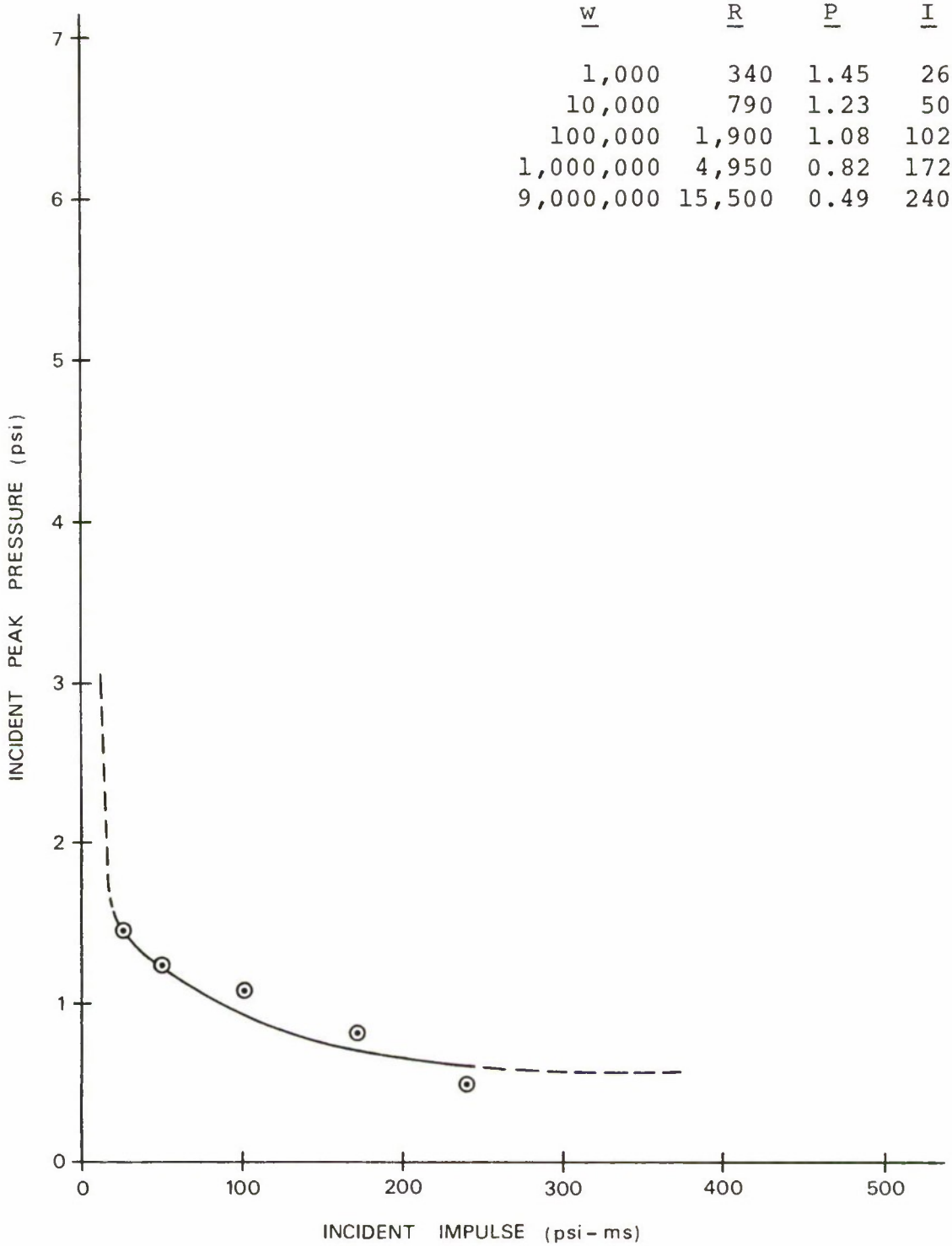

Figure 43. Acceptable Incident Peak Pressure-Impulse Relationship for Constant Damage (80 Percent of Overturning Impulse) to the House Trailer

W	R	P	I
1,000	230	2.45	38
10,000	550	2.10	72
100,000	1,280	1.90	152
1,000,000	3,100	1.59	272
9,000,000	8,600	1.13	433

NOTE: Bus is rounding a 460-foot radius curve at 50 mph. Centrifugal and blast forces are additive.

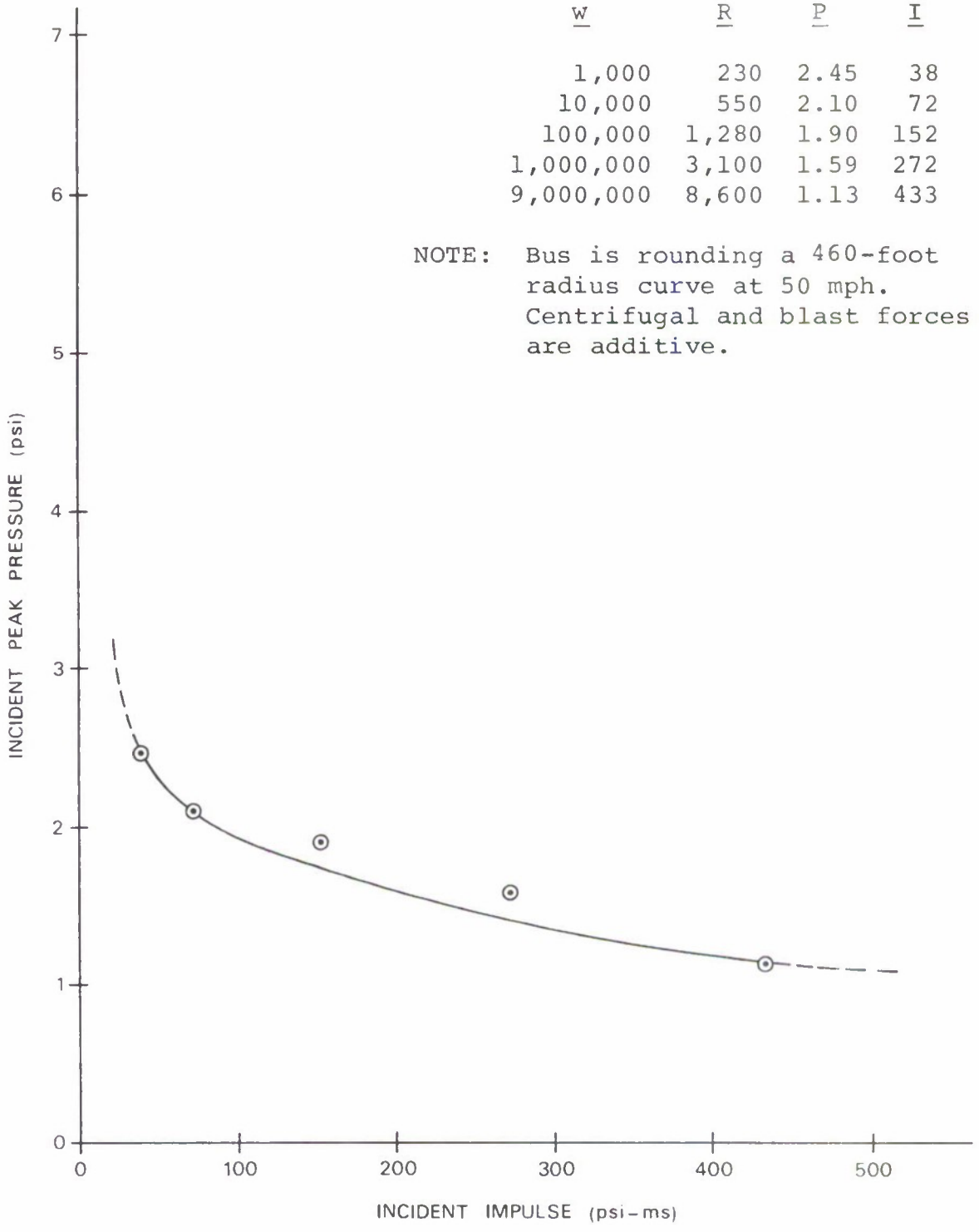

Figure 44. Acceptable Incident Peak Pressure-Impulse Relationship for Constant Damage (80 percent of Overturning Impulse) to a Highway Bus

W	R	P	I
1,000	250	2.20	35
10,000	620	1.75	64
100,000	1,520	1.45	128
1,000,000	4,000	1.10	212
9,000,000	11,700	0.72	320

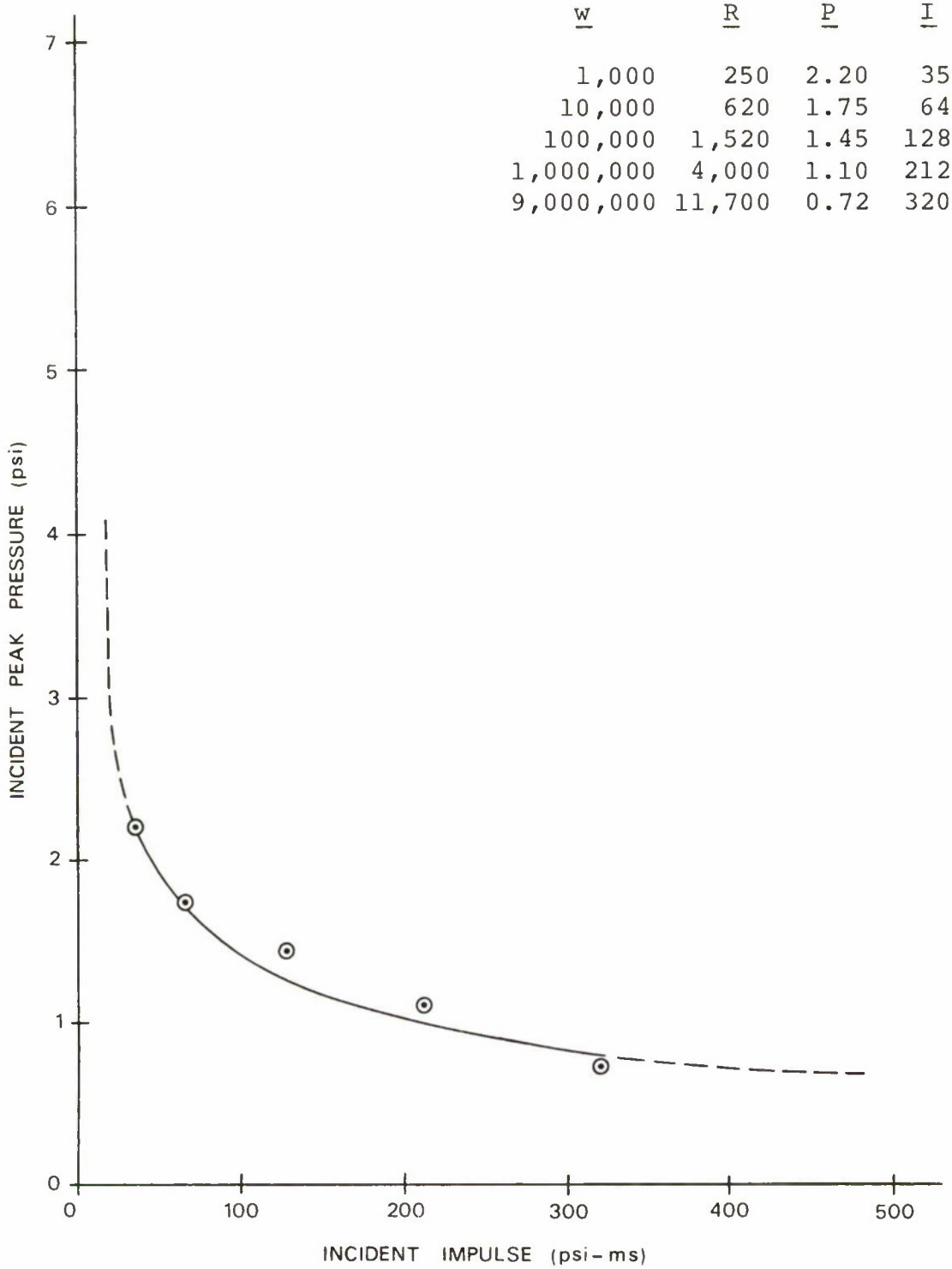

Figure 45. Acceptable Incident Peak Pressure-Impulse Relationship for Constant Damage (80 percent of Overturning Impulse) to the Camper-Pickup

W	R	P	I
1,000	200	3.00	43
10,000	539	2.15	73
100,000	1,253	1.97	155
1,000,000	2,700	1.97	315
9,000,000	5,616	1.97	650

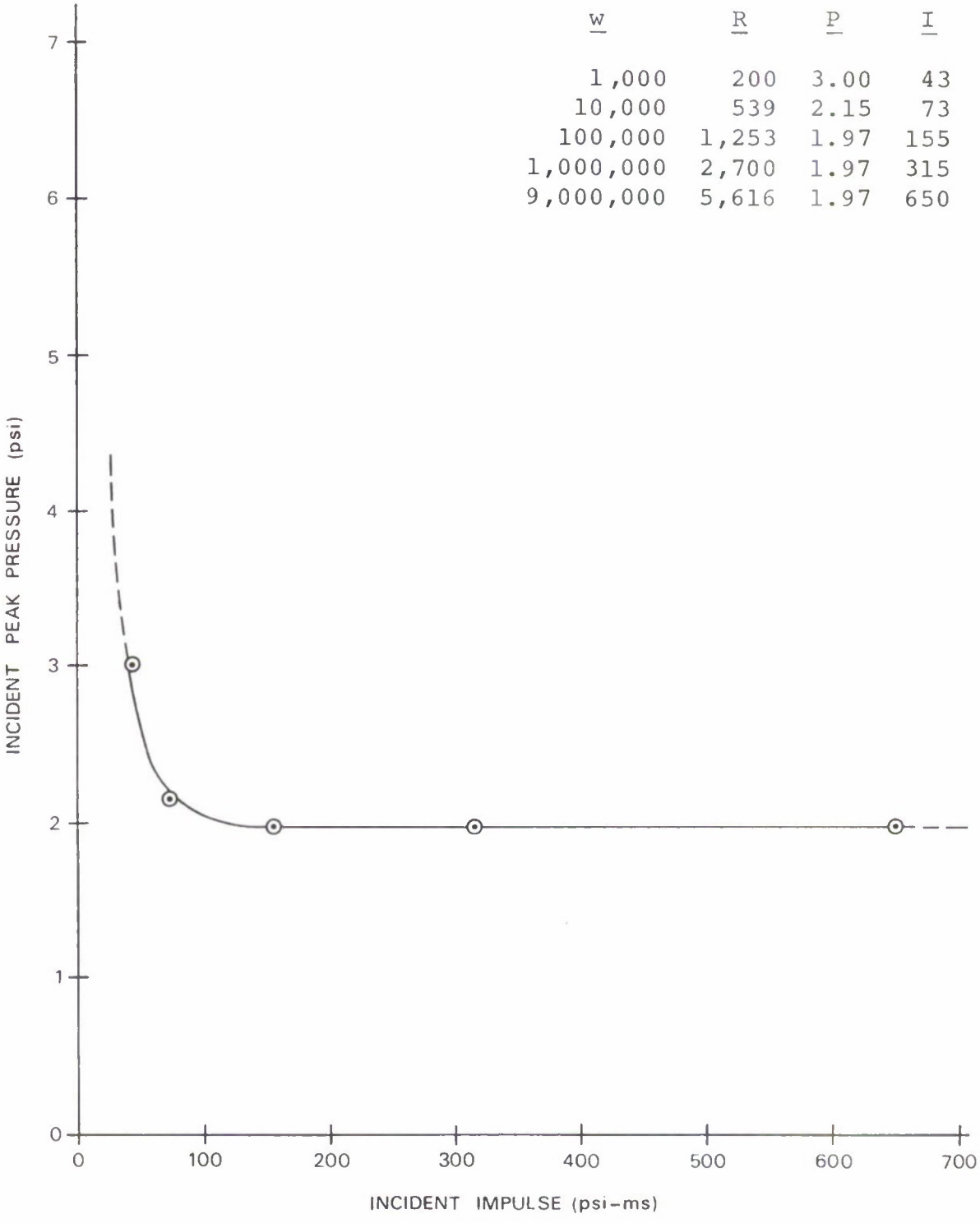

Figure 46. Acceptable Incident Peak Pressure-Impulse Relationship for Constant Damage to a Large Commercial Aircraft

It should once again be emphasized that these pressure-impulse results have been derived through analytical methods and that solid experimental evidence of target behavior under the appropriate levels of blast loading and damage response is frequently unavailable. The experimental data which have been found either confirm the computed values or at least do not contradict them.

There is, of course, an extensive body of experimental data for many types of targets exposed to blast waves. The project staff has reviewed most of these data and used the most pertinent values in deriving the analytical procedures. Some of the experimental evidence was not useable directly for reasons such as the following:

1. Much of the nuclear test data involved charge size equivalents which were substantially beyond the charge size range of this study.

2. Target structures were often exposed to blast levels far above or below those associated with the damage levels of interest to this program.

3. For some of the nuclear tests and for nearly all accident data, the correct TNT equivalency of the charge is not known with sufficient accuracy to satisfy project requirements.

4. In some instances the test target structure was not defined with suitable accuracy or the target structure was substantially different from the targets to be considered in this study.

5. Charge location (underground, air burst, etc.) was such as to make a determination of the blast wave at the target difficult to describe or difficult to translate to an equivalent surface burst charge.

D. CONSTANT DAMAGE SCALING FACTORS

The lack of applicable experimental data has precluded the direct uses of the equal damage scaling techniques described by O. T. Johnson in [52]. These scaling methods require that the quantity of explosive needed to cause the precise damage

level of interest be known for at least one combination of charge size and distance. Two or more experimental points would be preferable.

The data plotted in Johnson's report cover charge sizes up to 10,000 pounds; thus, the present study overlaps the explosive quantity range in that study only between 1,000- and 10,000-pound charge sizes. Figures 47 through 56 present the C_w, or constant damage distance ratios, for all the targets of this study. The five circled points correspond to the five charge sizes and the distance values shown in Figures 31 through 35. The dashed line represents Johnson's function for which:

$$C_w = 7.64\ w^{-0.435}$$

and extends only to the 10,000-pound level, since that was the limit of the experimental data treated. The experimental data points which fall within the region of interest to this study are also shown on these plots.

In order to make a meaningful comparison between the Johnson scaling factor and the values computed in this study, it has been assumed that the value for a 1,000-pound charge (the smallest in this study) was on the line and thus had a C_w value of 0.379. This is not substantially different from basing all data on a C_w value of 1.0 for a 100-pound charge as was done in BRL 1389.

An estimated best-fit straight line has been drawn through the calculated points as an aid to interpolation. These results agree very well with the function proposed by Johnson. The slope of the line varies somewhat with the type of target and appears to be slightly less for eight of the targets and slightly more for the other two.

In the case of the large wooden structures, the house roof and the church roof, a straight line function does not fit the data as well as a slightly curved function would. These targets are different from all of the others in that they absorb energy only through elastic deformation right up to the point of failure. All of the other targets have some form of plastic deformation or kinetic energy absorption process which exits between the elastic limit and the defined failure condition.

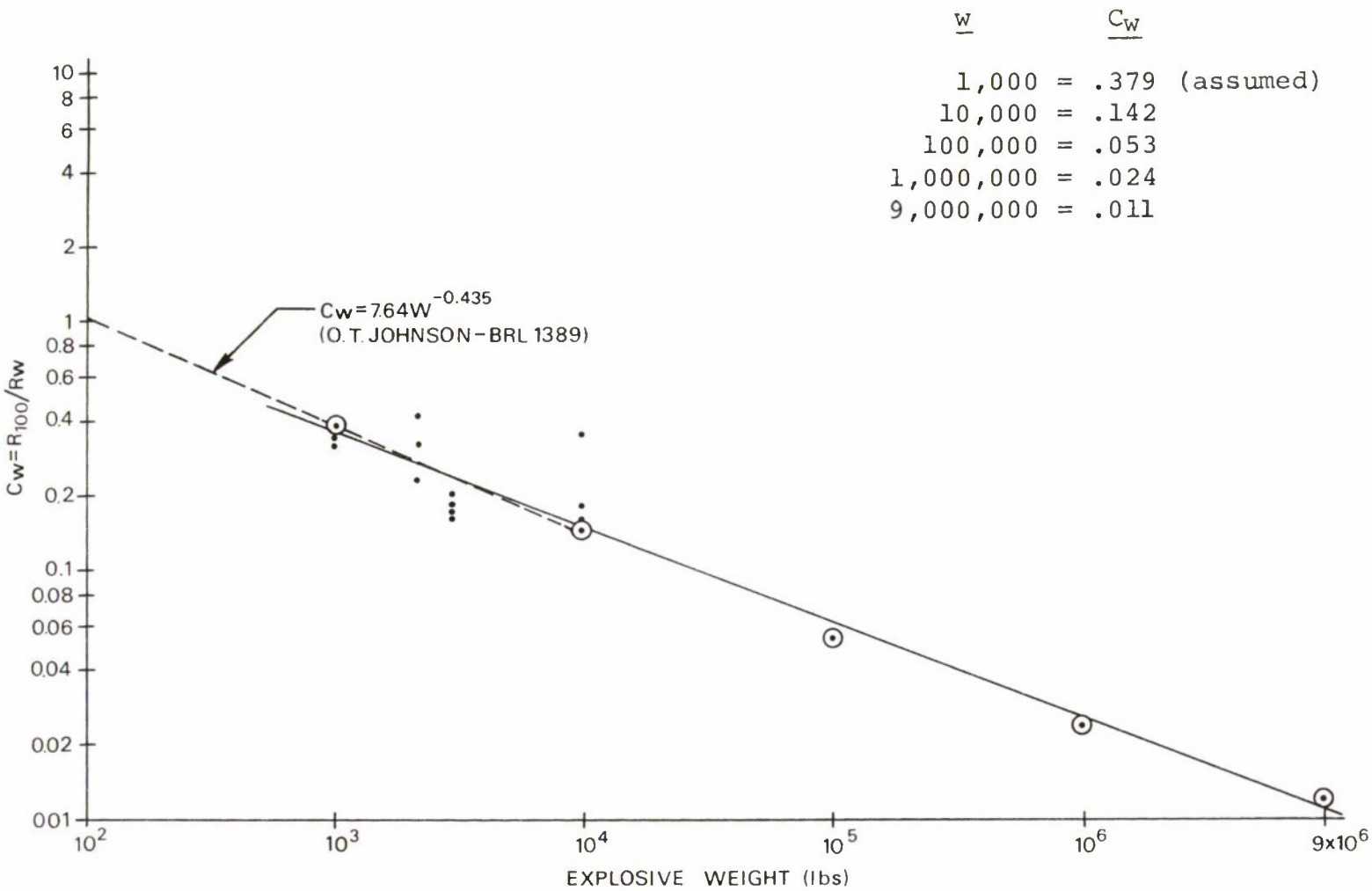

Figure 47. Scaling Relationships for Constant Acceptable Damage to the House

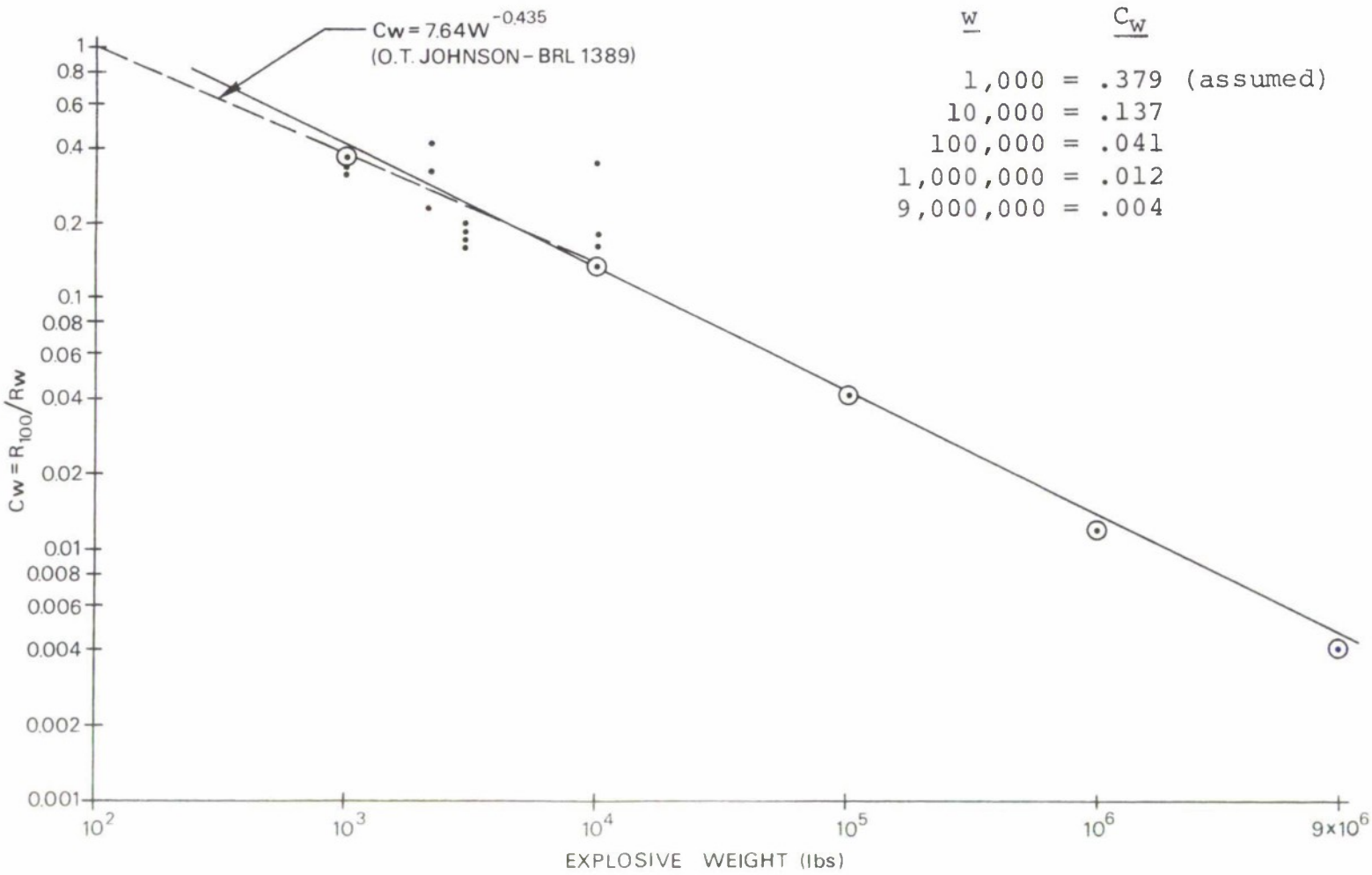

Figure 48. Scaling Relationships for Constant Acceptable Damage to the School

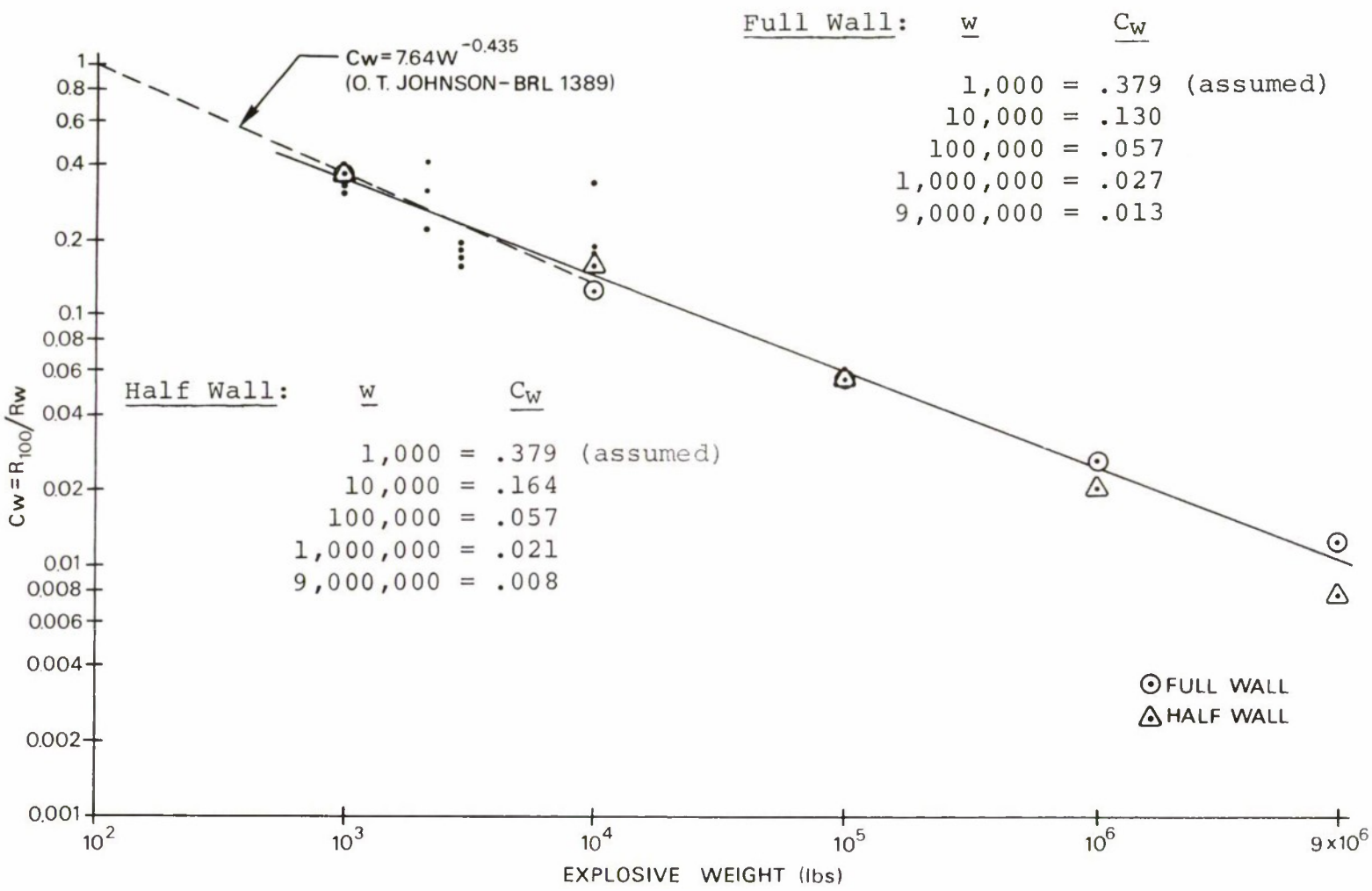

Figure 49. Scaling Relationships for Constant Acceptable Damage to the Office Building

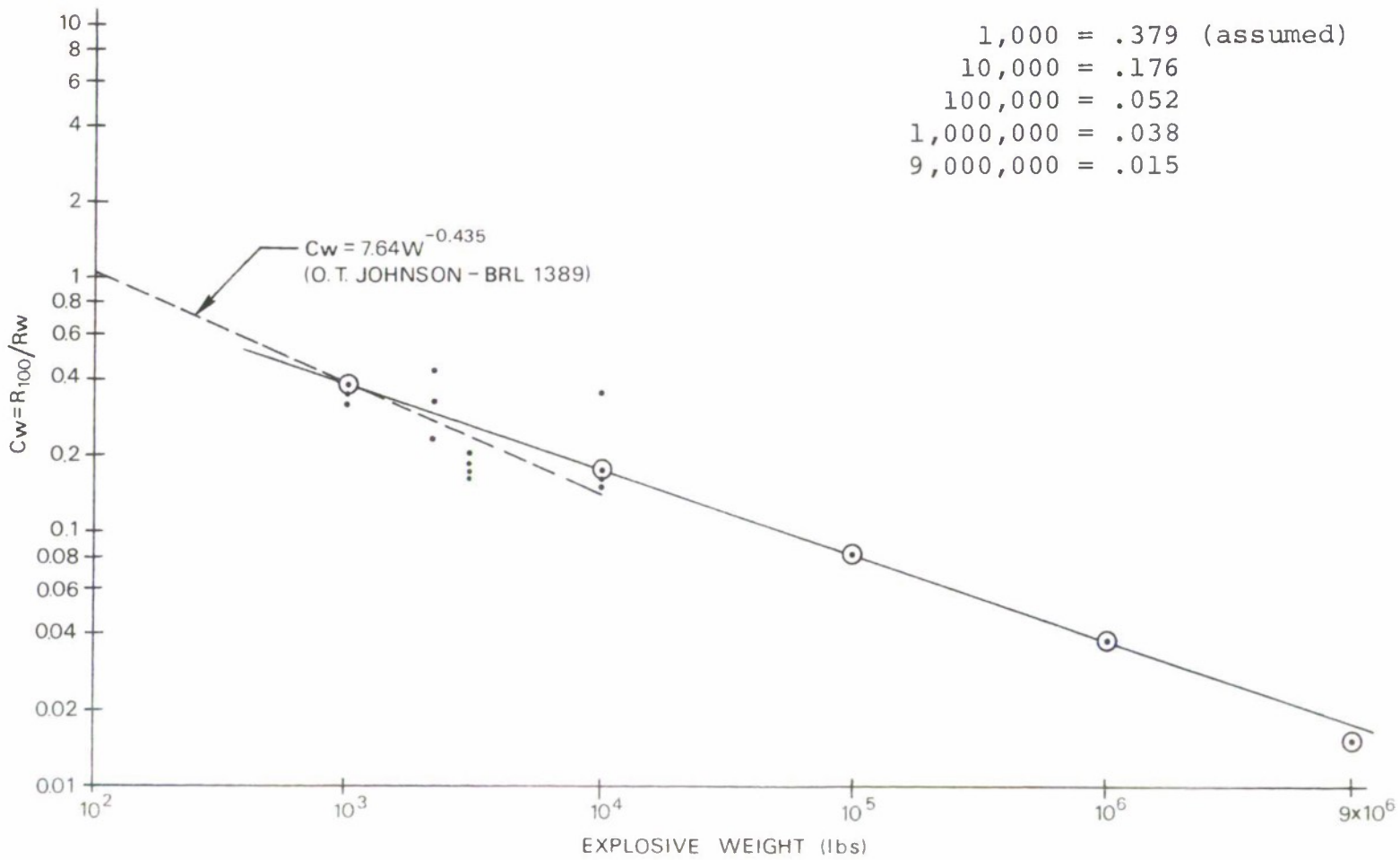

Figure 50. Scaling Relationships for Constant Acceptable Hazards to Personnel

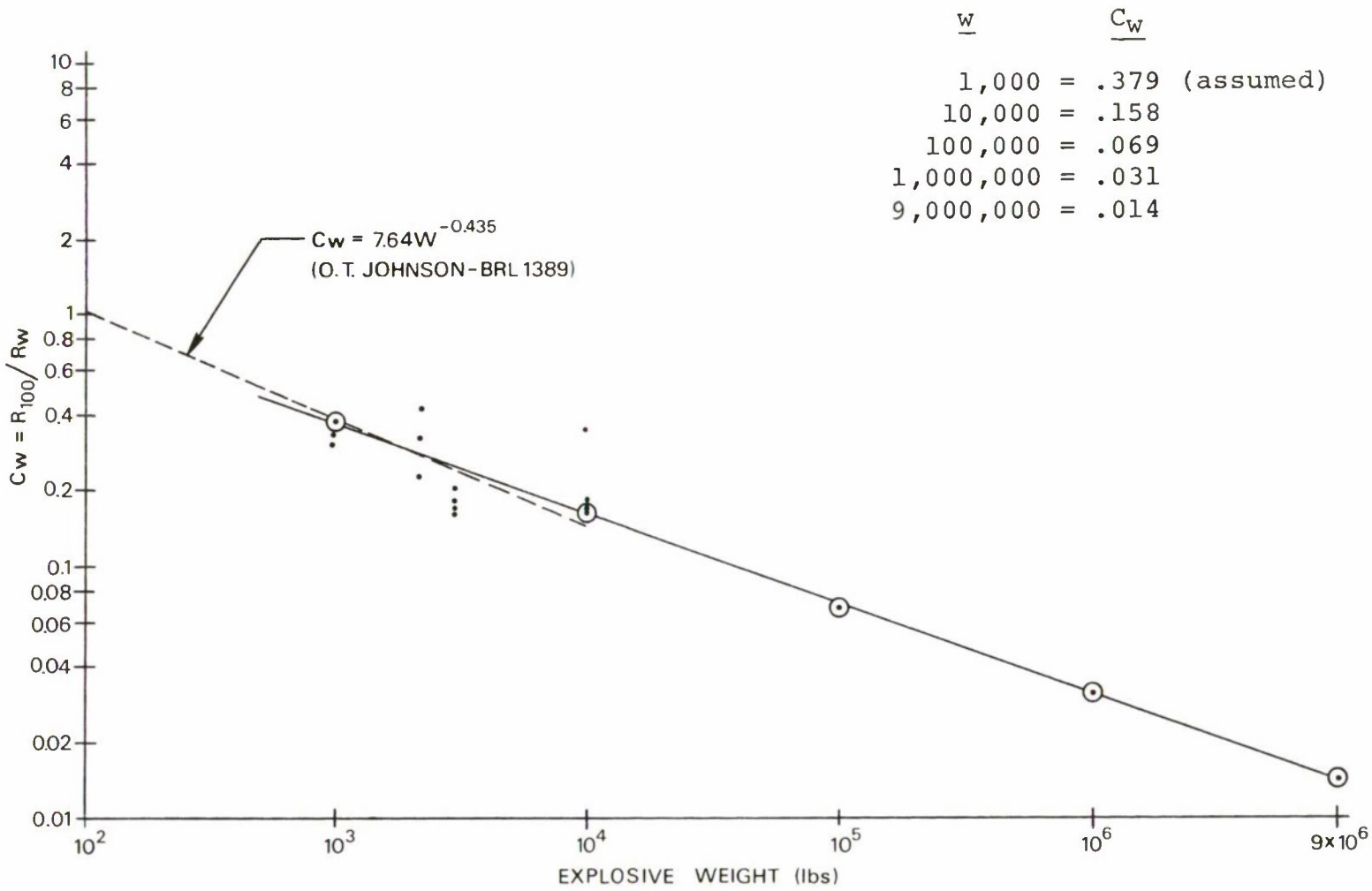

Figure 51. Scaling Relationship for Constant Acceptable Damage to the Igloo Doors

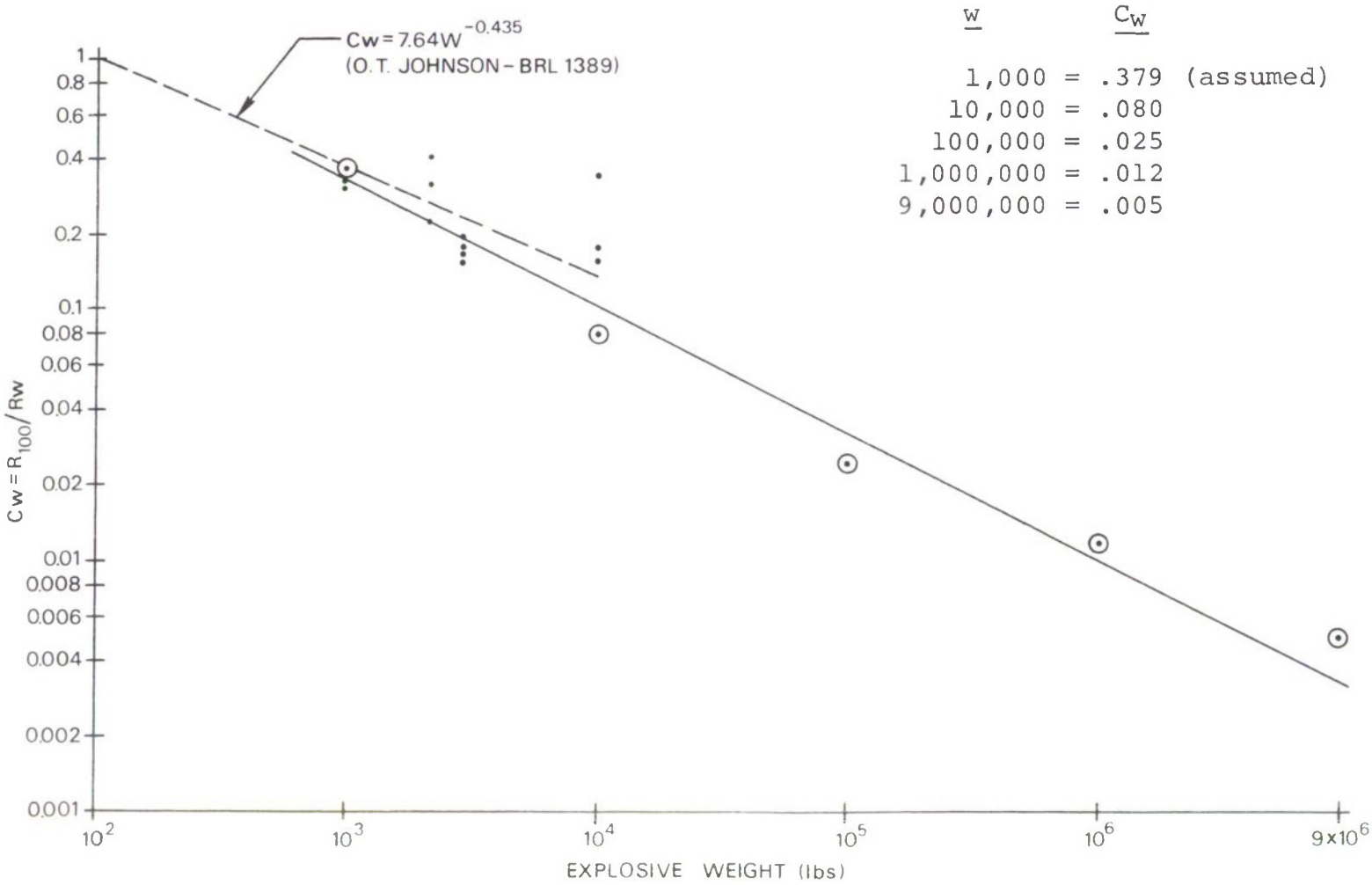

Figure 52. Scaling Relationships for Constant Acceptable Damage to the Church Roof

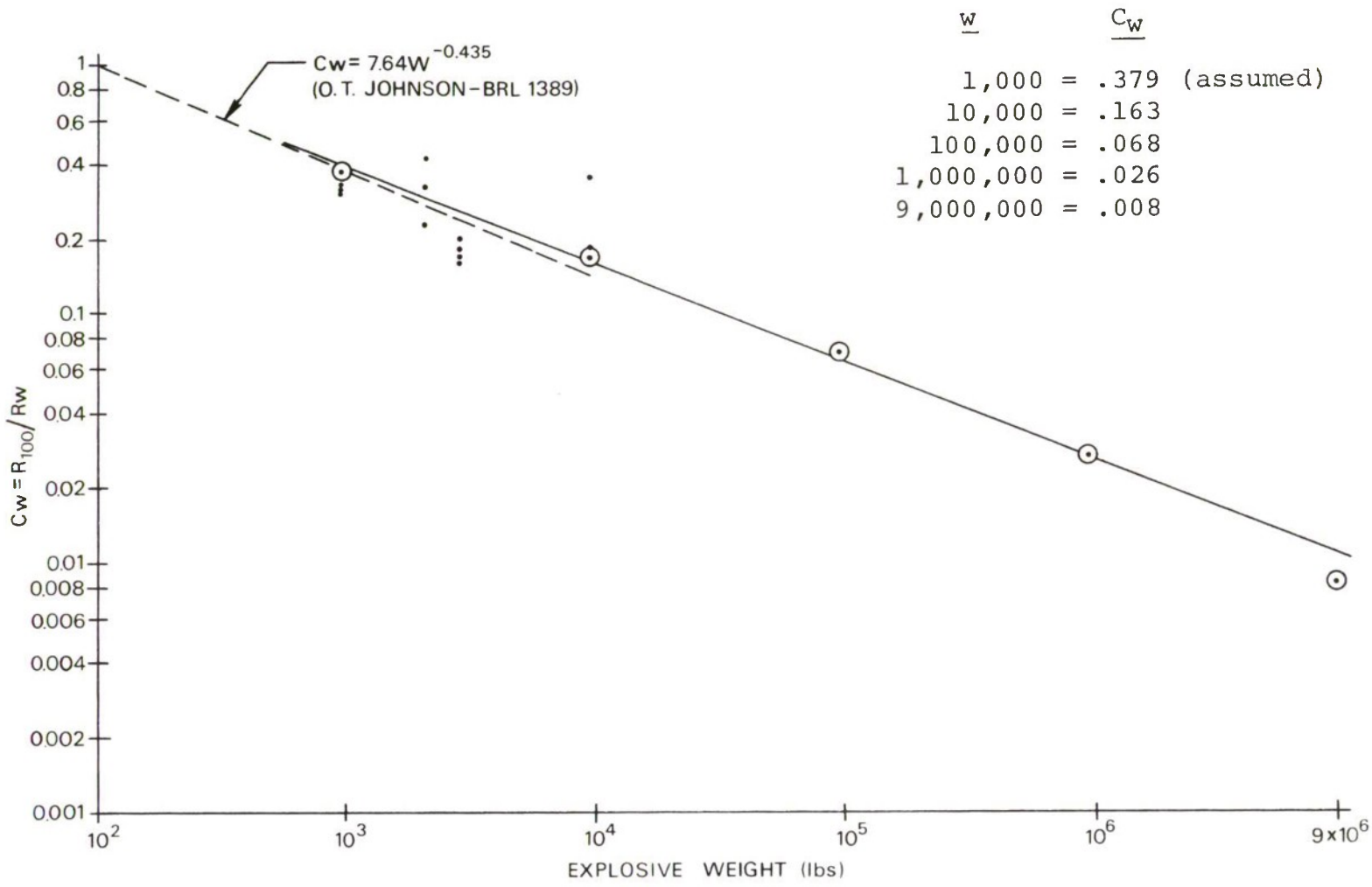

Figure 53. Scaling Relationships for Constant Acceptable Damage to the House Trailer

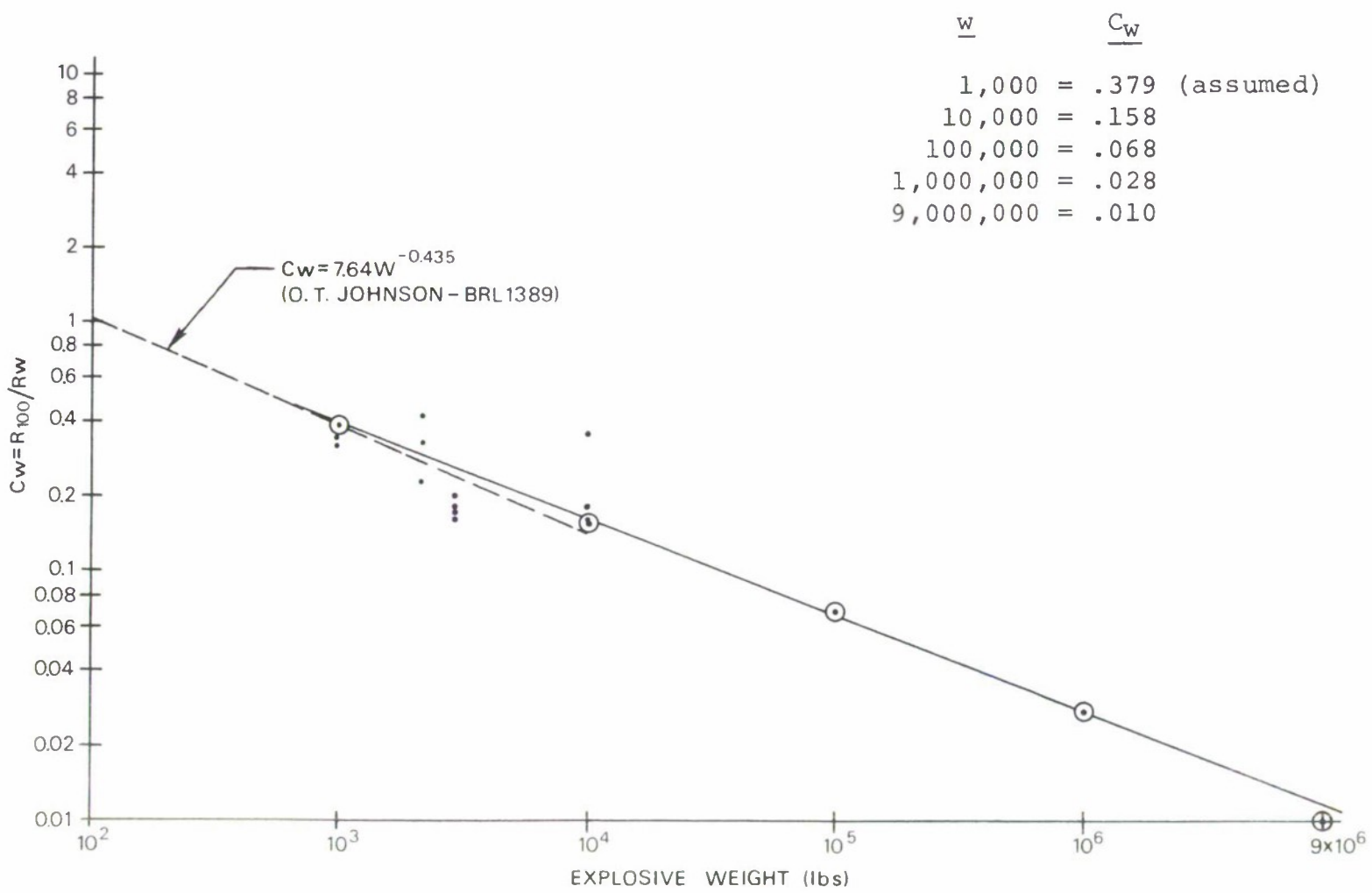

Figure 54. Scaling Relationships for Constant Acceptable Damage to the Bus

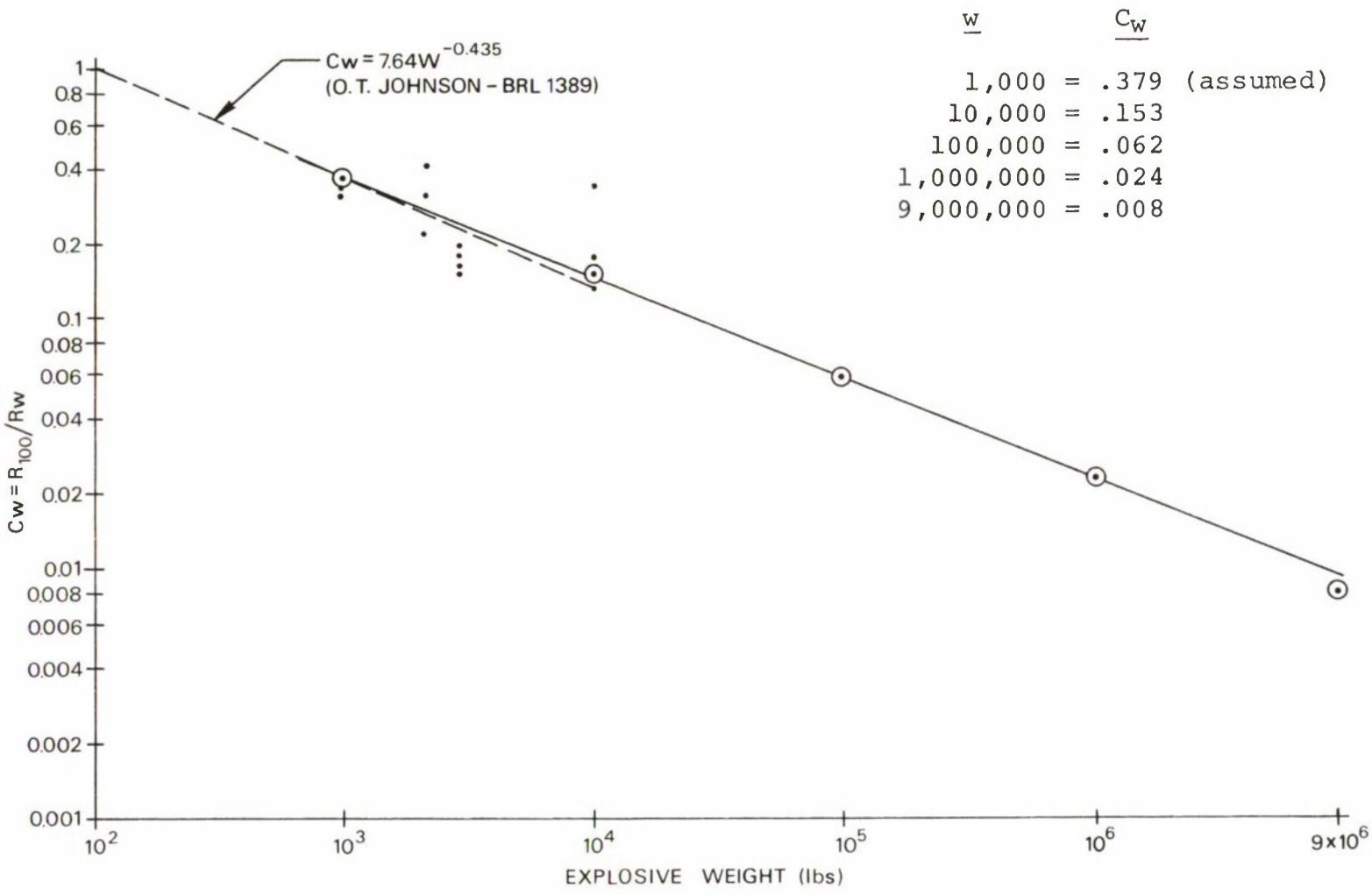

Figure 55. Scaling Relationships for Constant Acceptable Damage to the Camper-Pickup

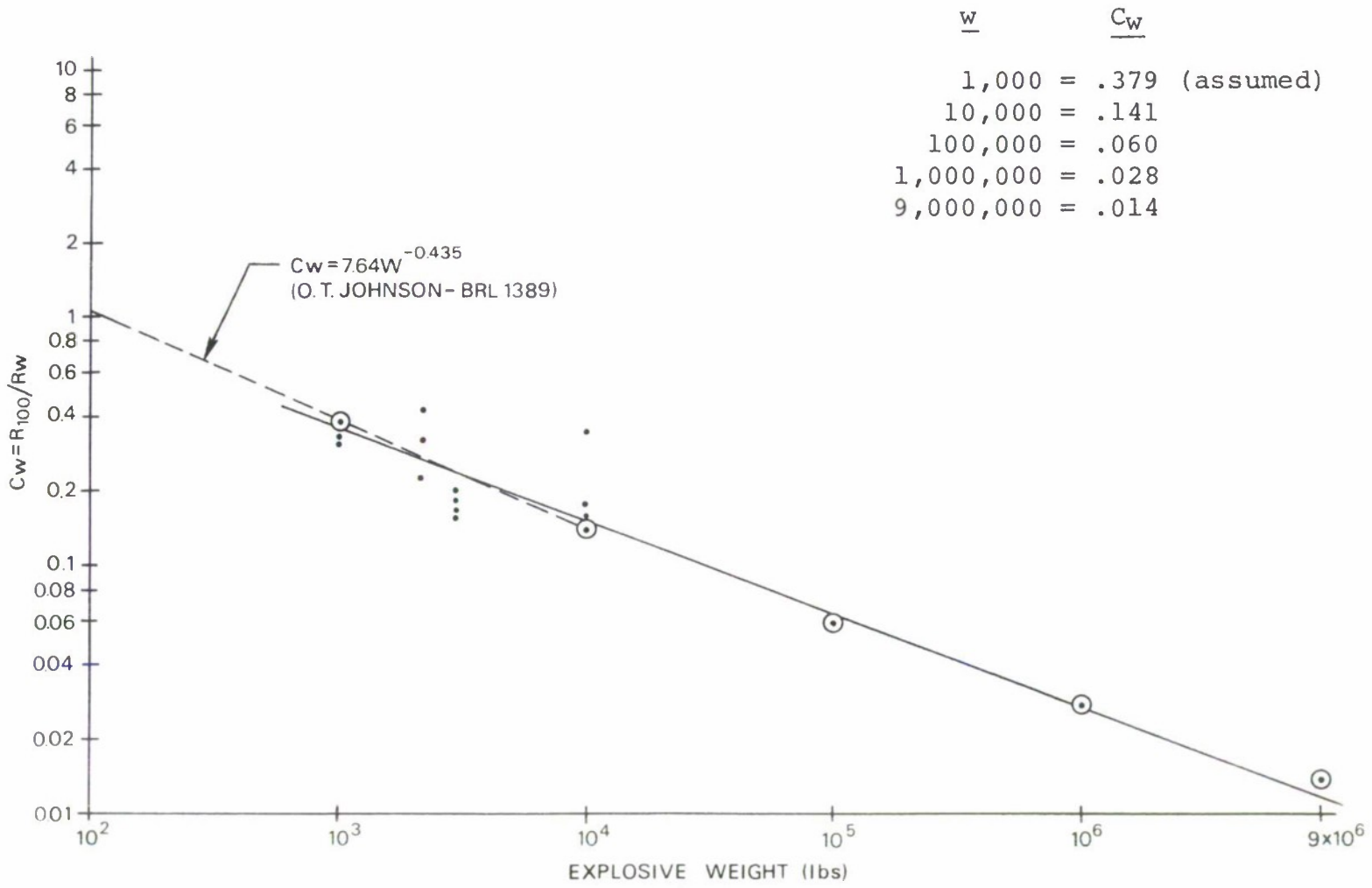

Figure 56. Scaling Relationships for Constant Acceptable Damage to the Aircraft

The results presented in these ten figures are of direct value for determining quantity-distance relationships for charges between the specific quantities used in this study, and should be of substantial additional value in extending the understanding of target-blast wave interactions.

E. THE EFFECTS OF EXPLOSIVE CHARGE SHAPE ON RESULTS

The results which have been provided are based upon spherical charges and hemispherical blast wave data. In some instances, it is probable that a quantity of stored explosives may have a shape which is substantially different from a sphere. While there are no direct tests of this shape factor for large charges, there are clear indications in the literature as to the magnitude of the changes in the blast wave which are to be expected.

Work performed by Falcon staff members with cylindrical explosive charges of varying length-to-diameter ratio [76] has shown a substantial variation in peak pressure with changes in this parameter. Increases in peak pressure measured at the side of the cylinder (90 degrees to the axis) were shown for increases up to 10 in L/D ratio for charges of equal weight. Beyond 10, little or no further increase appears possible. The increased peak pressure values varied with the distance from the charge for all L/D ratios. For λ_d (scaled distance) values of five, peak pressure increases of as much as 30 percent were observed. At λ_d values of ten, the maximum peak pressure enhancement was no more than 15 percent, and at λ_d values of 20 the shape enhancement was no more than 5 percent. These percentage increases are for comparison with L/D ratios of one.

It is thus indicated that for stored explosives which had length and width factors which would approximate L/D ratios up to ten, some enhancement of the pressure levels in the blast wave are to be expected. This enhancement will be greatest close to the charge and will not exceed 5 percent at a scaled distance of 20. (A scaled distance of 20 is 200 feet from a 1,000-pound charge or 2,000 feet from a 1-million-pound charge.) The masonry walls of the school building and office building as well as the igloo doors are within $\lambda_d = 20$ for the 1,000-pound charge at the acceptable damage level. For the largest charge sizes, only the igloo doors remain

within a scaled distance of 20. Thus, while explosive charge shape can have a substantial effect on blast properties close to the charge, it will not seriously alter calculated target responses at the distances of interest to inhabited building safety.

F. THE EFFECT OF BARRICADES ON RESULTS

Recent work at the Research Triangle Institute and at the Southwest Research Institute [85] has involved the influence of barricades upon blast wave parameters. While a substantial reduction in both peak pressure and impulse was shown immediatly behind the barricades, the effect generally did not extend beyond about five barricade heights. At some specific distances beyond barricades, it is even possible to get slightly higher pressure and impulse values than would have been the case for unbarricaded conditions.

These findings indicate that barricade effects on blast waves are of major importance only for locations within a few barricade heights of the barricade considered. Thus, the targets considered in this study will be generally unaffected by barricades in the vicinity of the charge and will seldom have barricades in the vicinity of the target unless they are natural features of the terrain.

No shielding modifications to the computed results which have been presented are believed to be necessary unless it can be shown that a barricade exists within 100 to 200 feet of the target structure. These distances apply to all targets except the church and office building which are too high for barricade protection. The other targets are generally no more than 15 feet high.

VI. CONCLUSIONS

The work which has been accomplished within the scope of this contract has provided a basis for a number of significant conclusions. The most pertinent are outlined in the following statements.

1. A scarcity of appropriate experimental data applicable to the civilian targets of interest has required the model which has been developed to be based largely upon analytical procedures for the description of the targets to blast energy.

2. It has been found necessary to consider the resonant and elastic properties of the structural elements as well as the strength, weight, size, and orientation of the targets in a blast field to achieve useful models of target response for a wide range of charge sizes.

3. A program for the experimental verification of these modeled interactions should be undertaken. This can be done most economically with small charge and target component tests.

4. Except for the following specific instance, the computed results indicate that the present quantity-distance criteria are at least adequate for all explosive quantities of interest.

    a. The church roof may suffer unacceptable damage from a 1,000,000-pound charge at the inhabited building distance of 7,000 feet.

    b. The trailer, school building, and church roof may suffer unacceptable damage from a 9,000,000-pound charge at the inhabited building distance of 10,400 feet.

    c. Vehicles on public highways may be subject to overturning from a 9,000,000-pound charge at the public highway distance of 6,240 feet.

d. The computed response data for the igloo door indicates an unacceptable risk to this target for all five charge sizes considered. The computed acceptable distance is never very far beyond the present limit for unbarricaded above-ground magazines and the igloo door selected for analysis was the lightest of the standard types. A rather small change in either the type of door analyzed or in the criteria level for acceptable damage would eliminate this apparent unacceptable risk. Thus, the present distance values for above-ground magazines may be very realistic and appropriate.

5. Targets which have very large surfaces, such as the church roof, or which are easily overturned, such as the trailer, respond efficiently to the impulse from large explosive charges and thus are endangered at greater distances than other types of targets. It may be desirable to consider such targets on an individual case basis rather than extending the distance for all targets to a limit which would protect these, most vulnerable, types.

6. From the standpoint of blast damage alone, the present runway separation distances may be conservative.

7. The pressure-impulse relationships which have been developed for these ten targets confirm both the damage scaling approach proposed by O. T. Johnson and the critical period and impulse blast damage criterion, proposed by R. G. Sewell. It is believed that no real inconsistency between these two approaches exists if the blast interaction with the target is fully understood and modeled.

8. The refinement of the models of dynamic explosive blast-target interaction which have been used in this study should be undertaken when more specific experimental evidence of the behavior of target elements becomes available.

VII. RECOMMENDATIONS

1. It is recommended that these models of blast-structure interactions be used for validating present quantity distance standards and for estimating risks to existing or proposed structures near stored explosives.

2. It is recommended that certain aspects of these models be tested experimentally, either through full-scale tests with large charges or target component tests with small charges. Specific types of tests which are believed most needed include the following:

a. Tests of wooden frame components should be performed which would validate the critical impulse in a critical period concept. A series of tests should be planned in which wood frame structures of known resonant frequency are exposed to three types of blast waves as follows:

(1) A wave that just provides the computed critical impulse in a time interval equal to one-fourth the resonant period.

(2) A wave that provides substantially more total impulse than (1) but which fails to provide it fast enough to meet the critical energy level within the quarter period.

(3) A wave which provides less total impulse than (1) but which exposes the target to substantially higher incident pressure levels.

b. Tests of damaged (cracked) masonry structures should be performed to determine the maximum uniform lateral loads that can be sustained without further deformation. A value of 0.2 psi has been used in the models involving such walls as a damage threshold; however, there is very little experimental evidence to support any specific pressure level.

c. Tests designed to determine the "effective impulse" imparted to masonry walls under a variety of loading conditions are needed. It is believed that appropriate tests are being performed under OCD sponsorship.

d. Tests of the vehicle overturning model are needed. A preliminary test involving a bus and a camper-pickup are planned for March or April 1970. Further tests may be required involving larger charge sizes.

e. Tests are required to determine the hazards associated with the breakage of plate glass windows, particularly at the threshold pressure levels where large pieces of glass may be produced. A significant hazard may be associated with falling glass from such breakage. It is believed that velocities for such pieces can be computed with reasonable accuracy, but it is not possible to predict the size of the pieces which are to be expected.

f. If an exposed igloo door, such as the one treated in this analysis, is of substantial concern to the Armed Services Explosive Safety Board, a full-scale test of such a structure exposed to the blast from at least a 500,000-pound bare charge should be planned. This type of test should be planned to evaluate the model of door failure rather than just as a test of the strength of the door.

3. It is recommended that consideration be given to establishing a consistent single value for the inhabited building distance requirement for one million-pound charges. The results from this study indicate that an appropriate requirement lies between 5000 and 7000 feet.

4. It is recommended that consideration be given to the need for a moderate increase in the public highway distance for 9,000,000-pound charges. An increase to the inhabited building distance of 10,400 feet may be justified.

5. It is recommended that further consideration be given to the definition of an acceptable damage level for the igloo door. More damage than simply opening the doors may be acceptable if all factors are considered.

REFERENCE DOCUMENTS

1. Air Force Technical Manual, "Structural Repair Instructions for Aircraft", T.O. 1C-135(K)A-3-1, 15 February 1962.

2. Air Force Weapons Laboratory, "Systems Applications of Nuclear Technology - Blast Effects on Aerospace Vehicles", AFSC Manual No. 500-2, March 1964.

3. Amman & Whitney Consulting Engineers, "Design of Structures to Resist the Effects of Atomic Weapons, Weapons Effects Data", Department of the Army Technical Manual 5-856-1, July 1959.

4. -----, "Design of Structures to Resist the Effects of Atomic Weapons, Strength of Materials and Structural Elements", Department of the Army Technical Manual 5-856-2, March 1957.

5. -----, "Design of Structures to Resist the Effects of Atomic Weapons, Principles of Dynamic Analysis and Design", Department of the Army Technical Manual 5-856-3, March 1957.

6. -----, "Design of Structures to Resist the Effects of Atomic Weapons, Single-Story Frame Building", Department of the Army Technical Manual 5-856-5, January 1958.

7. -----, "Design of Structures to Resist the Effects of Atomic Weapons, Multi-Story Frame Buildings", Department of the Army Technical Manual 5-856-6, January 1960.

8. -----, "Design of Structures to Resist the Effects of Atomic Weapons, Shear Wall Structures", Department of the Army Technical Manual 5-856-7, January 1958.

9. -----, "Design of Structures to Resist the Effects of Atomic Weapons, Arches and Domes", Department of the Army Technical Manual 5-856-8, January 1960.

10. -----, "Design of Structures to Resist the Effects of Atomic Weapons, Buried and Semiburied Structures", Department of the Army Technical Manual 5-856-9, January 1960.

11. Armed Services Explosive Safety Board, "Explosives Accident/Incident Abstracts - September 1961-June 1967", Washington, D. C., October 1967, AD 660 020.

12. -----, "Minutes of the Eleventh Explosives Safety Seminar, Sheraton-Peabody Hotel, Memphis, Tennessee, 9-10 September 1969", Volume 1.

13. Army-Navy Explosives Safety Board, "The Present Status of the American Table of Distance", Explosives Safety Board Technical Paper No. 1, 1 July 1945, AD 223 339.

14. Baker, W. E., and Schuman, W. J., Jr., "Air Blast Data for Correlation With Moving Airfoil Tests", BRL Technical Note 1421, Ballistic Research Laboratories, August 1961, AD 610 391.

15. Beck, Christian, Editor, "Nuclear Weapons Effects Tests of Blast Type Shelters - A Documentary Compendium of Test Reports", CEX-68.3, Civil Effects Test Operations, U. S. Atomic Energy Commission, June 1969.

16. Bowen, I. G., et al., "Biophysical Mechanisms and Scaling Procedures Applicable in Assessing Responses of the Thorax Energized by Air Blast Overpressures or by Non-Penetrating Missiles", Lovelace Foundation for Medical Education and Research, Albuquerque, N. M., DASA 1857, November 1966.

17. Bowen, I. G., Fletcher, E. R., and Richmond, D. R., "Estimates of Man's Tolerance to the Direct Effects of Air Blast", Lovelace Foundation for Medical Education and Research, Albuquerque, N. M., DASA 2113, October 1968.

18. Bowen, I. Gerald, et al., "A Model Designed to Predict the Motion of Objects Translated by Classical Blast Waves", Lovelace Foundation for Medical Education and Research, Albuquerque, N. M., January 1961.

19. -----, "Translation Effects of Air Blast From High Explosives", Lovelace Foundation for Medical Education and Research, Albuquerque, N. M., November 7, 1962, DASA Report 1336.

20. Bowen, I. Gerald, Franklin, Mary E., and Fletcher, E. Royce, "Secondary Missiles Generated by Nuclear-Produced Blast Waves", Operation Blumbbob, WT-1468, Civil Effects Test Group, 28 October 1963.

21. Christensen, Wayne J., "Blast Effects on Miscellaneous Structures", Operation Castle, Defense Atomic Support Agency, Washington, D. C., July 1955, WT Document 901, AD 356 271L.

22. Clark, D. S., and Wood, D. S., "The Tensile Impact Properties of Some Metals and Alloys", Transactions, American Society of Metals, Vol. 42, 1950.

23. Cord, John N., "Behavior of Wall Panels Under Static and Dynamic Loads", Department of Civil and Sanitary Engineering of the MIT, August 1952, AD 2231.

24. Cox, P. A., et al., "Structural Response of Helicopters to Muzzle and Breech Blast--Structural Response of Specific Helicopters to Blast From Specific Weapons, Volume III (U)", Southwest Research Institute, June 1969, Confidential.

25. Criscione, E., and Hobbs, N. P., "The Prediction of Lethality Envelopes for Aircraft in Flight, Part 2. Detailed Theoretical Analysis (U)", WADC 56-150, MIT, October 1958, AD 302 202, Confidential.

26. Defense Atomic Support Agency, "Capabilities of Nuclear Weapons (U)", DASA Manual No. 1, 1 January 1968, AD 394 199, Confidential.

27. Department of the Army, Headquarters, "Design of Structures to Resist the Effects of Atomic Weapons--Structural Elements Subjected to Dynamic Loads", Department of the Army Technical Manual TM 5-856-4, December 1965.

28. Deaprtment of Defense, "Ammunition and Explosives Safety Standards", DOD 4145-27M, March 1969.

29. Departments of the Army, Navy, and Air Force Technical Manual, "Structures to Resist the Effects of Accidental Explosions", TM 5-1300, NAVFAC P-397, AFM 88-22, June 1969.

30. Dick, Richard A., "Factors in Selecting and Applying Commercial Explosives and Blasting Agents", Information Circular No. 8405, U. S. Department of Interior, Bureau of Mines, 1968.

31. Dickerson, Alan A., "Operation Prairie Flat", DASIAC Special Report No. 70, 15 May 1968.

32. Donahue, J. D., et al., "Explosives Storage Quantity-Distance Specification Computer Model--User's Manual", Falcon Research and Development Company, Denver, Colorado, March 1970.

33. Dudash, M. J., "Operation Prairie Flat, Preliminary Report, Vol. I", DASA Report 2228-1, January 1969.

34. Dunetz, Bryant R., and Kruse, Loren R., "Effects of Blast on Personnel and Materiel Targets (U)", Technical Memorandum No. 4, Army Materiel Systems Analysis Agency, September 1968, AD 393 444, Confidential.

35. Fletcher, E. Royce, "Glass Fragment Data From the Prairie Flat and China Lake Two-Story House Test", Lovelace Foundation for Medical Education and Research, Albuquerque, N. M., unpublished data.

36. Fletcher, E. Royce, and Bowen, I. Gerald, "Blast Induced Translational Effects", Lovelace Foundation for Medical Education and Research, Albuquerque, N. M., DASA 1859, November 1966.

37. Fletcher, E. R., et al., "An Estimation of the Personnel Hazards from a Multi-Ton Blast on a Coniferous Forest", Lovelace Foundation for Medical Education and Research, Albuquerque, N. M., DASA 2020, November 1967.

38. Gilstad, D. A., "Structural Response and Gas Dynamics of an Airship Exposed to a Nuclear Detonation (U)", WT-1431, Defense Atomic Support Agency, April 1960, AD 360 874L, Confidential.

39. Glasstone, Samuel, "The Effects of Nuclear Weapons", Department of Defense, February 1964.

40. Goldizen, V. C., et al., "Missile Studies With a Biological Target", Lovelace Foundation for Medical Education and Research, Albuquerque, N. M., Operation Plumbbob, WT 1470, January 1961.

41. Hackman, Emory E., "Notes on High Explosives Internal Blast and Target Damage - Hopkinson's Rule--Geometric Scaling", Paper presented to the Technical Cooperation Program at New Mexico Institute of Mining and Technology, Socorro, N. M., April 1969.

42. -----, "A Theoretical Basis for Johnson's Damage Rule", Paper presented to the Technical Cooperation Program at New Mexico Institute of Mining and Technology, Socorro, N. M., April 1969.

43. Hippensteel, Robert G., Hoffman, Alvan J., and Baker, Wilfred E., "Safety Tests of Nike-Hercules Missile Site (U)", BRL Report 1085, November 1959, AD 377 104, Confidential.

44. Hirsch, Frederick G., "Effects of Overpressure on the Ear, a Review", Lovelace Foundation for Medical Education and Research, Albuquerque, N. M., DASA 1858, November 1966.

45. Hobbs, Norman P., "The Prediction of Lethality Envelopes for Aircraft in Flight, Part 5, Simplified Prediction Methods (U)", WADC 56-150, MIT, June 1958, AD 155 603, Confidential.

46. Hoffman, D., "Comparison of Four Methods for Predicting Blast Damage to Structures (U)", USNRDL-TR-1011, U. S. Naval Radiological Defense Laboratories, 22 March 1968, AD 374 004, Confidential.

47. House of Representatives Document No. 199, "Ammunition Storage Conditions", Proceedings of the Joint Army-Navy Board to Survey Ammunition Storage Conditions Pursuant to Public Law No. 2, 70th Congress, 1928, AD 493 245.

48. Ilsley, Ralph, "The Port Chicago, California Ship Explosion of 17 July 1944", Technical Paper No. 6, Army-Navy Explosive Safety Board, Washington, D. C. March 1948, AD 223 344.

49. Interdepartmental Explosives Storage and Transport Committee of the United Kingdom, "Notes on the Basis of Outside Safety Distances for Explosives Involving the Risk of Mass Explosion", 1959, AD 221 164.

50. Iverson, J. H., "Existing Structures Evaluation, Part 2, Window Glass and Applications", Final Report, Stanford Research Institute Project No. MU6300-020, December 1968.

51. Jack, W. H., Jr., "Measurements of Normally Reflected Shock Waves From Explosive Charges", BRL Memorandum Report 1499, Ballistic Research Laboratories, July 1963, AD 422 886.

52. Johnson, O. T., "A Blast Damage Relationship", BRL Report No. 1389, September 1967.

53. Julian, A. N., "In-Flight Structural Response of FJ-4 Aircraft to Nuclear Detonations", Bureau of Aeronautics, Department of the Navy and North American Aviation, Inc., Columbus Division, February 1960, WT 1432, AD 360 875L.

54. Kaplan, K., and Davis, V. W., "Effectiveness of Barricades, Review of Basic Information", URS Report 677-4R, DASA Report 2014, June 1968.

55. Keenan, William A., "Strength and Behavior of Restrained Reinforced Concrete Slabs Under Static and Dynamic Loadings", Technical Report R-621, Naval Civil Engineering Laboratory, Port Hueneme, California, for the Defense Atomic Support Agency, April 1969.

56. -----, "Strength and Behavior of Laced Reinforced Concrete Slabs Under Static and Dynamic Loads", Technical Report R-620, Naval Civil Engineering Laboratory, Port Hueneme, California, for the Department of the Army, Picatinny Arsenal, April 1969.

57. Kingery, C. N., "Air Blast Parameters vs Distance for Hemispherical TNT Surface Bursts", BRL Report No. 1344, September 1966, AD 811 673.

58. -----, "Parametric Analysis of Sub-Kiloton Nuclear and High Explosive Air Blast", BRL Report 1393, Ballistic Research Laboratories, February 1968.

59. Kravitz, S. and Wiesenfeld, L., "Effects of a Bare Explosive Against a Metal Plate", Picatinny Arsenal, Dover, New Jersey, November 1963.

60. Long, Robert P., "High Explosive Blast Effects on 1/4-Ton Trucks (U)", BRL Memorandum Report No. 1610, October 1964, AD 359 168, Confidential.

61. Lyons, C. G., and Gardiner, P. C., "The Screening of Blast by Buildings", Ministry of Home Security Research and Experiment Departments, Great Britain, REN No. 523, about 1945.

62. Mann, R. L., "Igloo and Revetment Tests", Technical Paper No. 5, The Army-Navy Explosive Safety Board, October 1946, AD 223 343.

63. Mason, H., and Walter, D., "An Exploratory Study to Assess the Magnitude of OCD Foundation Problems", Final Report, URS Report 693-3, Prepared for the Stanford Research Institute and the Office of Civil Defense, November 1968.

64. McKee, K. E., "Studies of the Influence of Variations of Blast and Structural Parameters on Blast Damage to Structures (U)", Report No. 30, Armor Research Foundation of Illinois Institute of Technology, January 27, 1955, AD 53 470, Confidential.

65. Melichar, Joseph F., "The Propagation of Blast Waves Into Chambers", BRL Memorandum Report 1920, March 1968.

66. Merritt, Melvin L., "Blast Loading of Idealized Structures Using High Explosives", Sandia Corporation.

67. Moulton, James F., Jr., "Nuclear Weapons Blast Phenomena, Volume I (U)", DASA 1200, Defense Atomic Support Agency, March 1960, Secret.

68. -----, "Nuclear Weapons Blast Phenomena, Volume II (U)", DASA 1200, Defense Atomic Support Agency, March 1960, Secret.

69. -----, "Nuclear Weapons Blast Phenomena, Volume V (U)", DASA 1200, 1 June 1968, AD 503 077L, Secret.

70. Murphy, H. L., "Ground Motion Predictions for Nuclear Attack Area Studies", Stanford Research Project MU6300-470, SRI, Menlo Park, California, May 1967.

71. Naval Ordnance Laboratory, "Explosives - Effects and Properties (U)", NOLTR 65-218, White Oak, Maryland, February 1967, Confidential.

72. Newlin, J. S., "The Design for Strength of Flat Panels With Stressed Coverings", Bulletin R1220, U. S. Forest Products Laboratory, March 1940.

73. -----, "Existing Structures Evaluation, Part II: Window Glass and Applications", Office of Civil Defense, Washington, D. C., Stanford Research Institute, December 1968.

74. Newmark, N. M., "Effect of Long Positive Phase Blast Waves on Drag and Diffraction Type Targets", University of Illinois, Urbana, Illinois, Report No. AFSWP-494, 21 August 1953, AD 270 653.

75. Parks, Daniel K., "The Development of Equations for the Prediction of Explosive Effectiveness (U)", Denver Research Institute Progress and Fund Report No. 8, 15 March 1961, AD 323 207, Confidential.

76. Parks, D. K., and Weeding, G. S., "Investigations of Air Blast Parameters Around Cylindrical Charges (U)", Denver Research Institute, January 1959, AD 305 334, Confidential.

77. Parrack, Horace O., "Hazard to Man Created by Environmental Acoustic Energy", Aerospace Medical Research Laboratories, Wright-Patterson AFB, Ohio, about 1968.

78. Peterson, Frederick H., Lemont, Charles J., and Vergnolle, Robert R., "High Explosive Storage Tests, Big Papa", Technical Report No. AFWL-TR-67-132, AFWL, Kirtland AFB, N. M., May 1968.

79. Purkey, Glen F., Lounsbery, W. R., "Destructive Loads on Aircraft in Flight", Radiation, Inc., January 1958, WT 1132, AD 357 980L.

80. Purkey, Glen F., and Mitchell, R. F., "Structural Response of F-84F Aircraft in Flight", Cook Research Laboratories, WT 1133, AD 362 111L, July 1958.

81. Randall, Phillip A., "Damage to Conventional and Special Types of Residences Exposed to Nuclear Effects", Operation Teapot, WT 1194, 12 April 1961, AD 611 160.

82. Richmond, Donald R., et al., "The Relationship Between Selected Blast Wave Parameters and the Response of Mammals Exposed to Air Blast", Lovelace Foundation for Medical Education and Research, Albuquerque, N. M., DASA 1860, November 1966.

83. Rinehart, J. S., and Pearson, J., "Behavior of Metals Under Impulsive Loads", American Society of Metals, Cleveland, Ohio, 1954.

84. Rotz, Julius V., "Detail Damage of NFSS Structures With Detailed Descriptions of Damage and Degraded PF", Final Report, URS Report 658-7, Prepared for the Office of Civil Defense, September 1967.

85. Schleicher, A. R., "Analytical Development and Experimental Testing of a Model for Barricade Blast Interactions", Second Progress Report, Research Triangle Institute for the Armed Services Explosive Safety Board, July 1969.

86. Schuman, William J., Jr., "The Response of Cylindrical Shells to External Blast Loading", BRL Memorandum Report 1461, Ballistic Research Laboratories, March 1963.

87. -----, "A Failure Criterion for Blast Loaded Cylindrical Shells", BRL Report 1292, Ballistic Research Laboratories, Aberdeen Proving Ground, Maryland May 1965.

88. Schwartz, Robert B., "Safe Overpressure Limit for the C-135 Aircraft Exposed to Nuclear Detonations", Technical Report SEG-TR-64-69, University of Dayton Research Institute, January 1965, AD 459 375.

89. Sewell, Robert G. S., "A Blast Damage Criterion", Weapons Development Department, U. S. Naval Ordnance Test Station, China Lake, California, March 1964, AD 349 335.

90. Shaw, Ebe R., and McNea, Frank P., "Exposure of Mobile Homes and Emergency Vehicles to Nuclear Explosions", Federal Defense Administration, July 1957, WT 1181, AD 611 318.

91. Sinnamon, G. K., et al., "Effect of Positive Phase Length of Blast on Drag and Semidrag Industrial Buildings, Part 1", Air Force Special Weapons Center, Air Research and Development Command, Kirtland AFB, N. M., in cooperation with the University of Illinois, December 1958, WT 1129, AD 617 174.

92. Sinnamon, G. K., Haltiwanger, J. D., and Newmark, N. M., "Effects of Length of Positive Phase of Blast on Drag-Type and Semidrag-Type Industrial Buildings (U)", WT 1325, University of Illinois, Urbana, Illinois, AD 357 972L, Secret.

93. Stalk, G., Gee, R. E., and Vednar, J. P., "In-flight Structure Response of an F-89D Aircraft to a Nuclear Detonation", Northrop Aircraft, Inc., Hawthorne, California, WE 1434, AD 357 975L, October 1957.

94. Taylor, Benjamin C., "Blast Effects of Atomic Weapons Upon Curtain Walls and Partitions of Masonry and Other Materials", Operation Upshot-Knothole, Federal Civil Defense Administration, August 1956, AD 636 766.

95. Timoshenko, S., "Vibration Problem in Engineering", D. Van Nostrand, Inc., January 1955.

96. -----, "The Effects of Nuclear Weapons", Atomic Energy Commission, April 1952.

97. The Boeing Company, "Boeing 707 Intercontinental Structural Repair Manual", Renton, Washington.

98. URS Research Company, "Evaluation of Explosive Simultaneity Tests", Prepared for the Naval Weapons Center, China Lake, California, May 1969.

99. Van Dolah, R. W., Gibson, F. C., and Murphy, J. N., "Sympathetic Detonation of Ammonium Nitrate and Ammonium Nitrate-Fuel Oil", Bureau of Mines Report of Investigations 6746, U. S. Department of Interior, Bureau of Mines, 1966.

100. -----, "Further Studies on Sympathetic Detonation", Bureau of Mines Report of Investigation No. 6903, U.S. Department of Interior, Bureau of Mines, 1966.

101. Von Karman, T., and Duwey, P., "The Propagation of Plastic Deformations in Solids", Journal of Applied Physics, Vol. 21, 1950.

102. Walls, J. H., "In-flight Structure Response of the Model A-4D-1 Aircraft to a Nuclear Explosion", Douglass Aircraft Company, El Segundo, California, October 1957, WT 1433, AD 355 562L.

103. Walls, J. H., and Heslin, N. C., "In-flight Structural Response of an HSS-1 Helicopter to a Nuclear Detonation", Bureau of Aeronautics, Department of the Navy and Sikorsky Aircraft Division, United Aircraft Corp., July 1960, WT 1430, AD 360 873L.

104. White, Clayton S., "The Scope of Blast and Shock Biology and Problem Areas in Relating Physical and Biological Parameters", Lovelace Foundation for Medical Education and Research, Albuquerque, N. M., DASA 1856, November 1966.

105. Whitney, C. S., et al., "Design of Blast Resistant Construction for Atomic Explosions", J. American Concrete Institute, Proceedings, Vol. 51, March 1955.

106. Wiehle, C. K., and Bockholt, J. L., "Existing Structures Evaluation, Part 1. Walls", SRI Project No. MU6300-020, Stanford Research Institute, Menlo Park, California, for the Office of Civil Defense, November 1968.

107. Wiehle, Carl K., and Durbin, William L., "Combined Effects of Nuclear Weapons on NFSS Type Structures", Final Report by URS Corp., September 1966, URS Report No. 658-3, AD 642 502.

108. Willoughby, A. B., Wilton, C., and Gabrielsen, B., "Development and Evaluation of a Shock Tunnel Facility for Conducting Full-scale Tests of Loading Response and Debris Characteristics of Structural Elements", URS Corp., for the Stanford Research Institute and the

Office of Civil Defense, URS Report No. 680-2, December 1967, AD 674 256.

109. -----, "A Study of Loading, Structural Response, and Debris Characteristics of Wall Panels", URS 680-5, URS Research Company, July 1969.

110. -----, "Strength Values of Clear Wood and Related Factors", Agriculture Handbook No. 72, Forest Products Laboratory.

111. Wisotski, John, and Snyer, W. H., "Characteristics of Blast Waves Obtained From Cylindrical High Explosive Charges", Denver Research Institute, November 1965, AD 367 625.

112. Witmer, Emmett A., "The Prediction of Lethality Envelopes for Aircraft in Flight, Part 1. General Considerations (U)", WADC Technical Report 56-150, MIT, June 1958, AD 155 602, Confidential.

DISTRIBUTION LIST

Armed Services Explosives Safety Board (5)
Washington, D. C. 20314

Defense Documentation Center, Cameron Station (20)
Alexandria, Virginia 22314

Director of Defense Research & Engineering (1)
Department of Defense
Washington, D. C. 20301

Assistant Secretary of Defense (I&L) (1)
ATTN: Mr. Howard Metcalf, IT
Washington, D. C. 20301

Chief of Research & Development (1)
Department of the Army
ATTN: LTC A. E. Grum, CRDCM
Washington, D. C. 20310

Assistant Chief of Staff for Force Development (1)
Department of the Army
Director of Doctrine & Systems
Washington, D. C. 20310

Assistant Chief of Staff for Intelligence (1)
Department of the Army
Director, Combat Intelligence
Washington, D. C. 20310

Deputy Chief of Staff for Logistics (2)
Department of the Army
ATTN: Col. K. S. Whittemore
LOG-DPD
Washington, D. C. 20310

Deputy Chief of Staff for Personnel (1)
Department of the Army
ATTN: Director of Safety
Washington, D. C. 20310

Commanding General (1)
Army Materiel Command
ATTN: AMCRD-SP-A
Washington, D. C. 20315

Commanding General (2)
Army Materiel Command
ATTN: Mr. G. L. Feazell, AMCSF
Washington, D. C. 20315

Commanding General (1)
Army Materiel Command
Mobility Equipment R&D Center
Ft. Belvoir, Virginia 22060

Office, Chief of Engineers (1)
Department of the Army
ATTN: ENGSA
Washington, D. C. 20314

Office, Chief of Engineers (1)
Department of the Army
ATTN: Mr. G. F. Wigger
ENGMC-EM
Washington, D. C. 20314

Commanding Officer (1)
Picatinny Arsenal
ATTN: SMUPA-DE
Dover, New Jersey 07801

Commanding General (1)
Army Munitions Command
ATTN: Mr. E. W. Van Patten
Dover, New Jersey 07801

Commanding Officer (1)
Aberdeen R&D Center
ATTN: Mr. O. T. Johnson
Aberdeen Proving Ground
Maryland 21005

Chief of Naval Material (1)
Department of the Navy
ATTN: MAT 0441B
Washington, D. C. 20360

Chief of Naval Material (1)
Department of the Navy
ATTN: MAT 046
Washington, D. C. 20360

Chief of Naval Operations (1)
Department of the Navy
ATTN: Mr. J. W. Connelly,
OP-41D
Washington, D. C. 20350

Chief of Naval Operations (1)
Department of the Navy
ATTN: Capt. G. J. Davis
OP-098B
Washington, D. C. 20350

Commander (1)
Naval Ordnance Systems Command
ATTN: ORD-0332
Washington, D. C. 20360

Commander (1)
Naval Ordnance Systems Command
ATTN: Mr. H. M. Roylance,
ORD-048
Washington, D. C. 20360

Commander (1)
Naval Ordnance Systems Command
ATTN: ORD-04612
Washington, D. C. 20360

Commander (1)
Naval Facilities Engineering
Command
ATTN: Mr. C. J. Stevens,
Code 04122D
Washington, D. C. 20390

Commander (1)
Naval Facilities Engineering
Command
ATTN: Mr. A. D. Tolins, 04122D
Washington, D. C. 20390

Commander (1)
Naval Ord Lab, White Oak
ATTN: EA Div. Mr. W.S. Filler
Silver Spring, Md. 20910

Commander (1)
Naval Weapons Center
ATTN: Code 3022
China Lake, Calif. 93555

US Atomic Energy Commission (1)
Div. of Operational Safety
ATTN: Mr. John P. Kelly
Washington, D. C. 20545

Commanding Officer (1)
Naval Ammunition Depot
ATTN: WEPEC
Crane, Indiana 47522

Commanding Officer (1)
Naval Civil Engineering Lab
Pt. Hueneme, Calif. 93041

Director (1)
Defense Atomic Support Agency
ATTN: Mr. J. R. Kelso, SPLN
Thomas Building
Washington, D. C. 20305

Director (1)
Defense Atomic Support Agency
ATTN: Mr. E. L. Eagles, LGCI
Thomas Building
Washington, D. C. 20305

Director of Aerospace (2)
Safety, Hq, US Air Force
ATTN: Col. A.A. Biretta
AFIAS-G2
Norton, AFB, Calif. 92409

Hq, USAF (AFIIS) (1)
ATTN: LTC W. K. Hillyer
Washington, D. C. 20330

Hq, USAF (AFSSS) (1)
Washington, D. C. 20330

AFSC (SCTSW) (1)
Andrews AFB
Washington, D. C. 20331

AFSC (SCIZG) (1)
ATTN: Mr. B. C. Mann
Andrews AFB
Washington, D. C. 20331

AFATL (ATBT) (1)
ATTN: Mr. Ralph L. McGuire
Eglin AFB, Fla. 32542

SAMSO (SMNM) (1)
ATTN: Mr. Daniel Sheriff
Norton AFB, Calif. 92409

Hq, USAF (AFOCE-K) (1)
ATTN: Mr. Walter Buchholtz
Bolling AFB
Washington, D. C. 20332

Director, AFWL (WLDC) (1)
ATTN: Mr. F. Peterson
Kirtland AFB, N. M. 87117

Central Intelligence Agency (1)
Washington, D. C. 20505

Albuquerque Operations (1)
Office, US Atomic Energy
Commission, ATTN: ODI
PO Box 5400
Albuquerque, N.M. 87115

Mason & Hanger-Silas Mason (1)
& Co., Inc.
Pantex Plant - AEC
ATTN: Mr. I. B. Akst
Director of Development
PO Box 647
Amarillo, Texas 79105

Commanding Officer (1)
Savanna Army Depot
ATTN: Mr. A. G. Ehringer
Savanna, Illinois 61074

Office of Civil Defense (1)
Department of the Army
Room 3D-336, Pentagon
Washington, D. C. 20310

E. I. du Pont De Nemours (1)
& Co.
ATTN: Mr. Frank A. Loving
Potomac River Development Labs
Martinsburg, W. Va. 52401

Directorate of Safety (1)
(Army Department)
Ministry of Defense
ATTN: Mr. Reginald R. Watson
Lansdowne House, Berkeley
Square
London W1, England

Black & Veatch (1)
ATTN: Mr. Harry Callahan
1500 Meadowlake Parkway
Kansas City, Mo. 64114

Mechanics Research, Inc. (1)
1200 University Blvd., NE
Albuquerque, N. M. 87106

IIT Research Institute (1)
ATTN: Mrs. Hyla S.
Napadensky
10 West 35th Street
Chicago, Illinois 60616

John F. Kennedy Space (1)
Center
ATTN: Mr. Fred X. Hartman
Kennedy Space Center
Florida 32899

NASA Headquarters (Code DY) (1)
ATTN: Mr. John Donovan
Washington, D. C. 20546

UNCLASSIFIED
Security Classification

DOCUMENT CONTROL DATA - R & D

(Security classification of title, body of abstract and indexing annotation must be entered when the overall report is classified)

1. ORIGINATING ACTIVITY (Corporate author) Falcon Research and Development Co., 1441 Ogden Street, Denver, Colorado 80218	2a. REPORT SECURITY CLASSIFICATION UNCLASSIFIED 2b. GROUP ---

3. REPORT TITLE

Evaluation of Explosives Storage Safety Criteria

4. DESCRIPTIVE NOTES (Type of report and inclusive dates)

Final Report - 1 July 1969 to 28 February 1970

5. AUTHOR(S) (First name, middle initial, last name)

George H. Custard, James D. Donahue, John R. Thayer

6. REPORT DATE	7a. TOTAL NO. OF PAGES	7b. NO. OF REFS
March 1970	157	112

8a. CONTRACT OR GRANT NO.	9a. ORIGINATOR'S REPORT NUMBER(S)
DAHC04-69-C-0095 b. PROJECT NO. c. d.	Falcon R&D Project 3040 9b. OTHER REPORT NO(S) (Any other numbers that may be assigned this report)

10. DISTRIBUTION STATEMENT

11. SUPPLEMENTARY NOTES	12. SPONSORING MILITARY ACTIVITY
	Armed Services Explosive Safety Baord, Washington, D. C.

13. ABSTRACT

This project has sought to develop greater understanding of the interaction of explosive blast forces with the structural targets which require protection from the accidental detonation of stored explosives. The relationships which have been developed will be helpful in understanding the risks which are implied in the established explosive quantity-distance criteria and will provide a basis for estimating the potential damage to structures exposed in a blast field which is sufficient to cause incipient structural failure.

This study has been implemented through the definition of ten specific structures which have been "exposed" to the blast forces from five charge sizes through analytical modeling techniques. All charges considered have been spherical, surface burst, bare TNT. The charges considered were limited to the following five sizes: 1,000, 10,000, 100,000, 1,000,000, and 9,000,000 pounds.

14 KEY WORDS	LINK A		LINK B		LINK C	
	ROLE	WT	ROLE	WT	ROLE	WT
EXPLOSIVE EFFECTS						
STRUCTURAL RESPONSE TO BLAST						
BUILDINGS						
VEHICLES						
AIRCRAFT						
SAFE EXPLOSIVE STORAGE						
DAMAGE LEVELS						
SURFACE BURST TNT						
PRESSURE						
IMPULSE						
STRUCTURAL RESONANT FREQUENCY						
COMPUTER PROGRAM						
ANALYTICAL MODEL						
SAFETY STANDARDS						